Fault Tolerant Control of Run of River Hydropower Plant

Ahmad Saeed

Registration No.85-FET/PhDEE-S15

A dissertation submitted to I.I.U. in partial fulfillment of the

requirements of the degree of

DOCTOR OF PHILOSOPHY

in Electronic Engineering at the

Department of Electrical and Computer Engineering

Faculty of Engineering and Technology,

International Islamic University, Islamabad

2023

Fault Tolerant Control of Run of River Hydropower Plant

Ahmad Saeed

Registration No.85-FET/PhDEE-S15

Supervisor:

Dr. Adnan Umar Khan

Department of Electrical & Computer Engineering

Faculty of Engineering and Technology,

International Islamic University,

Islamabad.

Fault Tolerant compiling - Programming

Hydropower Plant

software engineering

CERTIFICATE OF APPROVAL

Title of Thesis: **"Fault Tolerant Control of Run of River Hydropower Plant".**

Name of Student: Ahmad Saeed

Registration No: 85-FET/PHDEE/S15

Accepted by the Department of Electrical Engineering, Faculty of Engineering and Technology, International Islamic University, Islamabad, in partial fulfillment of the requirements for the Doctor of Philosophy Degree in Electronic Engineering.

Viva voce committee:

Dr. Adnan Umar Khan (Supervisor)
Assistant Professor,
DECE,FET, IIUI

Dr. Wasim Khan (Internal)
Assistant Professor,
DECE, FET, IIUI.

Dr. Noaman Ahmed Khan (Externa-I)
Associate Professor/Chairman,
DECE,Sir Syed CASE, Institute of Technology,
Islamabad.

Dr. Muhammad Mukhtar Talha (External -II)
Principle Scientist, KRL, Islamabad.

Dr. Shahid Ikram (Chairman)
Chairman, DECE, FET, IIUI.

Prof. Dr. Nadeem Ahmed Shaikh
Professor /Dean
FET, IIUI.

August 30, 2023

IN THE MEMORY OF:

Dr. Ijaz Mansoor Qureshi (10th January 2021)

Aapa Phupho (26th August 2020),

Sofi Phupho (24th August 2020),

and

My Father, Haroon Anis (9th July 2017).

ABSTRACT

Hydropower generation is one of the most prominent renewable sources of power. Run-of-river hydropower is like traditional hydropower but has a significantly less environmental impact. Faults in industrial processes cause large losses in monetary value and off times in industrial processes and consumer utilities. It is more efficient for the system to identify the occurring faults and, if possible, to have the processes running without interruption with the occurrence of a fault. This work proposes a new model—the three-pond hydraulic run-of-river system and integrates it with a turbine and regulated power generation. After integrating the hydraulic system with the turbine andpower generation, we design a diagnostic system for commonly occurring faults within the system. Mathematical models of the faults are formulated and residues are calculated. Fault detection and identification is achieved by analyzing the residues and then a fault-tolerant control is proposed. The Fault Diagnostic Module can correctly detect the faults present and offers sufficient fault compensation to make the system run nearly normally in the event of fault occurrence. With the emergence of distributed power generation smart grids and renewable energy, this fault diagnostic can reliably offer uninterrupted power to the grid and thus to consumers.

PUBLICATIONS

[A] **Saeed, Ahmad**, Shahzad, Ebrahim, Khan, Adnan U., Waseem, Athar, Iqbal, Muhammad, Ullah, Kaleem, and Sheraz Aslam. "Three-Pond Model with Fuzzy Inference System-Based Water Level Regulation Scheme for Run-of-River Hydropower Plant." *Energies 16*, no. 6 (2023): 2678.
(Archive version: https://arxiv.org/abs/2011.13131)

[B] **Saeed, Ahmad**, Adnan Umar Khan, Muhammad Iqbal, Fahad R. Albogamy, Sadia Murawwat, Ebrahim Shahzad, Athar Waseem, and Ghulam Hafeez. "Power Regulation and Fault Diagnostics of a Three-Pond Run-of-River Hydropower Plant." *Processes* 10, no. 2 (2022): 392.

ACKNOWLEDGEMENTS

All praise to Allah (SWT) for letting me take this task and to complete it. I pray to Allah (SWT) to guide me towards the righteous path in this world and Hereafter.

I would like to thank my late supervisor Dr. Ijaz Mansoor Qureshi, who was my supervisor during my MS and partway through PhD until his untimely passing. Dr. IM Qureshi has taught me a lot during his time since I met him first in 2010. He gave the basis of this thesis and research and even a week before his passing he gave detailed outlines and ideas for my research. May Allah be pleased with him and enter him in the everlasting Jannah (Aameen). I thank my supervisor Dr. Adnan Umar Khan, who took over from the position of our co-supervisor after Dr. Qureshi's passing. He took care of the power generation side of this research. He was always there for us whenever we hit a wall in our research and pushed us over the finish line. I thank Dr. Muhammad Iqbal, a core member and coauthor of our research group. I always dreaded his reviews of my papers. However, his detailed and minute reviews were pivotal in making our papers acceptable for publication and taught us a lot in the process. I thank Dr. Athar Wasim, who came to my help in securing research funding for the publication, his help will always be remembered.I thank Dr. Wasim Khan for his moral support and all the ungodly times I bothered him for help again and again. I thank Dr. Hafeez from UET Mardan, and all the coauthors for their help and coordination in publishing my paper. I thank Dr. Sheroz for his valuable insights to my paper.

I would like to thank the Higher Education Commission (HEC) for funding my PhD and giving me stipends.

I thank my friend and brother in research Ebrahim Shahzad; he was the core and the most trusted member of our research team. He not only helped me in my research a lot but also provided me with very strong moral support whenever I was down for the count. I thank my friend and lab member Ahmed Saleem, who helped me everywhere in research. I thank our lab memher Laeeq Aslam for his support. I thank hrother Umer Naseer for his support, and his insights into psychology helped me overcome my severe stress during the PhD. I thank Khalid Ibrahim for his moral support and encouragement during this PhD journey. I thank Mr. Imran Iftakhar for all his moral and administrative support during the PhD.

I thank Professor Abdul Lateef (Hazrat G) for his ever-present prayers for me which helped me out. I thank Hakeem Shahbaz sb who gave me tools to get rid of my stress and start working.

I would like to thank my father, Aapa Phupho, and Sofi Phupho, who could not see me complete my PhD and may Allah enter them in Jannah (Aameen). I thank all my family, Shafia Pbupho, mother, Aali chacha, chachi and my younger brother and sister, for their patience with me, support and prayers. I especially thank my sister Dr. Ain ul Aisha, who not only supported me in the research and gave me moral support but also never hesitated to buy me premium tools to help me in paper and thesis writing. I thank Tariq bhai for his prayers. Last, but not the least, I thank my wife and child for their prayers and support for me. My wife was especially patient with me and supported me everywhere.

TABLE OF CONTENTS

LIST OF FIGURES

CHAPTER 1

INTRODUCTION

This thesis deals with fault-tolerant control of run of river hydropower plants. The title is of two distinct parts, hydropower plants or specifically run-of-river hydropower plants and fault tolerant control. Therefore before diving into the topic in detail, we shall briefly introduce the run of river hydro power plants.

Rivers and water bodies contain kinetic and potential energy. This energy is transformed in to mechanical energy and then to electricity which is known as hydroelectric power or hydropower in popular terms. Hydropower has been used since aneient times by use of water wheels to provide power to grind mills and other industrial tools. It provides almost 20% of the world's energy requirements in the modern world [1] and is considered the most cost effective energy source, comprising nearly 80% of all the renewable energy. Hydro power plants (HPPs) can be classified as conventional and non-conventional HPPs where conventional power plants consist of a dam, lake, penstock and a power house; however, non-conventional ones include run-of-river power plants, tidal and offshore wave power plants. This classification is based on size, water head, storage capacity, and type of generation facility. Today the majority of the HPPs in practice are conventional HPPs. However, since the suitable sites for conventional HPPs are limited and have far-reaching impacts on the eco-system; therefore, small and non-conventional methods for harnessing hydro-energy are being utilized now a days with the increasing research trends of distributed power-based

smart grids. One of the frequently used non-conventional HPPs is Run of River Hydro power plant (ROR HPP).

In the run of ROR HPPs the reservoir is mostly absent or altematively there is a very small pond or reservoir; however one of the major issues with ROR HPPs is its inconsistent output due to weather and temperature changes resulting in changing river's rate of flow [2]. The available power may peak during the rainy season the available power may be less in the dry season. The water level is regulated by constructing a weir at the riverbed. In some sites where river water is redirected to flow in power plant, a small pond is required at the head of plant to provide it with some energy storage capacity. Therefore it differs from a conventional power plant in terms of less power storage capacity.

Another important part of industrial process and power generation is the field of fault diagnostics. During the industrial processes many known and unknown faults or errors can occur, which results in undesirable outputs or off times which in turn can result in monetary loss and loss of service on the consumer side. It is often not desired to shut down the system for maintenance at the occurrence of every fault, as unexpected system shutdown may cause monetary loss and inconvenience. Therefore, it is required for the control system to be able to identify the occurring faults and make the system operate in such a way that minimizes the loss and inconvenience. A fault diagnostic system has two main factions, first to identify and isolate any fault that has occurred, and second to compensate the system so that the effects of the fault are minimized.

1.1. Literature Review for Run of River Hydropower

Plant control, plant power forecasting, and consequences on the power plant's environmental economics are all covered in the current literature on ROR HPPs. Classical control techniques are frequently employed in the control of ROR HPP [7]. However, as stated in [8], head pond level control is now via a fuzzy inference approach. ROR HPP's automatic generation control is implemented in two modes: constant power and frequency modes [9]. They are thought to be more general control techniques. To control a ROR HPP, a variable-speed Kaplan turbine [10] was devised and experimentally tested. A revolutionary idea is offered to supplement generated electricity with a bank of supercapacitors. It has recently developed a way to integrate the capacitor bank with the ROR HPP [11]. For use in a run-of-river hydropower plant, a software-based troubleshooting/fault diagnostic tool [12] is being developed. It is not a fault diagnostic system; but an end-user-based tool that identifies potential causes for unusual system behavior. To mimic a run-of-river hydroelectric plant, actual river flow data is used [13]. Simultaneously, another study [14] creates an electromechanical system for controlling generating frequency in the presence of electronic load controllers.

[14, 15] uses a mechanical gearbox speed increaser to boost the efficiency [15] of a turbine, as well as AC-DC-AC converters to regulate the output voltage. [16-21] proposes various methods for connecting run-of-river hydropower projects to the grid and with other power plants such as wind power. They also optimize electricity generation to reduce losses and [22] push developing of autonomous microgrids near run-of-river power stations.

Scheduling ROR hydropower output in response to changing power demands is also a hot topic in this field. [23-26] examine many kinds of power production scheduling, from the use

of reversible pumps [23] to the creation of a power production function [20] based on short-term scheduling using historical weather data. [27] and [28], which use Artificial Neural Network (ANN) to select on criteria to incorporate in forecast-related decision-making, discuss forecasting accuracy. Another study [29] looks at how to use water continuity equations for predicting while managing the water level in a power plant. According to the author, fluid continuity equations are unnecessary for short-term forecasting.

The economic and environmental implications of ROR HPPs have also been explored in [30-33]. For run-of-river hydropower facilities, cost economics optimization [33] and cost overrun prediction [30] have also been done, making run-of-river hydropower more sustainable and cost-effective [21,34-36]. A Study [37] in China on the effects of hydropower dams on change of the environment depending on river flow rate, channel depth and width, dissolved oxygen and ions, temperature etc on the biodiversity of river bed dwelling microalgae (benthic diatom). Due to the changing habitat conditions, the authors report that damming interferes with the benthic diatom. [38] looked at low-head run-of-river hydropower's environmental design in the United States. The assessment concludes that the ROR designs primarily maximize the projects' economic potential. The authors say that design models need to be expanded to include the effects of barriers, designs with low head technologies, and the tradeoffs associated with the run-of-river timescale. The authors also state that including enviromental impact on the design of run of river hydropower plants would make the ROR designs more feasible. Authors of [39] collected and reviewed 73 different papers based on hydropower and machine learning. While machine learning is widely employed in several disciplines, the authors argue that machine learning applications can considerably help areas such as optimal dispatch, maintenance, and general operations. [40] studied the variations and flow changes of different rivers in the Warta basin of Poland,

compiling the data for 70 years from 1950 to 2020. The author finds that analysis of historical data over a lengthy period of time is necessary for investment planning, design, operation, and economic efficiency in run-of-river hydropower projects. The authors in [41] propose a method for battery storage systems for nano and microgrids. The new methodology combines different optimization tools, clustering techniques, and softwares to lower daily operating costs for the considered grid. [42] proposes hydrogen production using the excess flow of water from a run-of-river hydropower plant by considering the load demand cycle of the power plant. The authors of [43] mapped river and stream flows of Japan in various conditions and used ANNs to determine the water-energy potential and find the optimal sites for the construction of ROR HPPs.

1.2. Literature Review for Fault Tolerance

[44] proposed a fault-tolerant control of a simulated hydropower plant. The faults of a hydropower plant discussed in [44] are the actuator fault, i.e., the response time of the actuator increases, the turbine flow fault, and the turbine speed sensor fault. The authors in [45] discuss different faults in Modular Multilevel Converters (MMCs) and present various fault diagnostics and fault-tolerant schemes. The faults of a 132 kV power distribution system are detected using a stationary wavelet transform to extract the features. Then these features were used with artificial neural networks to detect and classify faults [46,47]. Another researcher [48] presents fault diagnostics using a Markov model and fault regression vectors. Another interesting study of fault diagnostics is by [49], regarding fault detection and diagnostics of ventilation units in a building and using multiple readings from adjacent sensors and detecting the deviation in sensor readings. The sensors considered are

temperature, air, and fan-speed sensors. The authors in [50] proposed a contrastive learning algorithm for software and data-based fault diagnostics and a fault-detection system. In [51], fault detection and diagnostics of a vehicle's internal combustion engine and mechanical parts was achieved using chaos analysis and signal processing on the sound of the running vehicle. Similar to [52,53], they used spectrum analysis for fault diagnostics in rotating machines. In [54], for the fault diagnostics of a hydroelectric generator, they used two sensors: a vibration sensor with horizontal and vertical movement and a pendulum and bond phase sensor. These sensors are attached to the generating unit. The faults of the generating unit are diagnosed by analyzing the sensor data over the data communication line. The authors of [55] discuss the fault diagnostics of the hydro turbine governing system. First, a simplified non-linear model of a hydro turbine non-linear system is taken and analyzed using Volterra models in the frequency domain. In addition, many theses, such as [56–58], have been done on fault detection and diagnostics using observers and residues.

1.3. Research Gap

As the head pond of the Run of River hydroplants is dependant upon the flow of the river and is suseptable to disturbances. Therefore, there exists a research gap to make the head pond robust against disturbances. In this thesis, this is done by introducing a new three pond model and then its integration with the system is done. After that faults are modelled and fault tolerance is achieved.

1.4. Organization of Thesis

This thesis is organized into five parts. The introduction, explanation about faults and fault tolerance, then the two next chapters deal with the two research articles and fully conclude. The second chapter of this thesis delves into the background of hydropower and then fault diagnostics and tolerance. In the third chapter, the concept of having three ponds for a run of river hydropower plant is discussed in detail and simulation verification of the concept is discussed. The fourth chapter discusses the second publication continues the concept from the previous chapter, consolidates and completes the model and mathematical accuracy, and then applies the concept of fault tolerance to the three pond run of river power plant concept and then discusses its results and implication. Finally, future directions and conclusion are drawn in the fifth and the final chapter.

CHAPTER 2

BACKGROUND INFORMATION

This thesis consists of two parts, run-of-river hydropower plants and fault-tolerant control. We shall be briefly discussing both of these topics in this chapter.

2.1 Hydropower

Hydropower is the use of flowing or falling water to run machines or to produce electricity. Since the ancient times water wheels or watermills have been used to power grind mills, saw mills trip hammers and other machines [3,4]. Hydroelectricity is almost exclusively known as hydropower, as hydropower is mostly used for electricity generation. Hydropower is one of the most common sources of renewable energy. Renewable energy is known as 'renewable' because it does not use any traditional fuel to burn or use naturally occurring energy source and harnesses them for energy generation. These energy sources do not have a significant carbon footprint or emission as they are also 'repeatable' as long as the natural phenomenon exists. Examples of renewable power include solar energy, wind energy, geothermal energy and hydropower.

Hydropower generation can be divided into several categories depending on how we categorize hydropower plants. The categorization of hydropower plants is based on their size or power output. Another categorization is based on whether the hydropower plant is traditional or nontraditional. A traditional hydropower plant is made by constructing a dam

and a reservoir for the power plant. Nontraditional hydropower plants may do away with dams and even reservoirs. Nontraditional hydropower plants include run of river hydropower plants, tidal and wave power plants. In this thesis, only run-of-river hydropower plant is discussed.

A simplified diagram of a traditional hydropower plant is shown is Figure 1. In a traditional hydro power plant we have a dam and reservoir built in the path of a river. A large amount of water is kept stored in the reservoir. It is used to generate power and is often supplied for household uses. The maximum amount of water stored in a dam is controlled by spillway over flow gates near the top of the dam. Due to the dam construction there is a height difference between the reservoir and the continuing outward river. Near the base of the dam a water tunnel or pipe exists from which water enters the turbine. This tunnel is known as a *penstock*. At the end of the penstock there exists a turbine or a group of turbines coupled with generators with or without the involvement of gear trains. The exiting water of the turbine is thrown out through another tunnel to the river is known as the *tail race*. The mouth of the penstock is closed with a gate through which the flow of water is controlled through the turbine. The actual height difference between the intake of penstock and the exit of tail race is known as the *head* of a power plant which is directly related to the amount of power produceable with it.

Now with the basic structure of a traditional known, we shall look at the basic structure of a run of river power plant and know its similarities and differences with a traditional hydro power plant.

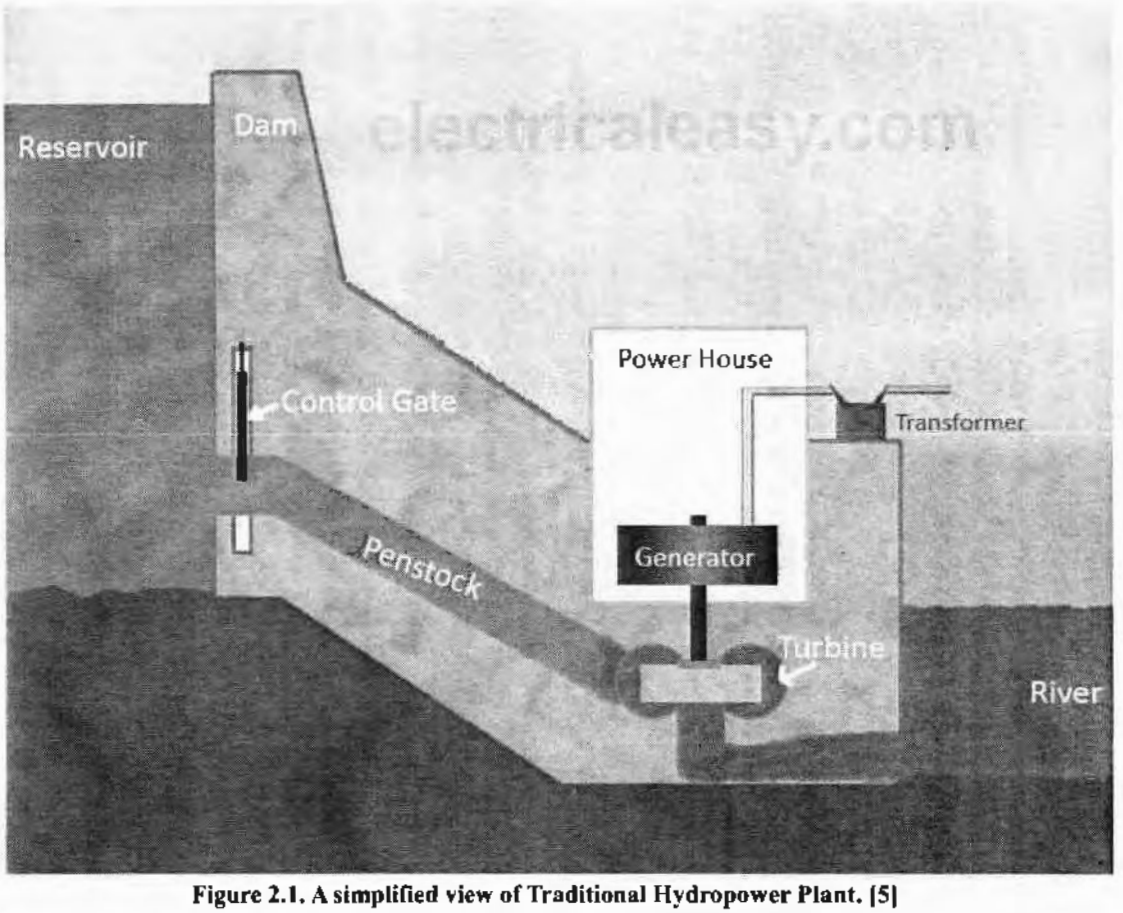

Figure 2.1. A simplified view of Traditional Hydropower Plant. [5]

A traditional hydropower plant has the main disadvantages of its large size, and its environmental or socio-economic effects due to its size. Due to the fact that a traditional hydropower plant requires constructing a dam and then flooding the reservoir, it requires specific geographic sites which are feasible for the construction of the hydropower plant. Once a site is found feasible for the construction of the dam and reservoir, the valley which will be flooded to become is reservoir has villages settled in it which have to be displaced. This displacement of people can cause socio-economic problems if the government does not settle them in an alternate place. Another undesirable impact of traditional hydropower plants is due to changing the topography of the land to a water reservoir which disturbs the natural ecosystem and its effects are long term.

Due to the ever-increasing energy demands, there is a renewed interest in renewable power sources. As stated earlier, feasible sites for constructing traditional hydropower plants are becoming rare, so the alternative to the traditional hydropower plant is a run of the river hydropower plant. In the run-of-river hydropower plant, the main difference is that the dam is absent. A reservoir or a head pond may or may not be present. In the presence of a head pond, its size is significantly smaller than the reservoir of a traditional hydropower plant. A wall is almost always constructed on the river bed to achieve some level of regulation in the power plant. This river wall is known as a weir. The main difference between a weir and a dam is that the water is meant to flow over the weir but not the dam. Water from the river or head pond enters the headrace or penstock to the turbine and exits through the tail race to the river. Depending on the geography of the system, the river may be redirected to the powerhouse rather than constructing the powerhouse near the river. Also, dependending on the length of the headrace and penstock a surge tank is added before the turbine. In that case, the tunnel before the surge tank is called headrace, while it is called penstock after the surge tank to the turbine. The basic structure of a run of river hydropower plant is shown is Figure 2.2.

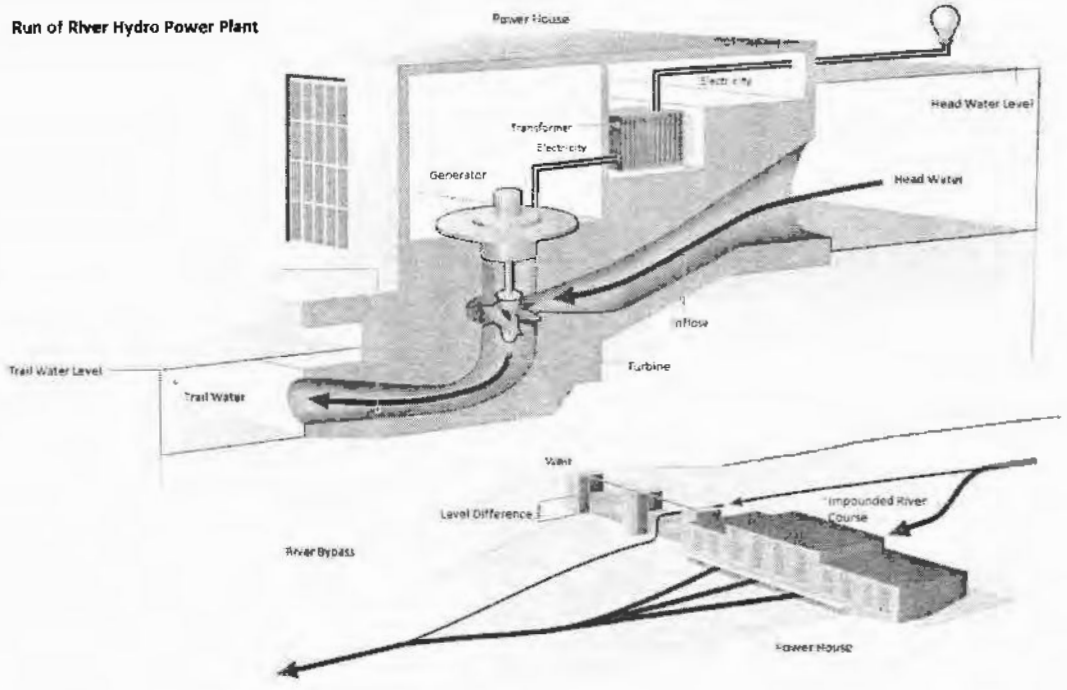

Figure 2.2. Run of River Hydropower Plant with external structure and weir. [6]

2.1.1 Turbine

The turbine is the part of the hydropower plant which is the linkage between the hydro-energy and electrical energy. The turbine converts the hydro energy to mechanical energy, which is converted to electrical energy by the generator. The scope of this thesis is only up to the turbine. The turbines in the power house are of different types which depend upon the water head (difference of water level between the headrace and tail race), water flow rate and the variability of water flow. Generally, three main types of turbines are used in run of river hydropower plants. A Pelton turbine is used in the case of a high head but a relatively low flow, while a Francis turbine is used for medium to low heads and medium to high flows. While Kaplan turbines are utilized if there is a noticeable change in water flow rates as the pitch angle of a Kaplan turbine can also be changed in addition to its wicket and control

gates. The power output of the turbine is a function of the rate of flow of water through it, its rotational speed and the wicket gate position. These relationships of the turbine are usually expressed in a set of points and graphs known as hill curves. Usually, during calculations an operating point of the turbine is set and all the calculations are done against that point.

2.2 Fault Diagnostics and Fault Tolerant Control

Fault diagnostics and fault tolerant control is one of the relatively new field which uses control techniques on a natural phenomenon. Any component, if it is faulty, behaves undesirably with the occurrence of fault and may change its, physical and operational characteristics. The reason fault is being called a natural phenomenon is because due to aging and time, faults are bound to occur, even if it takes a very long time. Another reason for the occurrence of fault is due to natural disturbances like storms, earthquakes or other natural disasters. Another reason for fault occurrence is artificial like sabotage or war. Like a control system design makes the system operate to our requirements and controls its processes and variables, fault-tolerant control aims to function like traditional control in the presence of fault.

Fault-tolerant control can be broadly categorized into passive and active fault-tolerant control. Passive fault tolerant control is more like robust control and it uses the property of robust control to deal with uncertainties and variations of the system parameters in the presence of faults to be able to operate desirably in the presence of faults. A disadvantage of passive fault tolerant control is that while it may behave more or less desirably during the occurrence of a fault, it cannot identify the fault. Active fault tolerant control covers this disadvantage of the passive fault tolerant control.

Active fault tolerant control or simply fault tolerant control consists of fault identification, isolation and then finally fault tolerance. The process of fault identification and isolation is also known as fault diagnostics. After fault identification and isolation, fault tolerance is initiated. Fault tolerance simply modifies the control law according to the fault identified so that the effect of the fault is minimized on the system output. In case of severe faults, shutting down the system to avoid further damage is also the responsibility of the fault tolerant control.

2.2.1 Types of Faults

Faults can be classified into two categories Based on the location of fault occurrence. One is a sensor fault, while the other is an actuator fault. Sensor fault occurs when the sensors do not work properly and give incorrect state values to the control. Sensor faults are distinctly different from actuator faults as they do not have any noticeable physical damage, the sensor may be giving wrong state information due to its damage, or it may be physically disconnected or dead. As the control of the system depends upon the state information, with the malfunctioning sensor, the degradation in the control of the system is amplified by the faulty sensor. The other type of fault is the actuator fault. As indicated by the name, actuators are unable to properly implement the control law, as the control law is unable to be properly implemented, and the system is unable to be properly controlled. Another category of fault is the actual system fault, in which the parameters of the system are disturbed by the fault. The effects of disruption of system parameters result in unpredictable output. However, instead of dealing with system faults using fault tolerant control, robust control or some other form of control is used and system parameter disturbance is modeled using uncertainty or disturbances. Therefore, faults are categorized in only two types, sensor and actuator as only these are specifically dealt with using fault tolerant control.

For fault identification or diagnostics, different techniques exist, many times; special filters and observers are used to estimate the true state values. These state values are then used to form the correct theoretical output and then estimate and locate the fault. Observers and filters are especially useful for diagnosing and correcting sensor faults. Another method is finding a difference between the system output and the observer or faultless system model output. This difference is known as a residue of the system, and the residue is analyzed to determine the occurrence and location of fault.

For sensor faults, the observer or filter achieves fault tolerance by providing the corrective terms to the faulty sensor state and then allowing the system to correct itself. In the case of actuator faults, the control law is modified in order to minimize the effects of the faults on the system output. Sometimes, when the effects of the faults appear only in these outputs, which are not very important or appear only during the transition state, then the system may be declared inherently fault tolerant and special control laws or fault tolerant actions may not be required.

CHAPTER 3

RUN OF RIVER HYDROPOWER WITH THREE PONDS

In a typical diverted ROR HPP, a weir or a short wall is placed on the riverbed to keep the water level in check. A weir varies from a dam in that it is designed to allow water to flow across it. The river is channeled and the water is directed towards the head pond. The penstock or headrace is connected to the head pond (when a surge tank is present).

3.1 Hydraulic System Model

Figure 3.1 depicts the three head ponds or tanks of our run-of-river hydropower plant: T_0, T_1 and T_2. The ponds T_1 and T_2 are allowed to receive water from the river. Ponds T_1 and T_2 are connected to pond T_0 at the bottom. A surge tank connects the pond T_0 to the headrace tunnel, which leads to the penstock and turbine. The controllable valves s_1 and s_2 are located in the connecting tunnels between T_1, T_0 and T_2, T_0. Also, keep in mind that Figure 1 was adapted from [7,8] as a model with a single reservoir and then modified to fit our needs as a three-pond system. Figure 3.1 shows the proposed hydraulic system diagram.

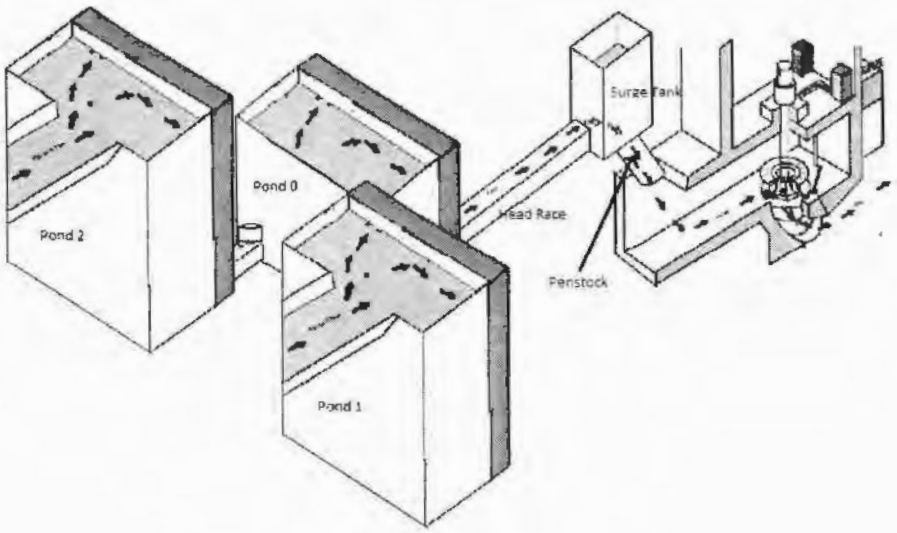

Figure 3.1. Proposed Three Pond Run of River Hydropower Plant

While dealing with each part, the system is modeled as a series of equations. There are five equations because our hydraulic system comprises of three ponds, a head race, and a surge tank. Ponds and tanks use the same mathematical model in terms of water level change. This is determined by the overall flow into and out of the pond or tank. Because the headrace is a long tunnel, the water levels at each end determine the flow. The equations for the system are listed below. Also, using the conclusions of [29], detailed fluid continuity equations can be ignored without losing accuracy for the system model.

As the main interest is in tbe water levels and flows, we formulate the equations of the ponds. The rate at which the water level changes in a pond or tank depends on the difference between inflows and outflows. The equation of such a pond is:

$$A\frac{d}{dt}x = inflow - outflow \tag{3.1}$$

Where, A is the the pond's cross-sectional area and x is the level of water. The inflows and outflows between connected tanks 1 and 2 is a function of the difference between the water levels.

$$flow_{1\to 2} = f(x_1 - x_2, a) \tag{3.2}$$

Where $x_1, x_2$are the two ponds' water levels, and a is the duct's cross-sectional area or opening between the two ponds.. For ponds 1 and 2, the inflow from the river and the outflow is to pond 0. We assume that the inflow from the river is completely controllable.

The outflow to the pond 0 is dependent on the levels of the pond 1 and 0 and the the duct's cross-sectional area between them. Therefore, by combining Equation 3.1 and 3.2 and expanding them, the equations for pond 1 and 2 are obtained.

Pond 1 has the following equation:

$$\frac{d}{dt}x_1 = -\frac{na}{A}s_1\sqrt{2g|x_1 - x_0|}sgn(x_1 - x_0) + \frac{U_1}{A} \tag{3.3}$$

Pond 2 has the following equation:

$$\frac{d}{dt}x_2 = -\frac{na}{A}s_2\sqrt{2g|x_2 - x_0|}sgn(x_2 - x_0) + \frac{U_2}{A} \tag{3.4}$$

where $sgn(z)$ is defined as:

$$sgn(z) = \begin{cases} 1 & z > 0 \\ 0 & z = 0 \\ -1 & z < 0 \end{cases} \tag{3.5}$$

and $|a|$ is defined as:

$$|z| = \begin{cases} z & z \geq 0 \\ -z & z < 0 \end{cases} \tag{3.6}$$

In Equations 3.3 and 3.4, U_1 and U_2 are the controllable river inflows to pond 1 and pond 2. The signum function included in the flow expression for the above equations determines the direction of water flow. Also, note that the equations of pond 1 and 2 outflows are intentionally written before the inflow to be in line with the classical representation of a system as we assume we have control over the inflow of water. For pond 0, it has three

inflows and outflows. Water flows in from ponds 1 and 2 and flows out to the headrace. So, Pond 0 has the following equation:

$$\frac{d}{dt}x_0 = \frac{n_0 a}{A}\left[s_1\sqrt{2g|x_1 - x_0|}sgn(x_1 - x_0) + s_2\sqrt{2g|x_2 - x_0|}sgn(x_2 - x_0)\right] - \frac{Q_t}{A} \quad (3.7)$$

In the above equations (3.3,3.4,3.7) the control variables are s_1, s_2 and U_1, U_2, where U_1, U_2, are the controllable inflow of water in the ponds 1 and 2, while s_1 s_2 are the controllable valves between Pond 1 and 0 and Pond 2 and 0 respectively, and $Q_t$is the flow of water from the pond 0 to the headrace.

The equation of headrace is derived from the flow in a tube. For the flow of water in a closed channel between two water reservoirs, 1 and 2 is given by:

$$\frac{L}{ag}\frac{d}{dt}Q = x_1 - x_2 - frictionlosses \quad (3.8)$$

Where L and a are the length and cross-sectional area of the closed channel and g is the gravitational constant and x_1, x_2 are the levels in ponds 1 and 2, respectively , and Q is the water flow through that closed channed. Therefore, as the water level in the two reservoirs changes, the flow direction in the closed channel changes. So the equation for the headrace is:

$$\frac{d}{dt}Q_t = \frac{gA_t}{L_t}(x_0 - x_s) - C_t Q_t|Q_t| \quad (3.9)$$

The inflow is from the headrace for the surge tank, while the outflow is to the turbine penstock. As stated earlier, we are not including the turbine and penstock in this work, so the surge tank equation is:

$$\frac{d}{dt}x_s = \frac{Q_t}{A_s} - \frac{n_0 a}{A_s}\sqrt{2gx_s} \quad (3.10)$$

These five equations (3,4,7,9,10) can be put together to form a nonlinear system model:

$$\frac{d}{dt}\vec{x} = \vec{f}(\vec{x}, \vec{u}) \tag{3.11}$$

The state variables are defined as follows:

$$\vec{x} = [x_1\ x_2\ x_0\ Q_t\ x_s]^T \tag{3.12}$$

And the control variables are located as follows:

$$\vec{u} = [U_1, U_2, s_1, s_2]^T \tag{3.13}$$

The outputs are x_1, x_2. and x_0. The output equation is:

$$\vec{y} = C\vec{x} \tag{3.14}$$

Where C is defined as:

$$C = \begin{bmatrix} 1 & 0 & 0 & 0 & 0 \\ 0 & 1 & 0 & 0 & 0 \\ 0 & 0 & 1 & 0 & 0 \\ 0 & 0 & 0 & 0 & 0 \\ 0 & 0 & 0 & 0 & 0 \end{bmatrix} \tag{3.15}$$

Where U_1, U_2 are the controlled water flow rates into the ponds P_1 and P_2 and s_1, s_2 are the valves between the ponds P_1, P_0 and P_2, P_0 respectively. The valves s_1, s_2 can be adjusted from 0 to 1, while U_1, U_2 can be adjusted from 0 to U_{max}. As we are only interested in the water levels of the head ponds, the 4th and 5tb columns of the matrix in equation 3.15 are supposed to be zero. Figure 3.2 shows the Simulink implementation of the system model (equation 3.11). As equations 3.1-3.15 are from the initial [A] paper, the three pond model is slightly modified to be used in the concluding [B] paper which is discussed in the next chapter.

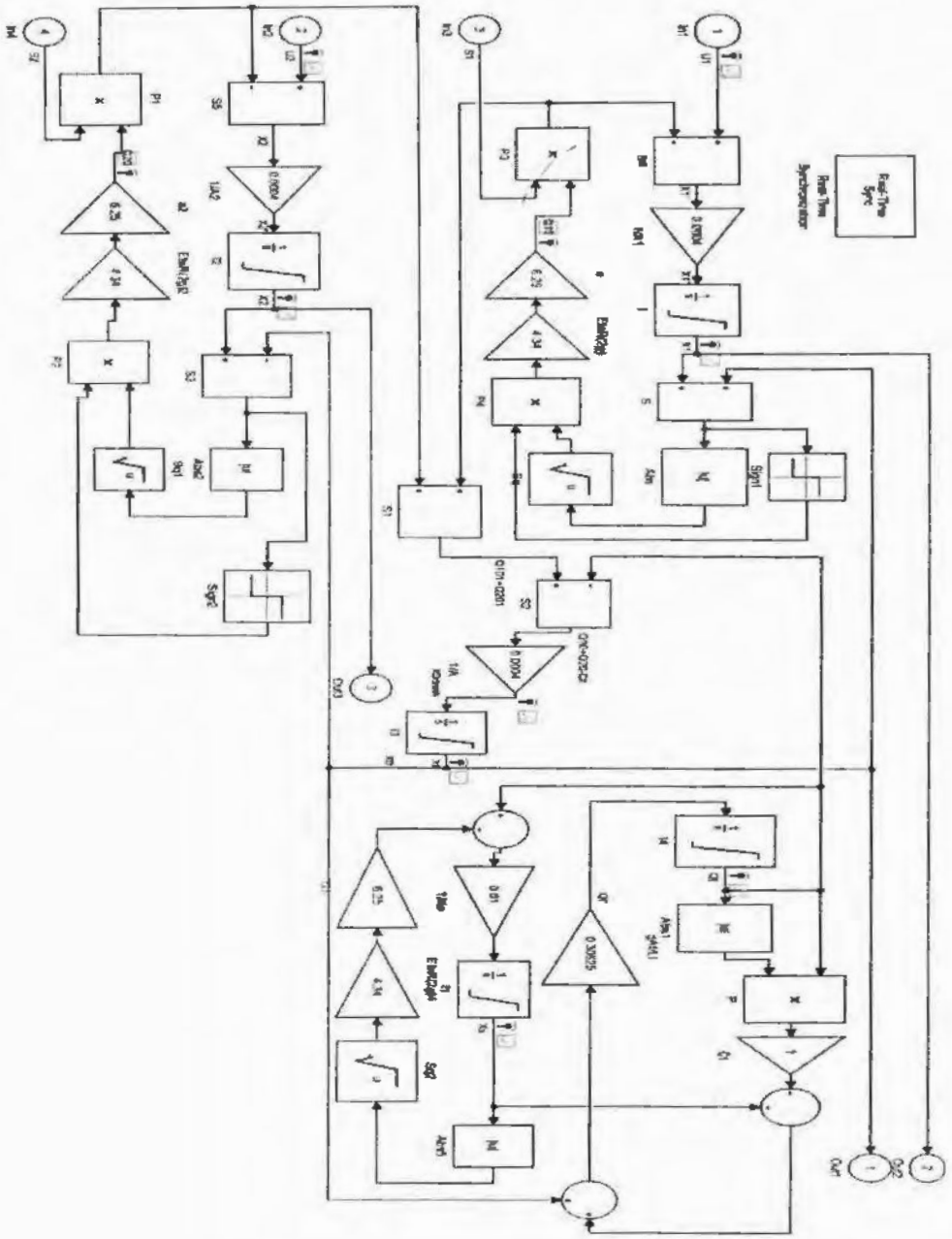

Figure 3.2. System model in Simulink

3.2 Control Design

The water level must be maintained in ponds at a predefined level using the three-pond system. Compared to a single pond, this system is distinguished from a conventional system by its three pond mechanism. This work models and analyses the water dynamics of the system. This work does not include a turbine, whereas the water level regulation of the system is performed by Fuzzy Inference Engine (FIE).Fuzzy Inference Engine or fuzzy control is used due to its flexibility for maintaining the water levels for the three ponds at different levels. Another advantage of using a fuzzy controller is its higher speed and accuracy when compared to traditional PID controllers. The generalized controller design is depicted in Figure 3.3.

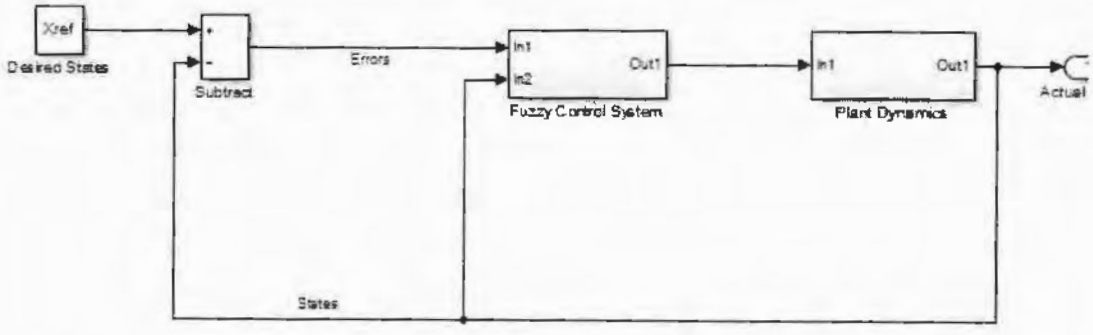

Figure 3.3. FIS Based Control scheme of system

3.2.1 Fuzzy Control

The control scheme is slightly unlike the traditional one, using the system output states and errors.

U_1,U_2, s_1, and $s_2$are control variables in the system defined in (eq 3.11) whereas x_0, x_1 and x_2 out of five states need to track their desired levels. The system control uses two fuzzy

inference engines and subtractors. Simulink based detailed control scheme is given in Figure 3.4.

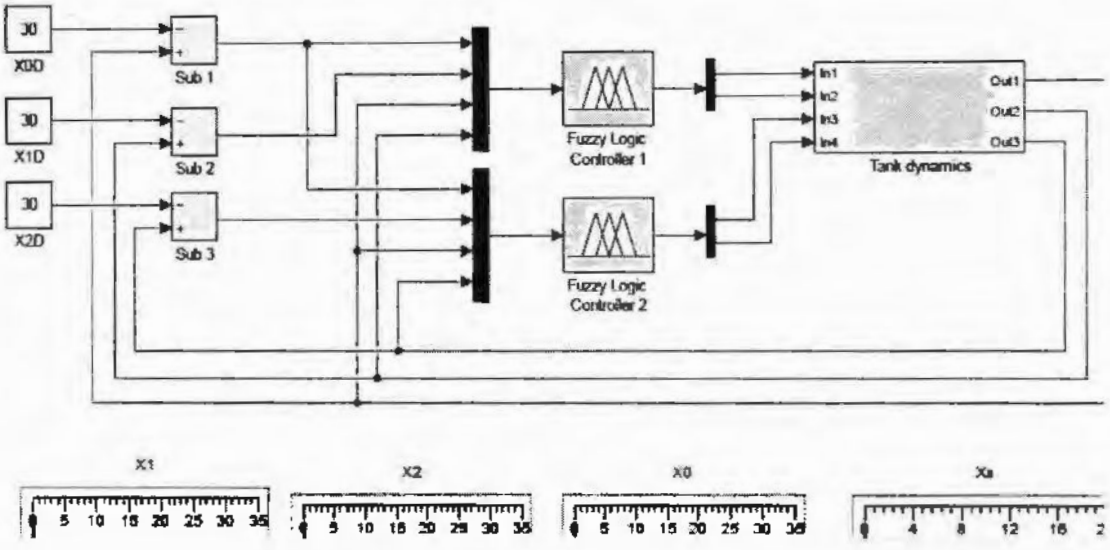

Figure 3.4. Fuzzy Control Scheme in Simulink

The subtractor is used to calculate the difference between current and intended state values. It provides the ease of changing required levels on the fly without creating new rules for FIS. Subtractors generate pond errors E_0, E_1 and $E_2$and depending on errors being positive, negative or zero FIS makes decisions. FIS is the most crucial component of the control system, which is constituted by IF-THEN rules. For example, if a system has two inputs and one output, the rules are formed as:

$$Rule\ 1\text{: } IF\ x_1\ is\ A_1^1\ and\ x_2\ is\ A_2^1\ THEN\ y\ is\ B^1 \tag{3.16}$$

A complete rules' set comprises of all possible input memberships' combinations. For example, if a two-input system has both inputs with 3 memberships, then all the possible memberships' combinations are 3×3 or $3^2 = 9$ rules. The outputs can have number of memberships same as the number of rules or less.

Because each rule has six inputs and four outputs, the complete rule base for this system requires $3^6 = 729$ rules for effective control of the system. Furthermore, each input has three levels, and output has five levels. This causes increased mathematical overhead and slowing of simulation. By replacing the one fuzzy system with two parallel ones, the problem is avoided. Fuzzy System 1 (FS_1) regulates U_1 and s_1 by dealing with Pond 0 and Pond 1, whereas Fuzzy System 2 (FS_2) regulates U_2 and s_2 by dealing with Pond 0 and Pond 2. So each Fuzzy system has four inputs and two outputs. The number of rules are now reduced to $3^4 = 81$ for each system.

It is required to maintain the ponds' water levels at the desired level in the three pond system. The inputs of FIE are current water levels and error values, whereas the value positions and the inflows are outputs. FIS regulates (maintains, increases, or decreases) the levels of ponds by varying the values of inflows U_1, U_2 and valves' positions s_1, s_2. The values can be varied from 0 to some positive maximum value for inflows and from 0 to 1 for valve position. The positive error can be reduced by stopping the inflow and depending on outflow to lower the level. In contrast, the management of negative error requires the inflows to be greater than outflows. The zero error is maintained by balancing the outflows and inflows. The valves are specifically used when the ponds need to be set at different levels.

Trapezoidal membership functions are assigned to heights with HIGH, *MEDIUM*, and *LOW* Levels of water. Trapezoidal membership functions are also assigned to *POSITIVE and NEGATIVE errors*, whereas *ZERO* is assigned with a triangular membership function. The membership functions used are self-explanatory and the ZERO membership function is meant for near zero error. Each output has five levels from 0 to 4, where Level '0' is stop and level '4' is maximum or full throttle. Level '0' is not defined for

'U' and valves s_i (for i =1,2) have impulse membership function which can be at zero or maximum. Membership functions assigned to all outputs are trapezoidal.

It is difficult and unnecessary to explain all the 81 rules for each fuzzy system, but few examples are given to justify their basis.

1) Considering zero initial conditions with a set desired level, x_1 and x_0 are at LOW and E_1 and E_0 are negative, the output $U_1$is required to have a high inflow rate L_4 and valve s_1 is to be set at open V_4. The conditions are given in the form of rule as:

$$IF\ E0\ is\ NEGATIVE\ and\ E1\ is\ NEGATIVE\ \ and\ X0\ is\ LOW\ \ and\ X1\ is\ LOW \\ THEN\ S1\ is\ V4\ and\ U1\ is\ L4 \tag{3.17}$$

2) If both levels are at similar high level and both errors are zero then it requires balancing of inflow and outflow rates, i.e. both U_1 and $s_1$are set at positions to maintain the system in equilibrium. This is depicted in the form of rule as:

$$IF\ E1\ is\ ZERO\ and\ E0\ is\ ZERO\ and\ X1\ is\ HIGHand\ X0\ is\ HIGH \\ THEN\ U1\ is\ L1\ and\ S1\ is\ V1 \tag{3.18}$$

3) If both errors are zero, level of x_0 is at mid-level and x_1 is high then it requires balancing of inflow and outflow rates, i.e. both U_1 and$s_1$are set at defined positions to maintain the system in equilibrium. This is depicted in the rule below:

$$IF\ E0\ is\ ZERO\ and\ E1\ is\ ZERO\ and\ X0\ is\ MEDIUMand\ X1\ is\ HIGH \\ THEN\ U1\ is\ L1\ and\ S1\ is\ V1 \tag{3.19}$$

4) If there is zero error for E_0 and positive error for E_1 but both the levels are similarly high, then the priority is set for Pond 0. The valve s_1 is set to a defined position and inflow is stopped at $L_0$to maintain the pond 0 in equilibrium whereas the level of Pond 1is reduced. This is depicted in the rule below:

$$IF\ E0\ is\ ZERO\ and\ E1\ is\ POSITIVE\ and\ X0\ is\ HIGH\ and\ X1\ is\ HIGH \\ THEN\ S1\ is\ V1\ \ and\ U1\ is\ L0 \tag{3.20}$$

5) If there is zero error for $E_1$and positive error for E_0 and both the levels are simmilarly high, then the priority is set for pond 0. The valve s_1 is set to a defined positionand inflow is stopped at $L_0$to get the pond 0 drained to pond 1 and the headrace. This is given in the rule below:

$$IF\ E0\ is\ POSITIVE\ and\ E1\ is\ ZERO\ and\ and\ X0\ isHIGH\ and\ X1\ is\ HIGH\ THEN\ S1\ is\ V1and\ U1\ is\ L0 \tag{3.21}$$

In this way all rules for FS1 are designed and the same are mirrored for FS2.

The fuzzy controller's output can be expressed in a generalized manner as follows:

$$u(t) = \frac{\sum_{j=1}^{81} \bar{u}_j \left(\prod_i^4 \mu_{A_i^j}(k_i)\right)}{\sum_{j=1}^{81} \left(\prod_i^4 \mu_{A_i^j}(k_i)\right)} \tag{3.22}$$

Where $u(t)$ is the controller's output for U_1 or s_1, k_i is the input value of $x_0, x_1, E_0$and E_2. The linguistic variable for input that can be $NEG, ZERO, POS$ or LOW, MED, HI is A, μ_A is the membership function of A and $\bar{u}_j$ is the firing strength of j^{th} fuzzy rule.

3.3 Testing the Three Pond System

Extensive simulations were used to analyze the proposed system in Simulink (MATLAB). The results are compared with the conventional redirected run of river hydropower plant. The proposed three-pond model is compared with a single pond model having the same storage capacity as the other three tanks combined.

As a case study, the following values for the model parameters are used for simulations.

$H_0 = H_1 = H_2$ = Height of pond 0, 1, 2 = 35m

H_s= Height of Surge Tank = 15m

a = The area of the cross-section of the ducts betweenT_1&T_0,T_2&T_0= $6.25m^2$

A = Area of the PondsT_0,T_1, T_2 = $50mx50m$= $2500m^2$

A_s = Area of Surge Tank. = $10mx10m$ = $100m^2$

L_t= Length of headrace. = $200m$

A_t = Cross section al area of head race = $6.25m^2$

U_{max} = The maximum controllable intake of water in ponds $T_1$and T_2 = $100\ ^{m^3}/_{sec}$

Traditional System: Single Pond Model.

Proposed System: Three Pond Model.

T_0, T_1, T_2: pond 0, pond 1, pond 2

For a fair comparison of the three-pond model with the classic single pond model, all parameters are the same except the pond area A of the traditional model is multiplied by 3 and U_{max} is multiplied by 2. This preserves generality as well as it is a fair and unbiased comparison between the two systems. Both systems' levels are managed through fuzzy inference control.

3.3.1 Level Regulation

This section discusses the results of the suggested FIS for managing water levels in the proposed model. Three different instances are considered. The case considers the water level in all three ponds to be the same. The second case considers the level of water in pond 0 to be less than that in ponds 1 and 2, where ponds 1 and 2 have the same water level. The third case considers the water levels in all of the three tanks to be different such that pond 0 has the lowest level of water, followed by pond 1 while pond 2 has the highest level of water. Provided following are the results and their discussion.

3.3.1.1 Case I: $(T_0 = 30, T_1 = 30, T_2 = 30)$

In this case, a water level of 30 meters is required for the three tanks. All three tanks are supposed to be empty initially. All states reach steady state in almost 30 minutes. The inaccuracy in steady-state is 0.5 meters. Ponds T_1 and T_2take different times, as compared to pond T_0, to reach steady state. They take 27 minutes to rise to the steady sate whereas T_0 takes 30 minutes. Figure 3.5 shows a graphical representation of these results. The findings suggest that the proposed scheme can maintain the desired water levels. A balance between water inflow and outflow is maintained when the system reaches a steady state.

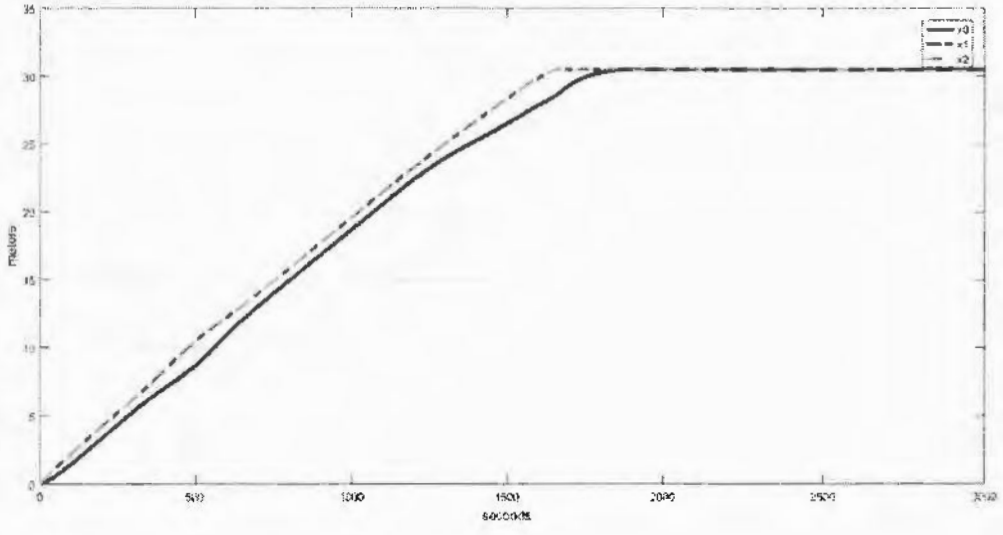

Figure 3.5. Desired water levels vs Time.T_0,T_1 and T_2 at 30m.

3.3.1.2Case II: $((T_0 = 25, T_1 = 30, T_2 = 30)$

Here, a water level of 25 meters is desired for pond 0, whereas 30 meters level is desired for pond 1. The system takes 30 minutes to reach desired water levels in ponds 1 and 2. It takes 24 minutes to reach the desired level in pond 0 as for pond 0, the desired water is 25 minutes, and the steady-state error is 0.5 meters. Figure 3.6 shows these results graphically, where the blue line represents the water level of pond 0, and the dotted green and red lines represent the water levels in ponds 1 and 2, respectively.

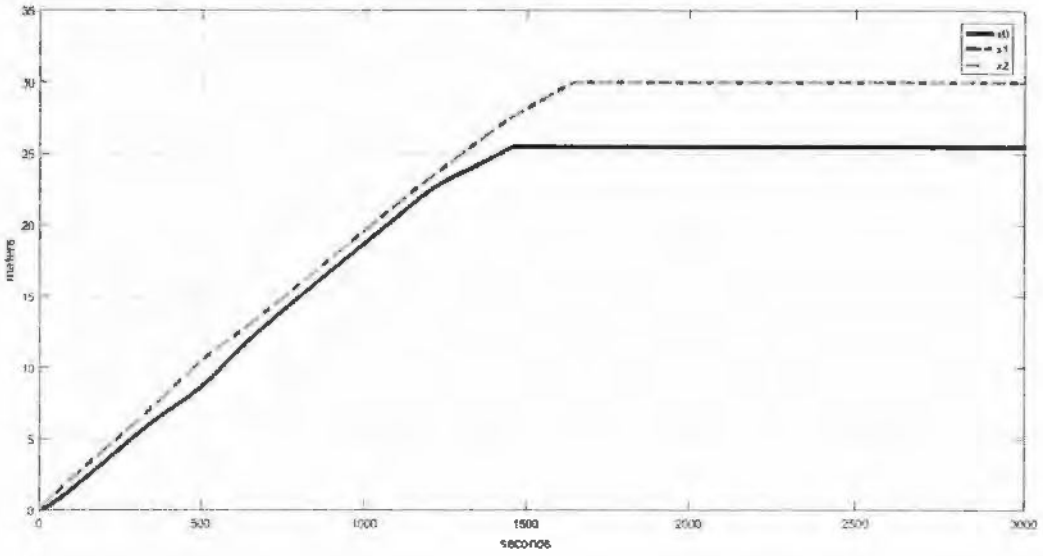

Figure 3.6. Desired water levels vs. Time. T_0 at 25m and T_1, T_2 at 30m.

3.3.1.3 Case III: ($T_0 = 20, T_1 = 25, T_2 = 30$)

The water levels of ponds 0 1 and 2 in this case are 20, 25, and 30 meters respectively. T_o reaches its desired level about 18 minutes, T_1 in 22 minutes and T_2 in 27 minutes. The system as a whole takes less than 30 minutes to reach the steady state. Where a steady state error of 0.5 meters is shown by T_o, an almost negligible steady state error is shown by T_1 and T_2. Figure 3.7 shows these results graphically.

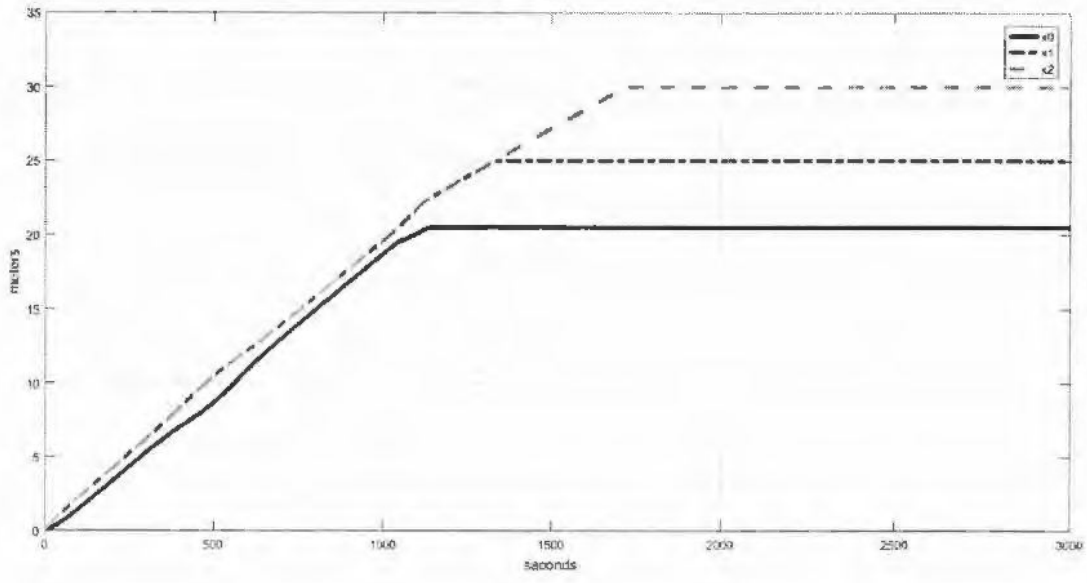

Figure 3.7. Desired Level T0 at 20m, T1 at 25m and T2 at 30m vs. Time

3.3.2 Robustness Analysis

This section provides analysis and discussion regarding the robustness of the proposed model of ROR HPP controlled with FIS. Simulations are done to check the system's response for four disturbances: white noise, sinusoidal, both positive and negative, and sudden surge. Next, these disturbances are utilized to check the response when the system has half capacity. The system's capacity may be halved by decreasing the depth of the pond or its area to half of the original. We have reduced the area instead of depth because reducing the depth/height of the pond necessitates redesigning or modifying the fuzzy inference system. The different cases are tested for the system at zero initial conditions (empty ponds) as well as initial steady-state conditions.

3.3.2.1 Case Ia: Sinusoidal Disturbance (Three pond system vs. Single pond system)

For a fair comparison between the two systems, the parameters of the three-pond system are matched with that of the traditional single-pond system. Comparison against disturbances is made because the two systems expectedly take the same time to reach desired steady states. An additive sinusoidal disturbance $d = a.sin(wt)$ with the controllable inflow of water is added to the system $U = [U_1, U_2]$. Differences in behavior begin to appear when two systems approach steady states. During transitory situations, both systems perform normally, as shown in Figure 3.8. In steady-state, the proposed three-pond system efficiently suppresses the effects of the disturbances, while the traditional single pond system does not suppress these effects so efficiently. This demonstrates the effectiveness and robustness of the FIS regulated proposed model against sinusoidal disturbances.

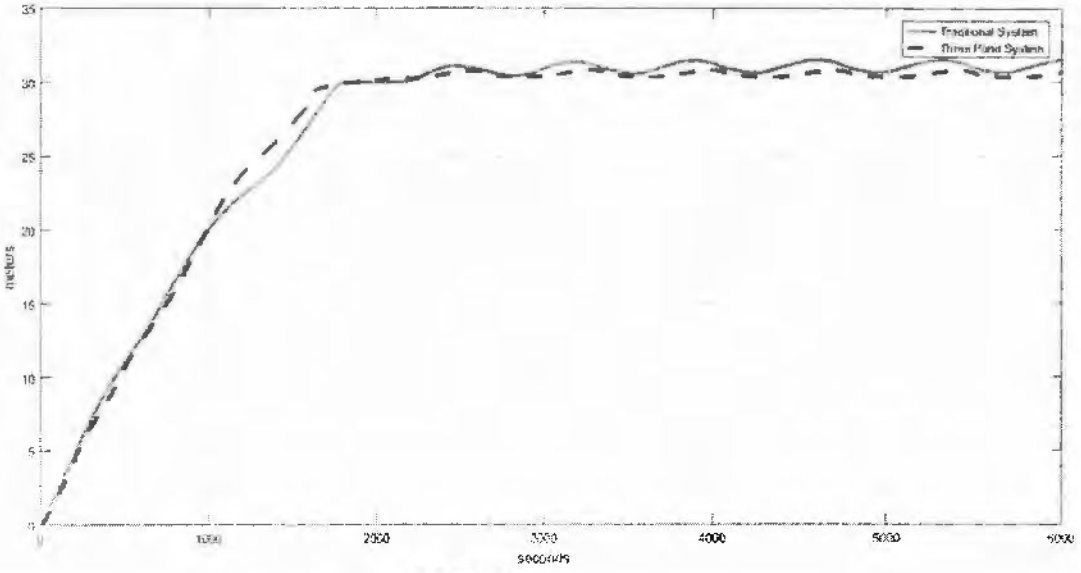

Figure 3.8. Comparison between the traditional system and the proposed system (sinusoidal disturbance)

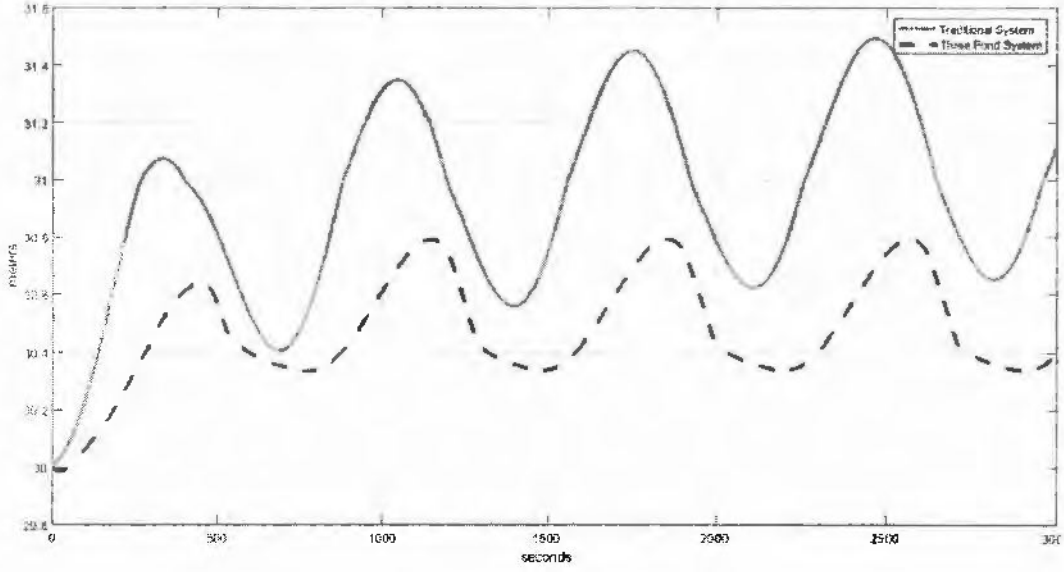

Figure 3.9. Traditional system vs Proposed systems (sinusoidal disturbance, steady state)

3.3.2.2 Case Ib: Sinusoidal Disturbance (Three pond system vs. Single pond system, Half Capacity)

The simulations described above are repeated for the half capacity case with some minor modifications. With the system capacity being half, the system rise time is faster. As in the previous case, the effects of disturbance are not so pronounced in the transient states, and difference in behavior appears only when the systems approach steady states. The responses of the two systems are shown in the figures below. As Figures 3.10 and 3.11 show, the proposed model efficiently mitigates the effects of the disturbances while they are much more pronounced for the traditional single pond system.

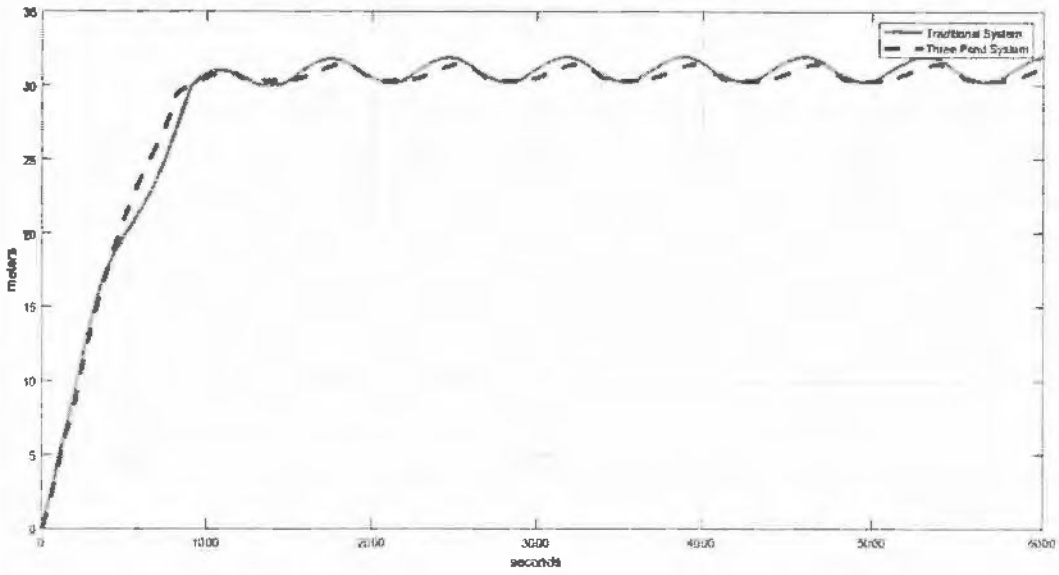

Figure 3.10.: Comparison between the proposed system (half capacity) and the traditional system (sinusoidal disturbance).

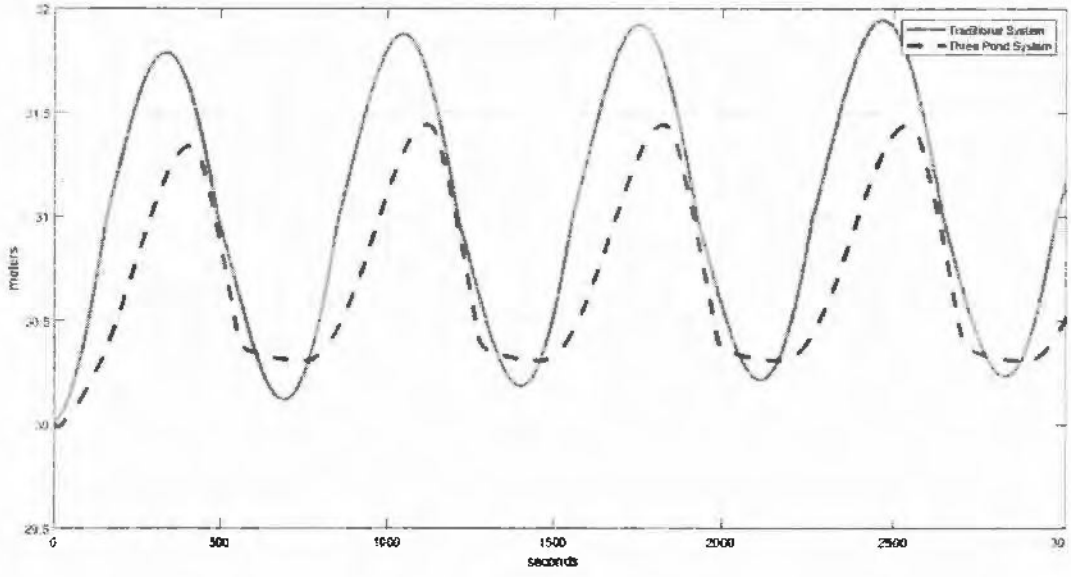

Figure 3.11. Proposed system (half capacity) vs traditional system (sinusoidal disturbance, steady state)

3.3.2.3 Case IIa: White noise disturbance (Three pond system vs Single pond system)

In the previous case, we added sinusoidal disturbances to the systems here. We add random additive white noise. Identical amounts of noise are added to two systems. In the case of three pond system, the noise is between the ponds T_1 and T_2. Contrary to the case of sinusoidal disturbances, the effects of disturbances are also visible in transient states. However, the proposed system suppresses the effects of the high-frequency components of the disturbance. Figures 3.12 and 3.13 show these results graphically.

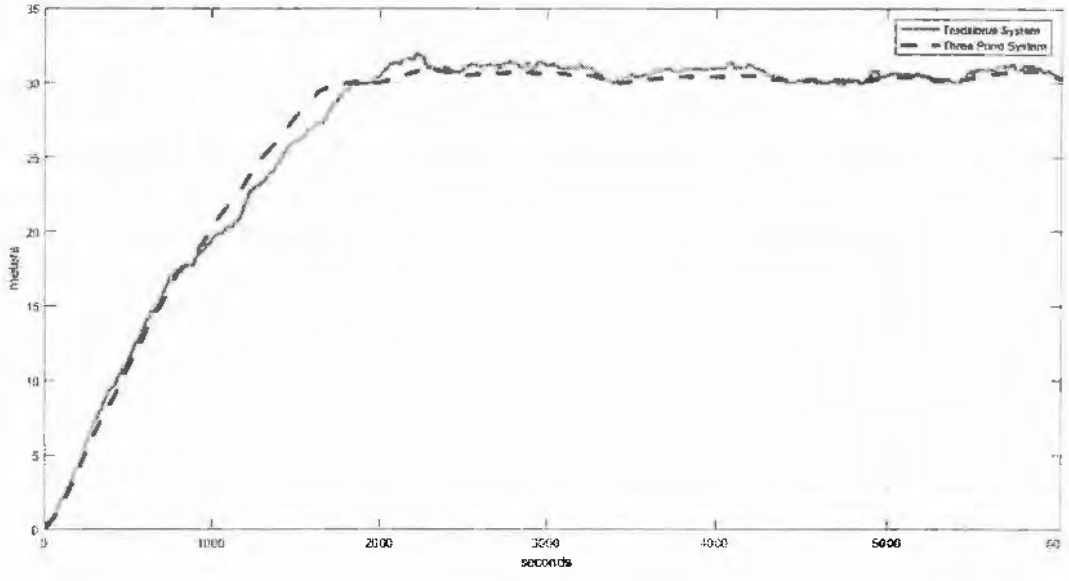

Figure 3.12. Comparison between the proposed and traditional system (white noise disturbance).

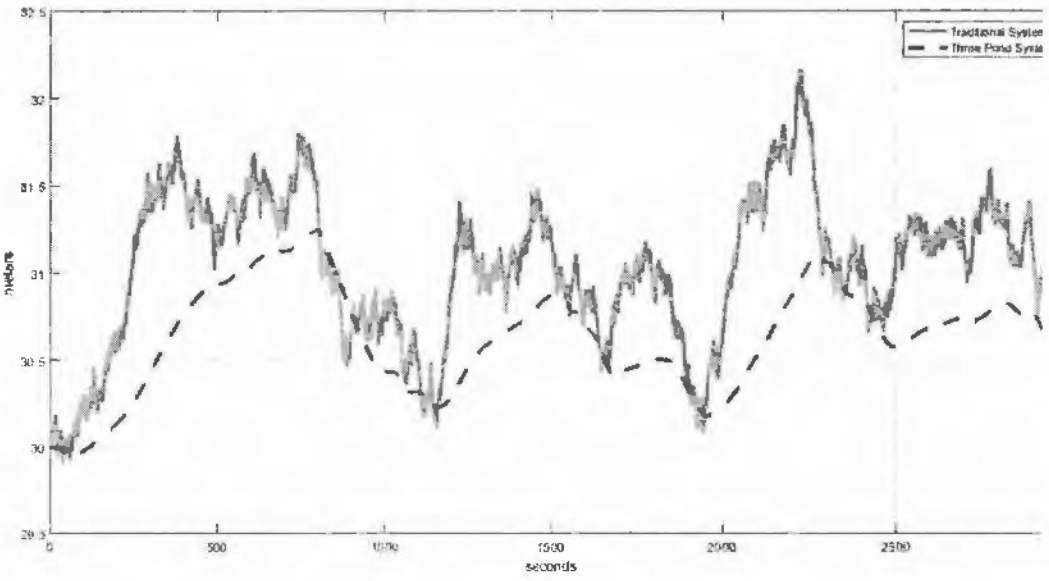

Figure 3.13 Traditional system vs the proposed system (white noise disturbance, steady state)

3.3.2.4 Case IIb : White noise disturbance(Three pond system vs. Single pond system, Half capacity case)

Here the two systems are supposed to be operating at half capacities. The effects of the disturbances are visible in the transient and steady states. However, these effects are much less in the case of the three-pond system. The high-frequency components of the disturbance are also suppressed by three pond system. The response of the two systems is graphically given in Figures 3.14 and 3.15.

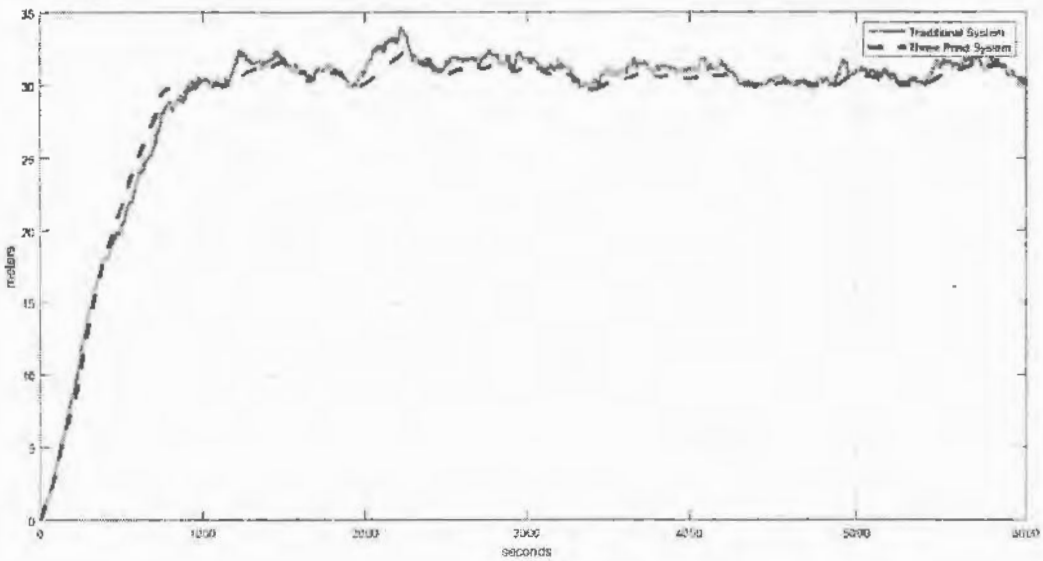

Figure 3.14. Comparison between the proposed system(half) and the traditional system (white noise disturbance).

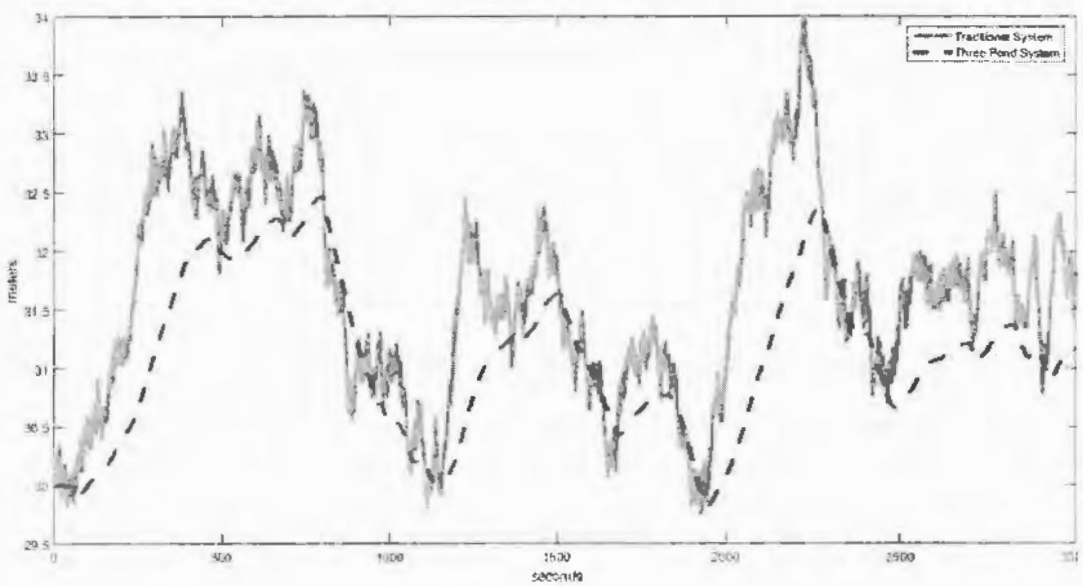

Figure 3.15 Traditional system vs the proposed system (half) (white noise disturbance, steady state)

3.3.2.5 Case IIIa Positive surge disturbance (Three pond system vs single pond system)

Equal amounts of positive surges of some predetermine durations are added to the system when they reach steady states, and their response is noted. In this case, it is observed that the proposed model suppresses the positive surge's effects efficiently. Also, the traditional system

is observed to have been overflown for some time. However, the proposed system does not overflow. Figures 3.16 and 3.17 show the behaviors of the two systems graphically.

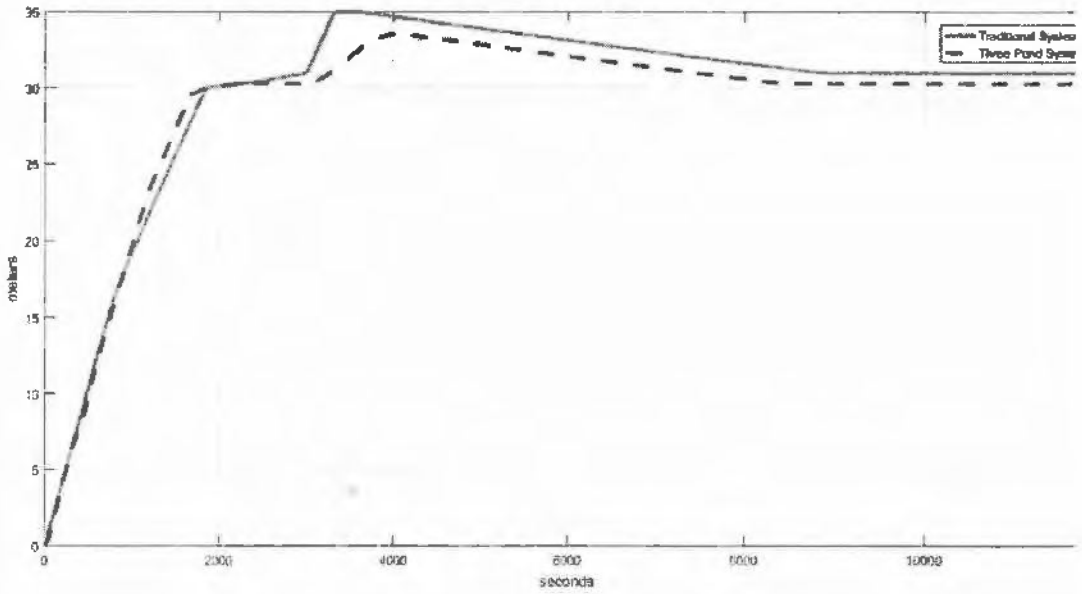

Figure 3.16. Comparison between the traditional system and the proposed system (positive surge)

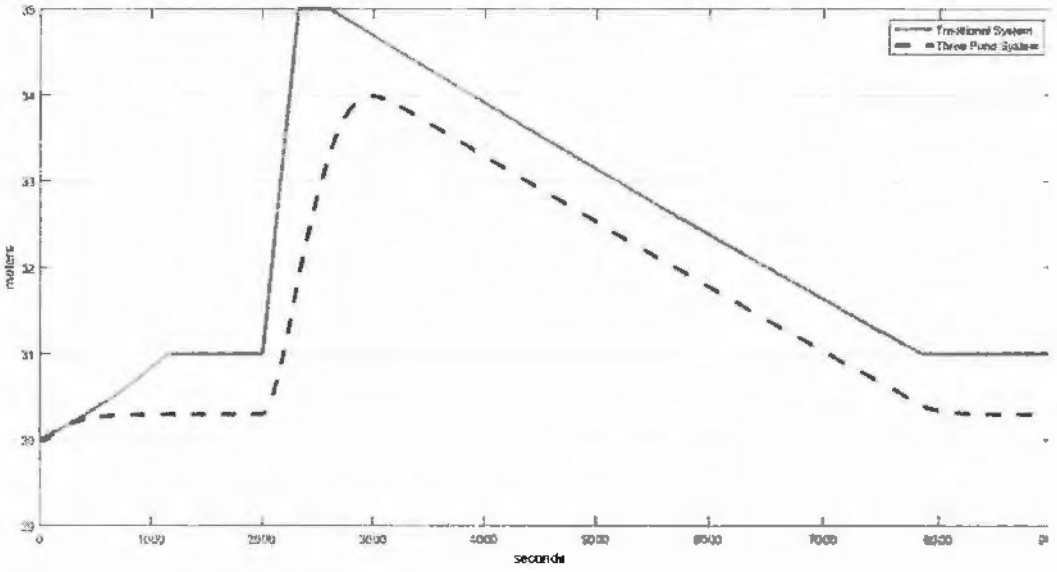

Figure 3.17. Traditional system vs the proposed system (positive surge, steady state)

3.3.2.6 Case IIIb Positive surge (Three pond system vs single pond system (Half Capacity)

The exact process as above is carried out in this instance for the half-capacity case. When the systems reach steady states, positive surges are added to them. More severity is observed in the two systems' behavior compared to the previous case when the systems were operating at full capacity. The proposed model can suppress the detrimental effects of the positive surge to some extent. The traditional system, in this case too, overflows. The overflow is more as compared to the previous case. The proposed model does not overflow. Figures 3.18 and 3.19 graphically show these results.

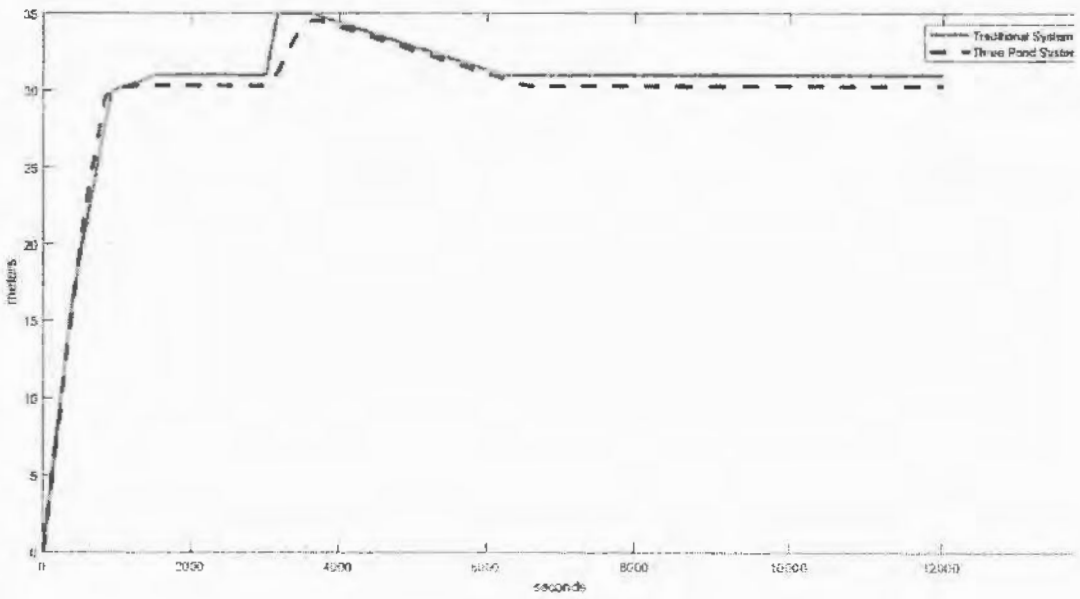

Figure 3.18. Comparison between the traditional system and the proposed system (half) (positive surge)

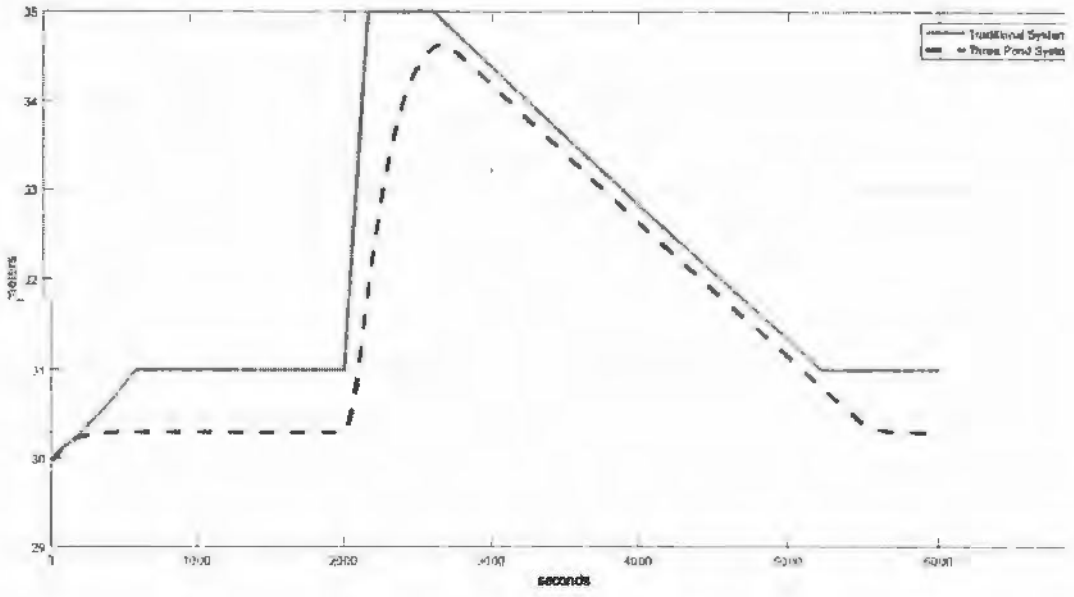

Figure 3.19. Traditional system vs the proposed system (half) (positive surge, steady state)

3.3.2.7 Case IVa Negative surge (Three pond system vs. single pond system)

This experiment is similar to the previous case, but a negative surge is provided to the system when they reach steady states instead of a positive surge. The effects of the negative surge in the proposed system are much less than that in the traditional system. The traditional system shows a sharp dip and then smoothes out. Figures 3.20 and 3.21 graphically show the behaviors of the two systems.

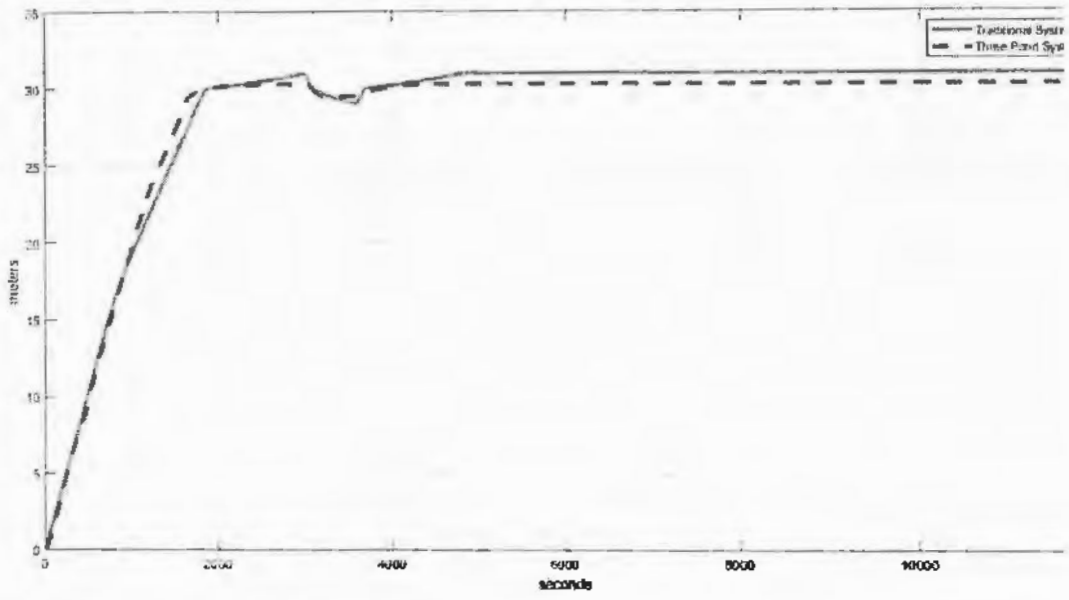

Figure 3.20. Comparison of the traditional system with the proposed system (negative surge)

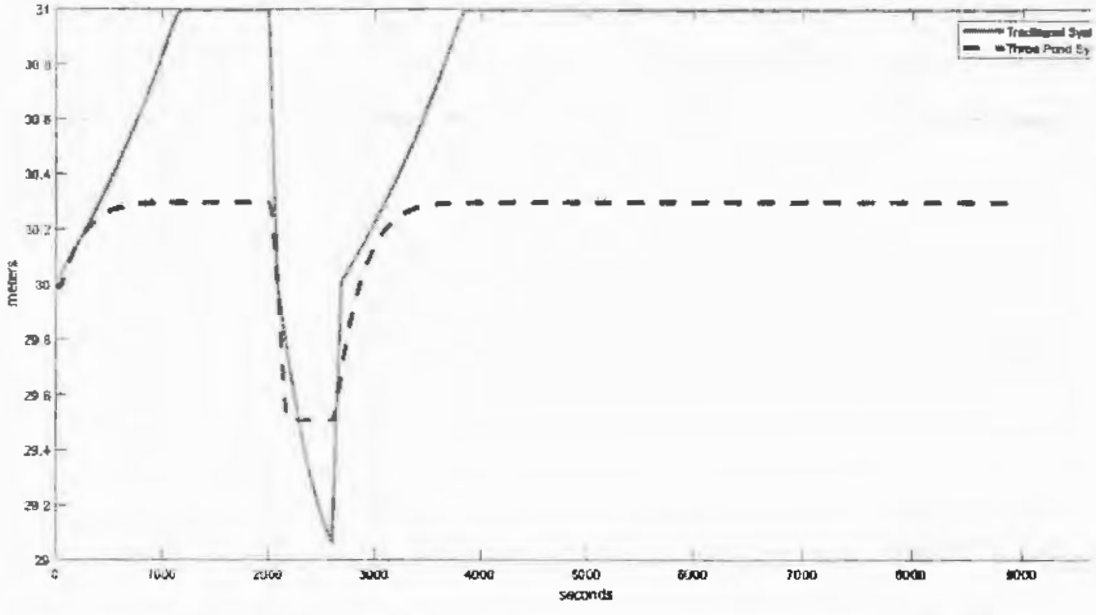

Figure 3.21. Traditional system vs proposed system (negative surge, steady state)

3.3.2.8 Case IVb Negative surge (Three pond system vs single pond system, half capacity)

This time, a negative surge is provided to the two systems operating at half capacity on reaching steady states. The effects of negative surge are observed to be same, but the severity

is more than the previous case. The system responses are graphically shown in figure 3.23 and 3.23.

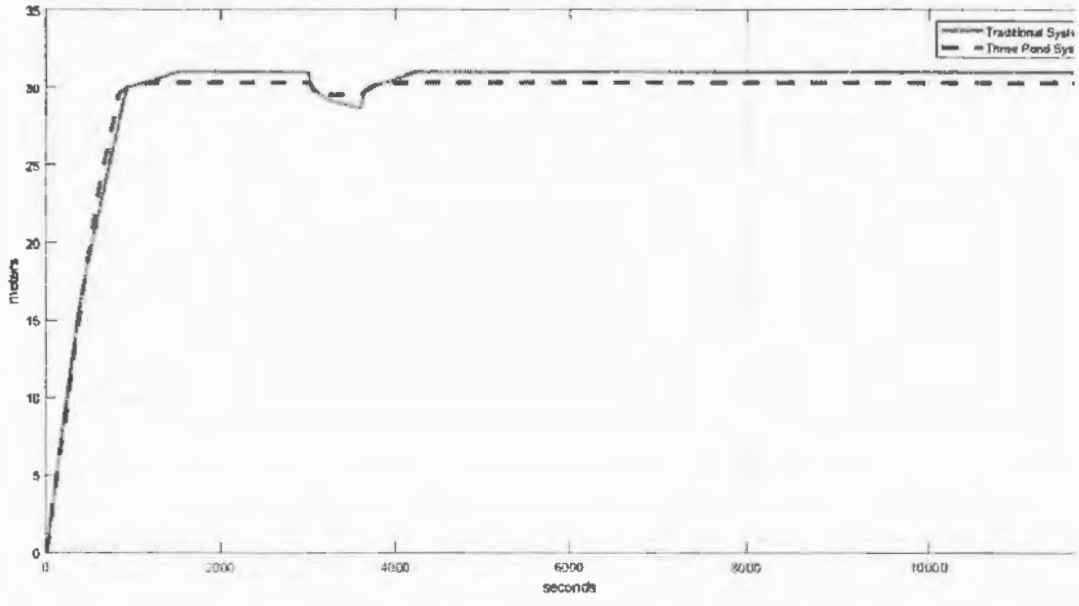

Figure 3.23. Comparison between traditional system and the proposed system (half) (negative surge)

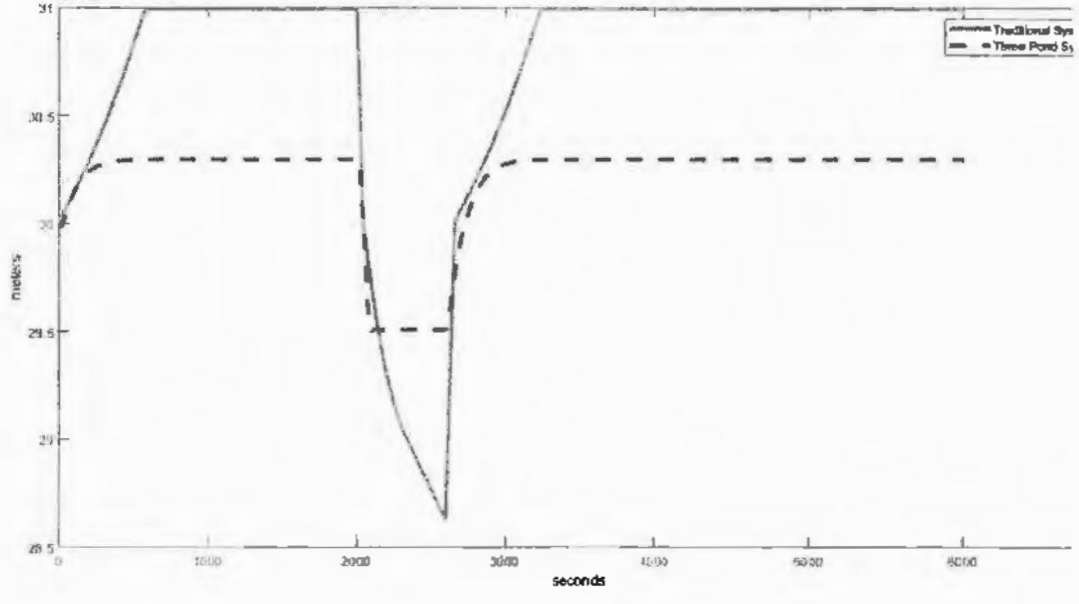

Figure 3.23. Traditional system vs Proposed system (half)(negative surge, steady state)

In this chapter, the concept of three pond model for hydropower plants is introduced and its control is developed. The system is then tested against disturbances to prove its viability over the tradition single pond model.

CHAPTER 4

POWER REGULATION AND FAULT TOLERANCE FOR THREE POND RUN OF RIVER HYDROPOWER PLANT

This chapter consists of the second publication, and the concept of three-pond model from the previous chapter is expanded and a power generation turbine is integrated to it.Next, fault tolerant control is explored for it.

4.1 System Model Modification and Turbine Coupling

We have proposed two modifications to the aforementioned three pond hydraulic system. The first is a modification to the flow of water entering ponds 1 and 2, and the second is to couple it with a turbine.

In the previous chapter, it is assumed that the inflow of river in ponds 1 and 2 are completely controllable; however, this is not practically achievable. The flow of the river can be controlled by adding a gate in its path. The river flow can have some short and long-term variations and some base flow rates. For simplicity, the river's flow is taken as a combination of the constant base and the short-term variable flow rate and is modeled by a sinusoidal function. In contrast, the long-term variation is considered constant and is included in the base flow rate. Therefore, the flow rate in cubic meter per second of the river is given by:

$$l = m + p \sin \omega t \tag{4.1}$$

where l is the total flow rate, m is the baseline constant flow rate, and $p \sin \omega t$ is the short-term variation in the flow rate. It is assumed that a controllable sluice gate w is present at the

mouth of the pond from the river. Now, U is the controllable flow rate in equations 3.3 and 3.4, and is given by:

$$U = wl \tag{4.2}$$

where w ranges from 0 to 1. Now, as a turbine with penstock is added to the hydraulic system, Equation (3.10) of the surge tank is modified. The out flow from the surge tank is changed to be a single variable instead of the expression. The outflow from the surge tank and inflow to the penstock and turbine is denoted by Q as:

$$n_a\sqrt{2gx_s} = Q \tag{4.3}$$

Now one substitutes the river and turbine flow values in the model and rewrite the equations. After substituting Equation (4.2) in Equations (3.3) and (3.4), the equations for pond 1 and 2 become:

$$\frac{d}{dt}x_1 = -\frac{n_a}{A}s_1\sqrt{2g|x_1 - x_0|}sgn(x_1 - x_0) + \frac{w_1 l_1}{A} \tag{4.4}$$

$$\frac{d}{dt}x_2 = -\frac{n_a}{A}s_2\sqrt{2g|x_2 - x_0|}sgn(x_2 - x_0) + \frac{w_2 l_2}{A} \tag{4.5}$$

Note that U_1 and U_2 are replaced by $w_1 l_1$ and $w_2 l_2$, which is the product of the river flow and the sluice gate opening into ponds 1 and 2. The equations for pond 0 and the headrace are unchanged.

$$\frac{d}{dt}x_0 = \frac{n_a}{A}\left[s_1\sqrt{2g|x_1 - x_0|}sgn(x_1 - x_0) + s_2\sqrt{2g|x_2 - x_0|}sgn(x_2 - x_0)\right] - \frac{Q_t}{A} \tag{4.6}$$

$$\frac{d}{dt}Q_t = \frac{gA_t}{L_t}(x_0 - x_s) - C_t Q_t|Q_t| \tag{4.7}$$

Finally, the equation of the surge tank is modified by plugging in Equation (4.3) in Equation (3.10) as:

$$\frac{d}{dt}x_s = \frac{Q_t}{A_s} - \frac{Q}{A_s} \tag{4.8}$$

As we are coupling the turbine with the hydraulic system here, the flow rate through the turbine is appended to the inputs of the hydraulic system as:

$$\vec{v} = [U_1 \quad U_2 \quad s_1 \quad s_2 \quad Q]^T \tag{4.9}$$

where Q is the flow through the turbine and is dictated by the equations of the turbine, while the rest of the inputs of the system are the control variables which are given as:

$$\vec{u} = [U_1 \quad U_2 \quad s_1 \quad s_2]^T \tag{4.10}$$

Note also that U_1, U_2 are given by the level controller, which was discussed in the previous section and is equated using Equation (4.2).

Comparing the above Equations (4.9) and (4.10), the input of the system is:

$$\vec{v} = [\vec{u}^T \quad Q]^T \tag{4.11}$$

The states vector $\vec{x}$ consisting of the state variables is:

$$\vec{x} = [x_1 \quad x_2 \quad x_0 \quad Q_t \quad x_s]^T \tag{4.12}$$

The output of the hydraulic system is:

$$\vec{y} = C\vec{x} \tag{4.13}$$

As the level of the surge tank is also important now, the matrix C is given by:

$$C = \begin{bmatrix} 0 & 0 & 1 & 0 & 0 \\ 1 & 0 & 0 & 0 & 0 \\ 0 & 1 & 0 & 0 & 0 \\ 0 & 0 & 0 & 0 & 1 \end{bmatrix} \tag{4.14}$$

Resultantly $\vec{y}$ becomes:

$$\vec{y} = [x_0 \quad x_1 \quad x_2 \quad x_s]^T \tag{4.15}$$

After the formulation of the hydraulic system model, the model of the turbine and penstock is needed to complete the hydropower system. In this thesis, the three-pond hydraulic system has a Francis turbine and penstock taken from [44]. The Francis turbine is described as a function of its rotational speed n and gate opening G to achieve a flow rate Q. The equation for the flow of water from the turbine is given as:

$$Q = h(G, n) \tag{4.16}$$

The characteristics of a Francis turbine are described by a set of points described by hill graphs [7]. For Hill graphs, a predetermined operating point of the turbine is set, and then the static values of G and n are used in the calculations. However, [44] describes the characteristics of the turbine in the form of a quadratic equation that is non dimensional. In addition to providing a dynamic model of the Francis turbine, this model is also completely scalable over different operating conditions and rated values. The equation for the Francis turbine from [44] is described as:

$$\frac{Q}{Q_r} = G\left[a_1 \frac{n^2}{n_r^2} + b_1 \frac{n}{n_r} + c_1\right] \tag{4.17}$$

where n_r and Q_r are the rated speed and the rated flow rate of the turbine, and the constants a_1, b_1, c_1 are the constants within the above quadratic equation, as stated by [44]. The torque generated by the turbine is given by the following equation [44]:

$$\frac{M}{M_r} = \frac{\frac{Q}{Q_r}\frac{H}{H_r}}{\frac{n}{n_r}} \tag{4.18}$$

where M and M_r are the torque and rated torque respectively. H and H_r are the height or level of water and the rated height, respectively. In the case of our system, the level or height (H) of concern is x_0 and the rated height (H_r) is the height of the pond 0 so the rated height is H_0. Now, rewriting Equation (4.18)for the generated torque of the turbine in our system, we get:

$$\frac{M}{M_r} = \frac{Q}{Q_r}\frac{x_0}{H_0}\frac{n_r}{n} \tag{4.19}$$

The power generated at the turbine is given by the product of rotational speed and torque of the turbine as in [44]:

$$P = nM \tag{4.20}$$

The total output of the system is the output of the hydraulic system and power.

$$\vec{Y} = [x_0 \quad x_1 \quad x_2 \quad x_s \quad P]^T \tag{4.21}$$

We shall be requiring the explicit values of $\vec{Y}$ in order to conveniently find the effects of the faults on the output. As the faults occur, we diagnose them by computing the values of the states by integrating the state equations rather than just taking the output value. The value of x_0 is computed by integrating Equation (4.6).

$$x_0 = \frac{n_r a}{A}\int_0^t \left[s_1\sqrt{2g|x_1 - x_0|}sgn(x_1 - x_0) + s_2\sqrt{2g|x_2 - x_0|}sgn(x_2 - x_0)\right]dt - \int_0^t \frac{Q_t}{A}dt \tag{4.22}$$

Similarly, for x_1,x_2, and x_s, Equations (4.4), (4.5), and (4.8) are integrated.

$$x_1 = -\frac{n_r a}{A}\int_0^t s_1\sqrt{2g|x_1 - x_0|}sgn(x_1 - x_0)dt + \int_0^t \frac{w_1 l_1}{A}dt \tag{4.23}$$

$$x_2 = -\frac{n_r a}{A}\int_0^t s_2\sqrt{2g|x_2 - x_0|}sgn(x_2 - x_0)dt + \int_0^t \frac{w_2 l_2}{A}dt \tag{4.24}$$

$$x_s = \int_0^t \frac{Q_t}{A_s}dt - \int_0^t \frac{Q}{A_s}dt \tag{4.25}$$

Furthermore, power is calculated by Equation (4.20), and we plug the value of the torque from Equation (4.19) into Equation (4.20) after simplifying.

$$P = \frac{Q M_r x_0 n_r}{Q_r H_0} \tag{4.26}$$

Now, plugging in the value of Q from Equation (4.17) to Equation (4.26) and simplifying.

$$P = \frac{M_r x_0 n_r}{H_0} G\left[a_1\frac{n^2}{n_r^2} + b_1\frac{n}{n_r} + c_1\right] \tag{4.27}$$

Although this step appears to be an unnecessary complication, it will help us find the residues easily in case of faults.

4.2 Control Design

The control for the system is done in a pseudo hierarchal and nested style. Three levels of control deal with level control, level reference, and gate (power) control. Now, these three controls will be discussed separately. The simplified form of the control system with the three levels of control is given in Figure 4.1.

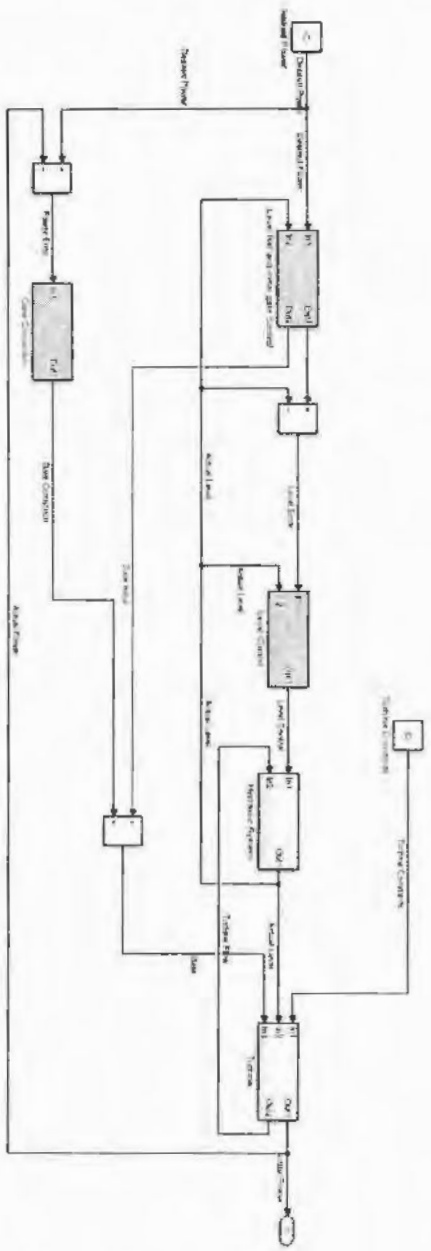

Figure 4.1. The control scheme for the system shows three different controllers (in color).

4.2.1 Level Controller

The primary level control governs the hydraulic part of the system. The primary level control is discussed in the previous chapter. Level control has the controllable variables s_1,s_2, and U_1,U_2. s_1 is the valve between pond 1 and 0 while s_2 is the valve between pond 2 and 0.

While U_1 and U_2 are the flow of river in the ponds 1 and 2 through the sluice gates. In this work's current scheme, the level control is essentially the same as in the previous chapter, with two differences. The first difference is discussed in the previous section regarding the controllable flow of river in the ponds 1 and 2. While the next change is just that the reference levels of the three ponds are set at the same level by the reference control, as opposed to the previous chapter, in which all the reference levels could be set at different levels. Combining Equations (3.3,3.4,3.7,3.9) and (3.11) of the hydraulic system gives us the nonlinear system of equations as:

$$\frac{d}{dt}\vec{x} = \vec{f}(\vec{x}, \vec{u}) \tag{4.28}$$

where the state variables are:

$$\vec{x} = [x_1 \quad x_2 \quad x_0 \quad Q_t \quad x_s]^T \tag{4.29}$$

and the control variables are:

$$\vec{u} = [U_1 \quad U_2 \quad s_1 \quad s_2]^T \tag{4.30}$$

Here, U_1, U_2 range from 0 to U_{Max} and s_1, s_2 range from 0 to 1. However, in the current system the flow U is equal to the product of the flow-rate of the river l and the opening of the sluice gate w, as shown in Equation (4.10). The controller gives U_1, U_2, the *required* flow-rate output to maintain the ponds' water levels at the desired reference level. According to Equation (4.2):

$$U_i = l_i w_i \tag{4.31}$$

where $i = 1,2$ for ponds 1 and 2. We have control input U_i and river flow rate l_i from the river. We control the sluice gate by the expression:

$$w_i = \begin{cases} \frac{U_i}{l_i} & \frac{U_i}{l_i} \leq 1 \\ 1 & \frac{U_i}{l_i} > 1 \end{cases} \tag{4.32}$$

This ensures that U_i cannot exceed l_i, the actual flow-rate in the river; the actual controlled system is slightly slower to reach its steady state as compared to the previous chapter, as it makes a more realistic approach towards the problem. The fuzzy controller used is the same as discussed in the previous chapter with the mentioned modifications in equations 4.2 and 4.3.

4.2.2 Level Reference Controller

The second controller that controls both the hydraulic system and turbine is also a fuzzy controller. The reference controller takes the input in the form of required power and the level of the pond 0. This controller requires the exact value of the required power or at least a scaled version of it. Therefore, the hydraulic system parameters are taken from the last chapter, and the parameters of the hydraulic turbine are taken arbitrarily to match the hydraulic system. After that, the total theoretical power is calculated, which comes around 2 Mega Watts of power. Next, the minimum level of the pond is also decided arbitrarily as it is very rare for the head pond of a power plant to be empty. That minimum level and minimum power are arbitrarily decided as 20 m and 800 kilo watts respectively.

The reference controller does not run the errors as opposed to the level controller but with the reference power and the feedback from the pond 0 (level). The head ponds' operating levels range from 20 m to a maximum of 35 m, and the operating power is between 800 kW and 2 MW.

The reference controller is in the form of the Takagi Sugeno Fuzzy Inference Engine instead of Mamdani Fuzzy Inference Engine for the previously discussed level controller. The Takagi Sugeno controller is different from the Mamdani controller in the form as its output is a constant or a linear combination of its inputs for each rule.

The function of the reference controller is to set a level reference for the ponds and give the initial base position to the gate of the turbine. As the power plant operates between 800 kW and 2 MW and from the 20 to 35 m pond level, the available power for the turbine is given by the following equation:

$$P = \eta \rho g H Q \tag{4.33}$$

where η is the turbine efficiency, ρ is the density of water, g is the gravitational constant, and H and Q are the level of water in pond and the flow rate through the turbine, respectively. As the efficiency of the turbine is not in our control, as the model taken from [2] assumes constant efficiency for the turbine, and the density of water and gravitational constants are fixed, the level of the water in head pond and the flow rate through the turbine can be adjusted. According to Equation (4.17), the turbine's rotational speed can also be used as a control parameter, but we kept it constant and is left for future work. The flow rate through the turbine is adjusted by adjusting the opening of the turbine wicket gate. The pond level is divided from 20 m to 35 m in increments of 1 m, and the operating power is adjusted from 800 kW to 2 MW in increments of 25 kW. The position of the turbine gate is estimated against the required power and water level while fixing the other parameters. This estimation is the basis for the rules of level reference and the initial gate position of the turbine.

The inputs of the level reference control are the required power and the level of pond 0. These inputs are assigned membership functions as follows: The pond level can vary from 20 to 35 m, so the level is assigned four membership functions. The first membership function deals with levels less than 20 m, while the rest three deal with from 20 to 35 m in increments of 5 m. The level membership functions are named as m_{20}, m_{25}, m_{30}, and m_{35}, respectively. All four level membership functions are trapezoidal, with the first membership function being non symmetric to describe all the levels less than 20 m. The required power level

$(REQP)$ is divided into increments of 25 kW between 800 kW and 1.95 MW. That means that 45+2 membership functions describe the required power. The 45 membership functions are between 800 kW and 1.95 MW, while the other two represent power levels less than 800 kW and greater than 1.95 MW. The inner 45 membership functions are triangular, while the boundary membership functions are trapezoidal. Therefore, the total number of rules for the level reference controller is 4 × 47 or 188. The controller requires the current level of the head pond to give the level reference; for when the required power level is reduced, and the current level of the pond is higher than the theoretical level, to stop the controller from quickly reducing the level of the pond. The other aspect to know about the current level is to set the initial position of the turbine gate according to the current level rather than the desired level. An example of a rule is given below:

$$IF\ REQP\ is\ 165P\ and\ LEVEL\ is\ m_{25}\ \ THEN\ LEVREF\ is\ 30\ and\ G_{Fuzzy}\ is\ 0.92 \tag{4.34}$$

All of the 188 rules for the level reference controller have a generalized form:

$$u(t) = \frac{\sum_{j=1}^{188} \bar{u}_j \left(\prod_i^2 \mu_{A_i^j}(k_i) \right)}{\sum_{j=1}^{188} \left(\prod_i^2 \mu_{A_i^j}(k_i) \right)} \tag{4.35}$$

where $u(t)$ is the output of the controller for $LEVREF$ or G_{Fuzzy}, k_i is the input value of $REQP$ and $LEVE$. The linguistic variable for the input, which has been described above is, A; μ_A is the membership function of A; and $\bar{u}_j$ is the firing strength of the j^{th} fuzzy rule.

4.2.3 Turbine Gate Correction Control

The turbine gate correction control is the final fine adjustment control for the turbine gate. The level reference control discussed earlier gives the required level to the level control and gives the turbine gate's initial gate position. The final adjustment to the turbine gate is made using a traditional PID controller. The output of the PID controller is

added to the previously assigned initial position of the gate by the level reference controller. Therefore, the final value of the turbine gate becomes:

$$G_{FINAL} = G_{Fuzzy} + G_{PID} \tag{4.36}$$

The PID control is a traditional control scheme that is driven by the error between the required power and generated power, and the output of the controller is given by:

$$G_{PID} = K_P e(t) + K_I \int_0^t e(t)dt + K_D \frac{d}{dt} e(t) \tag{4.37}$$

where $e(t)$ is the power error, and K_P, K_P, and K_P are the proportional, integral, and derivative constants of the PID controller respectively.

By the interaction of these three controllers, the required levels of the ponds are maintained, and the generated power comes within a hundred watts of the required power .

4.3. Fault Model

A few commonly occurring faults were modeled and added to the system to make fault diagnostics and fault-tolerant control. These faults were added to the system model, detected, and identified by the fault diagnostic module, and then suggested fault-tolerant control action was taken. In this thesis, only saturation and leakage faults are considered.

The saturation and leakage faults most commonly occur within the valves and gates due to age, obstruction, or a weakened or faulty actuator. Saturation fault occurs when the actuator cannot fully open the valve or gate; this reduces flow amplified by propagating through the system and affects the output by making it sluggish or lower than the desired value. Similarly, a leakage fault is the same as but opposite to a saturation fault. During a leakage fault, the gate or valve cannot close or shut completely, resulting in a constant leakage,

having the output creeping higher than the desired value, or having a sluggish response when braking or lowering the desired states of the system. During the normal mode of operation (i.e., from zero or lower initial conditions to higher desired states), the effects of saturation fault appear during the transient state but are not present during the steady state. In comparison, the case is vice-versa for leakage faults where their effects appear in the steady state but are invisible in the transient state. Although this rule is not strictly followed, and it will he seen later when these faults are added to the system. As a general rule of thumb, the faults that appear in the steady state are more severe than those whose effects only appear during the transient state.

From a purely fault-tolerant point of view, thc faults whose effects are only present during the transient state may not strictly require corrective action. As in this case, the system is merely somewhat slower than a normal system unless it is so slow that it becomes undesirable. In comparison, a fault whose effect is evident in the steady state has to be dealt with using corrective action to keep the undesirahle effects of the faults to a minimum. However, detecting, identifying, and isolating hoth kinds of faults are very important for early warning and avoiding the system from failing.

If we consider a single equation for a generalized linear system, then.

$$\dot{x} = Ax + Bu \tag{4.38}$$

where A is the state gain matrix and B is the input gain matrix. In case of the occurrence of a fault, the equation is modified as follows:

$$\dot{x} = Ax + Bu + Ef \tag{4.39}$$

where E is the fault gain and f is the fault. In case of a nonlinear system with a nonlinear fault, the system becomes:

$$\dot{x} = g(x, u, f) \tag{4.40}$$

Now let us consider our system equations and see how they are affected by the faults. The types of faults being considered are saturation, leakage, and a combination of the two. The components affected by these faults are the sluice gates w_1 and w_2, which allow the river's flow in ponds 1 and 2, the controllable valves s_1 and s_2 between the ponds T_1, T_0 and T_1, T_0, and finally, the wicket gate$G$of the Francis turbine. Sometimes the nonlinear fault can be separated as an additive or a multiplicative function, which is sometimes not easily possible. First, let us describe the faults mathematically before finding their effect on the components. The saturation fault, nonlinear in nature, is described as:

$$f^1(z) = \begin{cases} z & z < Sat \\ Sat & z \geq Sat \end{cases} \tag{4.41}$$

where z is an arbitrary faulty component, and Sat is the constant saturation limit of the effect of the fault. However, plugging this value of fault into the system is not feasible. Therefore, we transform this nonlinear fault as an additive fault to the system. The additive effect may be time varying or nonlinear, as is needed by the system. The fault f^1 is described in its additive form as:

$$f^1(z) = \begin{cases} z & z < Sat \\ z + f_z^1 & z \geq Sat \end{cases} \tag{4.42}$$

In the term f_z^1, z is the faulty component and f_z^1 is the time varying term that satisfies the equation below

$$z + f_z^1 = Sat \tag{4.43}$$

Similarly, the leakage fault is defined as:

$$f^2(z) = \begin{cases} Leak & z < Leak \\ z & z \geq Leak \end{cases} \tag{4.44}$$

Here, $Leak$ is the constant leakage effect of the fault. Now, one can describe the leakage fault in additive form as:

$$f^2(z) = \begin{cases} z + f_z^2 & z < Leak \\ z & z \geq Leak \end{cases} \tag{4.45}$$

The time-varying term f_z^2 satisfies the following equation:

$$z + f_z^2 = Leak \tag{4.46}$$

Similarly, when these two types of faults occur at the same time, it is defined as f^3, which is defined as:

$$f^3(z) = \begin{cases} Sat & z > Sat \\ z & Leak \leq z \leq Sat \\ Leak & z < Leak \end{cases} \tag{4.47}$$

To describe the f^3 type of fault, f_z^3 is not needed, as shown in the additive form of the fault below:

$$f^3(z) = \begin{cases} z + f_z^1 & z > Sat \\ z & Leak \leq z \leq Sat \\ z + f_z^2 & z < Leak \end{cases} \tag{4.48}$$

The above equations from Equation (4.41) to Equation (4.48) shall be referred to multiple times to define f_z^i, where the faulty component is z and $i = 1,2$, depending on whether the component is in saturation or leakage fault. This will be used extensively to convert the fault equations into additive forms.

Now let us look at how these faults affect the components of the system. In the thesis, we shall be discussing only the actuator faults. The sensor faults are left for future work. We shall examine the sluice gate, pond valve, and turbine wicket gate fault one by one. There are two sluice gates and pond valves; only one of each will be examined to avoid redundancy.

4.3.1 Sluice Gate Faults

The sluice gates are on the opening of the river to the ponds T_1 and T_2. Although, the level controller assumes that the flow of the river into the ponds is controllable explicitly, the sluice gates w_1 and w_2 control the inflow by monitoring the river flow using Equation (4.31). The equation for pond 1 T_1, Equation (4.4), is rewritten adding the effect of fault f^1 below.

$$\frac{d}{dt}x_1 = -\frac{n_v a}{A}s_1\sqrt{2g|x_1 - x_0|}sgn(x_1 - x_0) + \frac{f^1(w_1)l_1}{A} \tag{4.49}$$

According to Equation (4.41), the effect of the sluice gate fault in the saturation region can be written as a sum with the $f_{w_1}^1$ term. When the effect of the f^1 fault appears for the sluice gate, Equation (4.42) is written as:

$$\frac{d}{dt}x_1 = -\frac{n_v a}{A}s_1\sqrt{2g|x_1 - x_0|}sgn(x_1 - x_0) + \frac{w_1 l_1}{A} + \frac{f_{w_1}^1 l_1}{A} \tag{4.50}$$

Note that the value of $f_{w_1}^1$ is negative in the above case. To find the fault's total effect, we integrate the above Equation (4.50).

$$x_1 = -\frac{n_v a}{A}\int_0^t s_1\sqrt{2g|x_1 - x_0|}sgn(x_1 - x_0)dt + \int_0^t \frac{w_1 l_1}{A}dt + \int_0^t \frac{f_{w_1}^1 l_1}{A}dt \tag{4.51}$$

Similarly, for the case of a leakage fault, the equation becomes:

$$\frac{d}{dt}x_1 = -\frac{n_v a}{A}s_1\sqrt{2g|x_1 - x_0|}sgn(x_1 - x_0) + \frac{f^2(w_1)l_1}{A} \tag{4.52}$$

Going through similar steps and defining $f_{w_1}^2$ the fault f^2 is converted to an additive form and the effect of the fault in leakage mode is written as:

$$\frac{d}{dt}x_1 = -\frac{n_v a}{A}s_1\sqrt{2g|x_1 - x_0|}sgn(x_1 - x_0) + \frac{w_1 l_1}{A} + \frac{f_{w_1}^2 l_1}{A} \tag{4.53}$$

The total effect of the fault is given hy integrating the above Equation (4.53) as before.

$$x_1 = -\frac{n_v a}{A}\int_0^t s_1\sqrt{2g|x_1 - x_0|}sgn(x_1 - x_0)dt + \int_0^t \frac{w_1 l_1}{A}dt + \int_0^t \frac{f_{w_1}^2 l_1}{A}dt \tag{4.54}$$

Using the similar reasoning the effect of third type of fault appears in the equation as:

$$\frac{d}{dt}x_1 = -\frac{n_v a}{A}s_1\sqrt{2g|x_1 - x_0|}sgn(x_1 - x_0) + \frac{f^3(w_1)l_1}{A} \tag{4.55}$$

Since the f^3 fault is a combination of the saturation and leakage faults, the additive form of the fault f^3 on the sluice gate w_1 is described by Equations (4.50) and (4.53), depending on whether the fault is in the saturation or leakage region. The fault model for w_2 is the same as above and discussing it will be redundant.

4.3.2 Pond Valve Faults

In the case of a fault in the valve s_1, its effect appears in two equations. The equations are of pond 1 and pond 0. The equation for pond 1, Equation (4.4), with the occurrence of fault f^1, is modified as follows:

$$\frac{d}{dt}x_1 = -\frac{n_o a}{A} f^1(s_1)\sqrt{2g|x_1 - x_0|}sgn(x_1 - x_0) + \frac{w_1 l_1}{A} \tag{4.56}$$

Similarly, the equation for the head pond 0 equation (4.6) is modified as follows:

$$\frac{d}{dt}x_0 = \frac{n_o a}{A}\left[f^1(s_1)\sqrt{2g|x_1 - x_0|}sgn(x_1 - x_0) + s_2\sqrt{2g|x_2 - x_0|}sgn(x_2 - x_0)\right] - \frac{Q_t}{A} \tag{4.57}$$

Rewriting the faults in additive form according to Equation (4.42) and defining $f^1_{s_1}$, the equation for pond 1 in the saturation fault region is:

$$\frac{d}{dt}x_1 = -\frac{n_o a}{A}s_1\sqrt{2g|x_1 - x_0|}sgn(x_1 - x_0) - \frac{n_o a}{A}f^1_{s_1}\sqrt{2g|x_1 - x_0|}sgn(x_1 - x_0) + \frac{w_1 l_1}{A} \tag{4.58}$$

Likewise, the equation for pond 0 during the saturation region of the fault is:

$$\begin{aligned}\frac{d}{dt}x_0 = \frac{n_o a}{A}\Big[&s_1\sqrt{2g|x_1 - x_0|}sgn(x_1 - x_0) + f^1_{s_1}\sqrt{2g|x_1 - x_0|}sgn(x_1 - x_0) \\ &+ s_2\sqrt{2g|x_2 - x_0|}sgn(x_2 - x_0)\Big] - \frac{Q_t}{A}\end{aligned} \tag{4.59}$$

The total effect of the fault on pond 1 is given by integrating Equation (4.58).

$$\begin{aligned}x_1 = -\frac{n_o a}{A}\int_0^t s_1\sqrt{2g|x_1 - x_0|}sgn(x_1 - x_0)dt - \frac{n_o a}{A}\int_0^t f^1_{s_1}\sqrt{2g|x_1 - x_0|}sgn(x_1 - x_0)dt \\ + \int_0^t \frac{w_1 l_1}{A}dt\end{aligned} \tag{4.60}$$

Similarly, the total effect of fault on pond 0 is given by integrating Equation (4.59).

$$\begin{aligned}x_0 = \frac{n_o a}{A}\int_0^t \Big[&s_1\sqrt{2g|x_1 - x_0|}sgn(x_1 - x_0) + f^1_{s_1}\sqrt{2g|x_1 - x_0|}sgn(x_1 - x_0) \\ &+ s_2\sqrt{2g|x_2 - x_0|}sgn(x_2 - x_0)\Big]dt - \int_0^t \frac{Q_t}{A}dt\end{aligned} \tag{4.61}$$

We shall be delving more deeply into the effects of the saturation fault of the pond valve in the Appendix A. Using similar reasoning as above, the occurrence of fault f^2 on the valve s_1 modifies the equation of the pond 1 Equation (4.4) as follows:

$$\frac{d}{dt}x_1 = -\frac{n_a}{A}f^2(s_1)\sqrt{2g|x_1 - x_0|}sgn(x_1 - x_0) + \frac{w_1 l_1}{A} \tag{4.62}$$

Similarly, the equation of the pond 0 (4.6) with the occurrence of fault is:

$$\frac{d}{dt}x_0 = \frac{n_a}{A}\left[f^2(s_1)\sqrt{2g|x_1 - x_0|}sgn(x_1 - x_0) + s_2\sqrt{2g|x_2 - x_0|}sgn(x_2 - x_0)\right] - \frac{Q_t}{A} \tag{4.63}$$

Now, defining $f_{s_1}^2$ and rewriting the fault equations for pond 1 and pond 0, the equation for pond 1 during the effects of leakage fault is given as:

$$\frac{d}{dt}x_1 = -\frac{n_a}{A}s_1\sqrt{2g|x_1 - x_0|}sgn(x_1 - x_0) - \frac{n_a}{A}f_{s_1}^2\sqrt{2g|x_1 - x_0|}sgn(x_1 - x_0) + \frac{w_1 l_1}{A} \tag{4.64}$$

Similarly, the equation for pond 0 during the effects of leakage fault is:

$$\begin{aligned}\frac{d}{dt}x_0 = \frac{n_a}{A}\Big[&s_1\sqrt{2g|x_1 - x_0|}sgn(x_1 - x_0) + f_{s_1}^2\sqrt{2g|x_1 - x_0|}sgn(x_1 - x_0) \\ &+ s_2\sqrt{2g|x_2 - x_0|}sgn(x_2 - x_0)\Big] - \frac{Q_t}{A}\end{aligned} \tag{4.65}$$

The total effect of the fault on pond 1 is given by integrating Equation (4.64).

$$\begin{aligned}x_1 = -\frac{n_a}{A}\int_0^t s_1\sqrt{2g|x_1 - x_0|}sgn(x_1 - x_0)dt - \frac{n_a}{A}\int_0^t f_{s_1}^2\sqrt{2g|x_1 - x_0|}sgn(x_1 - x_0)dt \\ + \int_0^t \frac{w_1 l_1}{A}dt\end{aligned} \tag{4.66}$$

Similarly, the total effect of fault on pond 0 is given by integrating Equation (4.65).

$$\begin{aligned}x_0 = \frac{n_a}{A}\int_0^t \Big[&s_1\sqrt{2g|x_1 - x_0|}sgn(x_1 - x_0) + f_{s_1}^2\sqrt{2g|x_1 - x_0|}sgn(x_1 - x_0) \\ &+ s_2\sqrt{2g|x_2 - x_0|}sgn(x_2 - x_0)\Big]dt - \int_0^t \frac{Q_t}{A}dt\end{aligned} \tag{4.67}$$

Now when describing the fault combination f^3, which is actually a combination of the first two faults, the equation for pond 1 is:

$$\frac{d}{dt}x_1 = -\frac{n_r a}{A} f^3(s_1)\sqrt{2g|x_1 - x_0|}sgn(x_1 - x_0) + \frac{w_1 l_1}{A} \tag{4.68}$$

and the fault equation for pond 0 is:

$$\frac{d}{dt}x_0 = \frac{n_r a}{A}\left[f^3(s_1)\sqrt{2g|x_1 - x_0|}sgn(x_1 - x_0) + s_2\sqrt{2g|x_2 - x_0|}sgn(x_2 - x_0)\right] - \frac{Q_t}{A} \tag{4.69}$$

As the fault f^3 of the valve s_1 behaves like f^1 or f^2 depending on whether the fault is in the saturation or leakage region, the effects of f^3 are described by equations (4.59), (4.60), (4.66) and (4.67), respectively.

4.3.3 Turbine Wicket Gate Faults

Now let, us look at the fault model for the turbine wicket gate. In the case of the occurrence of fault f^1 in the turbine wicket gate, the effect appears in the turbine Equation (4.17) as:

$$\frac{Q}{Q_r} = f^1(G)\left[a_1\frac{n^2}{n_r^2} + b_1\frac{n}{n_r} + c_1\right] \tag{4.70}$$

Now, if we convert the fault to the additive form using Equation (4.42) and define f_G^1, the effect of the saturation fault for the turbine in the saturation region is given by the following equation:

$$\frac{Q}{Q_r} = G\left[a_1\frac{n^2}{n_r^2} + b_1\frac{n}{n_r} + c_1\right] + f_G^1\left[a_1\frac{n^2}{n_r^2} + b_1\frac{n}{n_r} + c_1\right] \tag{4.71}$$

We find the effect of turbine wicket gate fault on power by plugging in Equation (4.71) to Equation (4.27), so the faulty power becomes:

$$P = \frac{M_r x_0 n_r}{H_0} G\left[a_1\frac{n^2}{n_r^2} + b_1\frac{n}{n_r} + c_1\right] + \frac{M_r x_0 n_r}{H_0} f_G^1\left[a_1\frac{n^2}{n_r^2} + b_1\frac{n}{n_r} + c_1\right] \tag{4.72}$$

In the case of leakage fault f^2 of the turbine gate, the equation of the turbine is:

$$\frac{Q}{Q_r} = f^2(G)\left[a_1\frac{n^2}{n_r^2} + b_1\frac{n}{n_r} + c_1\right] \tag{4.73}$$

The effect of the leakage fault is written by converting the above Equation (4.73) to the additive form by defining f_G^2 using Equation (4.45). The additive form of the turbine wicket gate leakage fault in the faulty region is given by:

$$\frac{Q}{Q_r} = G\left[a_1\frac{n^2}{n_r^2} + b_1\frac{n}{n_r} + c_1\right] + f_G^2\left[a_1\frac{n^2}{n_r^2} + b_1\frac{n}{n_r} + c_1\right] \tag{4.74}$$

Similarly, the effect of the fault on power is given by:

$$P = \frac{M_r x_0 n_r}{H_0} G\left[a_1\frac{n^2}{n_r^2} + b_1\frac{n}{n_r} + c_1\right] + \frac{M_r x_0 n_r}{H_0} f_G^2\left[a_1\frac{n^2}{n_r^2} + b_1\frac{n}{n_r} + c_1\right] \tag{4.75}$$

Similarly, the case of the f^3 fault of the turbine wicket gate is given by:

$$\frac{Q}{Q_r} = f^3(G)\left[a_1\frac{n^2}{n_r^2} + b_1\frac{n}{n_r} + c_1\right] \tag{4.76}$$

As it was done in earlier cases, the additive form of the turbine gate fault f^3 is given as Equation (4.71) or (4.74) for flow through the turbine. Similarly, Equation (4.72) or (4.75) gives the effect of the faultf^3on power. These all depend on whether the turbine gate is in saturation or leakage fault mode. With the effects of the faults modeled, we shall find the effects of the faults on the residue in the next section.

4.4. Fault Diagnostics and Tolerance

The faults considered in this work are modeled in the previous section. Now there is the case of detection, identifying, and finally proposing a control action to mitigate the effect of the faults. In this thesis, fault diagnostics are done in three modes: residue generation, fault identification, and fault tolerance. The first step is residue generation and saving the said residue in a memory unit. The fault type is identified in the second diagnostic step and a relevant fault code is generated for the fault-tolerant control. In the last step, the fault tolerant

control reads the fault code and gives the corresponding corrective action to make the system fault tolerant.

A model-based fault diagnostic approach is used to detect and identify the faults and then suitable corrective action is taken to make the system fault tolerant. The first step in this direction is to generate residue for the faults.

4.4.1 Residue Generation

In the model-based fault-tolerant control, the residue is generated by the difference between the system's actual output and the output of the system model. As the system and its model are theoretically the same, the residues should be zero or near to it. However, there is almost always some disturbance or model uncertainties present in the residue. This makes the residue nonzero, but it is near to zero if there is minimum model mismatch and disturbance. Equations (4.77) and (4.78) give the generalized system with faults:

$$\dot{x} = Ax + Bu + Ed + Ff \tag{4.77}$$

$$y = Cx + Du + Hd + Jf \tag{4.78}$$

where E and F are the disturbance and fault distribution matrices for the state of the system, H and J are the output disturbance and fault distribution matrices, while d and f are the disturbance and fault, respectively. The system model is described by the equations:

$$\dot{x} = A_m x + B_m u \tag{4.79}$$

$$y = C_m x + D_m u \tag{4.80}$$

The residue of the system is given as the difference between Equations (4.78) and (4.80).

$$r = Cx + Du + Hd + Jf - C_m x - D_m u \tag{4.81}$$

In the absence of the model mismatch or uncertainty, the residue will only contain faults and disturbances; therefore,

$$r = Hd + Jf \tag{4.82}$$

This residue is processed to identify and isolate the faults for fault diagnostics and tolerance. In our system, which consists of the hydraulic system and the turbine, the outputs are Equation (4.15) and Power. The combined output of the system is given by:

$$\vec{Y} = [x_0 \quad x_1 \quad x_2 \quad x_s \quad P]^T \tag{4.83}$$

In the current case the residue is given by:

$$\vec{r} = \vec{Y} - \vec{Y}_{Faulty} \tag{4.84}$$

Now the residue in the case of the occurrence of the faults will be examined for each fault. The explicit effects of the faults on the states are given in the previous section. Although the effects of the faults tend to propagate through the system, due to the layered structure of the control, the effects of the faults are compensated for at the next level. Even with that, the faults can affect the system, thus requiring some kind of fault identification and tolerance. The implicit effects of the faults on the system are not mathematically discussed, but they are graphically shown in the residue graphs in the results section.

4.4.1.1 Residue Generation of Sluice Gate Faults

In the case of the saturation fault f^1 at the sluice gatew_1, directly affected is pond 1 T_1. The residue for this fault is given as the difference between Equations (4.23) and (4.51).

$$r_1^{f^1(w_1)} = \int_0^t \frac{f_{w_1}^1 l_1}{A} dt \tag{4.85}$$

Here, $r_1^{f^1(w_1)}$ is the residue of pond 1 with the occurrence of fault f^1 at sluice gate w_1. Although the rest of the residues may or may not be non zero due to the implicit effects of the saturation fault, these effects are shown graphically rather than mathematically. The total residue is given as:

$$\overrightarrow{r^{f^1(w_1)}} = \begin{bmatrix} r_0^{f^1(w_1)} \\ \int_0^t \frac{f_{w_1}^1 l_1}{A} dt \\ r_2^{f^1(w_1)} \\ r_s^{f^1(w_1)} \\ r_p^{f^1(w_1)} \end{bmatrix} \tag{4.86}$$

As this residue is due to the saturation fault of w_1, this residue will only be nonzero when the sluice gate w_1 is in the saturation region; this happens when the current levels of the ponds are less than the required level, and the sluice gate needs to open fully to allow the levels of the ponds to rise to the required level quickly. However, in the presence of the saturation fault in the sluice gate, the gate is not opened fully, thus restricting the water flow to the pond (pond 1 in this case). Due to this, the pond's level is less than the faultless state. Due to this pond level difference, the effect of the fault appears in the head pond 0 and is thus transmitted to power because at this level the turbine gate is also at its maximum opening, such as during normal operation, but the head pond level is lower; thus, there exists a power residue. However, once the required level is achieved, the sluice gate is no longer in saturation; thus, all residues drop to zero in steady-state mode.

In the case of the leakage fault f^2 at the sluice gatew_1, directly affected is pond 1. The residue for this fault is given as the difference between Equations (4.23) and (4.54).

$$r_1^{f^2(w_1)} = \int_0^t \frac{f_{w_1}^2 l_1}{A} dt \tag{4.87}$$

Here, $r_1^{f^2(w_1)}$ is the residue of pond 1 with the occurrence of fault f^2 at the sluice gate w_1. The rest of the residues will also be non zero due to the implicit effects of the saturation fault; these effects are shown graphically rather than mathematically. The total residue is given as:

$$\overrightarrow{r^{f^2(w_1)}} = \begin{bmatrix} r_0^{f^2(w_1)} \\ \int_0^t \frac{f_{w_1}^2 l_1}{A} dt \\ r_2^{f^2(w_1)} \\ r_s^{f^2(w_1)} \\ r_p^{f^2(w_1)} \end{bmatrix} \tag{4.88}$$

Unlike the saturation fault, the effects of the leakage fault are not present when the current levels of the ponds are below the required level as the sluice gate is in normal operating mode. However, once the system is in steady-state mode, the sluice gate enters the leakage mode, and the effects of the fault appear in the residue. The effects of this fault are constrained in pond 1 for a while until it propagates to head pond 0 and then later appears as an increase in power.

In the case of fault f^3 at the sluice gate w_1, this is a combination of the above two faults and the residue is given by either Equation (4.86) or Equation (4.88), depending on whether it is in transition or steady state.

4.4.1.2 Residue Generation of Pond Valve Faults

In the case of the saturation fault f^1 at the valve s_1, the primary affected are pond 1 and pond 0. The residue for pond 1 is the difference between Equations (4.23) and 4.60).

$$r_1^{f^1(s_1)} = -\frac{n_s a}{A} \int_0^t f_{s_1}^1 \sqrt{2g|x_1 - x_0|} sgn(x_1 - x_0) dt \tag{4.89}$$

The residue for pond 0 is given by the difference between Equations (4.22) and (4.61).

$$r_0^{f^1(s_1)} = \frac{n_s a}{A} \int_0^t f_{s_1}^1 \sqrt{2g|x_1 - x_0|} sgn(x_1 - x_0) dt \tag{4.90}$$

The rest of the residues may or may not be nonzero (its mathematics is shown in the Appendix A) due to the implicit effects of the faults, and the total residue is given as:

$$\overrightarrow{r^{f^1(s_1)}} = \begin{bmatrix} \frac{n_h a}{A}\int_0^t f_{s_1}^1 \sqrt{2g|x_1 - x_0|}\, sgn(x_1 - x_0)dt \\ -\frac{n_h a}{A}\int_0^t f_{s_1}^1 \sqrt{2g|x_1 - x_0|}\, sgn(x_1 - x_0)dt \\ r_2^{f^1(s_1)} \\ r_s^{f^1(s_1)} \\ r_P^{f^1(s_1)} \end{bmatrix} \tag{4.91}$$

This is the residue due to the saturation fault of the valve s_1. The effects of this fault occur as Equation (4.61), when the valve s_1 goes to the saturation region. The valve s_1 only goes in the saturation region when the current levels of the ponds are fairly below the required level and the valve s_1 has to be fully open to make the water levels quickly rise to the required level. Thus, the effects of this fault appear only in the transition state and show their effect by slightly increasing the level of pond 1 and decreasing the level of pond 0. The fault effects are transmitted to the other parts of the system, but they disappear as soon as the system reaches steady state.

In the case of leakage fault f^2 at the valve, s_1, the primary affected are pond 1 and pond 0. The residue for pond 1 is the difference between Equations (4.23) and (4.66).

$$r_1^{f^2(s_1)} = -\frac{n_h a}{A}\int_0^t f_{s_1}^2 \sqrt{2g|x_1 - x_0|}\, sgn(x_1 - x_0)dt \tag{4.92}$$

The residue for the pond 0 is given by the difference between Equations (4.22) and (4.67).

$$r_0^{f^2(s_1)} = \frac{n_h a}{A}\int_0^t f_{s_1}^2 \sqrt{2g|x_1 - x_0|}\, sgn(x_1 - x_0)dt \tag{4.93}$$

The rest of the residues may be nonzero due to the implicit effects of the faults, and the total residue is given as:

$$\overrightarrow{r^{f^2(s_1)}} = \begin{bmatrix} \frac{na}{A}\int_0^t f_{s_1}^2\sqrt{2g|x_1 - x_0|}sgn(x_1 - x_0)dt \\ -\frac{na}{A}\int_0^t f_{s_1}^2\sqrt{2g|x_1 - x_0|}sgn(x_1 - x_0)dt \\ r_2^{f^1(s_1)} \\ r_s^{f^1(s_1)} \\ r_p^{f^1(s_1)} \end{bmatrix} \tag{4.94}$$

Unlike the above discussed leakage fault f^2 at the sluice gate w_1, the valve's fault only affects the system when the current levels of the system are higher than the required level, and the water level in the ponds need to be reduced to the lower level. Unless the leakage fault is of very high magnitude, the effects of the fault disappear when the system reaches steady state. This is because the valve s_1 is open significantly during the steady state to equalize the inflows and the outflows.

In the case of fault f^3 to the valve s_1, the above two faults are combined. The residue is given by either Equation (4.91) or Equation (4.94) whether the current pond level of the system is lower or higher than the required level.

4.4.1.3 Residue Generation of Turbine Wicket Gate Faults

In the case of the saturation fault f^1 at the turbine wicket gate G, the effected part of the system is the turbine power output. Although due to some back propagation, the other parts of the residue may or may not he zero. The residue of the turbine is given by the difference between Equations (4.27) and (4.72).

$$r_p^{f^1(G)} = \frac{M_r x_0 n_r}{H_0} f_G^1 \left[a_1 \frac{n^2}{n_r^2} + b_1 \frac{n}{n_r} + c_1 \right] \tag{4.95}$$

The rest of the residues, which may or may not be zero, are given by:

$$\overrightarrow{r^{f^1(G)}} = \begin{bmatrix} r_0^{f^1(G)} \\ r_1^{f^1(G)} \\ r_2^{f^1(G)} \\ r_s^{f^1(G)} \\ \frac{M_r x_0 n_r}{H_0} f_G^1 \left[a_1 \frac{n^2}{n_r^2} + b_1 \frac{n}{n_r} + c_1 \right] \end{bmatrix} \tag{4.96}$$

The saturation fault f^1 of the turbine wicket gate is fairly critical as it directly affects the output power of the turbine. The effects of this fault occur whenever the turbine gate needs to be operated in a higher flow region, which is nearly all of the time other than when the system's power level needs to be reduced from a higher level. In the case of this fault, it is imperative to have some kind of fault-tolerant scheme for the system to run within acceptable levels of performance.

In the case of the leakage fault f^2 at the turbine wicket gate G, the primary affected part is the power output. The residue for the power output is given by the difference between Equations (4.27) and (4.75).

$$r_P^{f^2(G)} = \frac{M_r x_0 n_r}{H_0} f_G^2 \left[a_1 \frac{n^2}{n_r^2} + b_1 \frac{n}{n_r} + c_1 \right] \tag{4.97}$$

The rest of the residue, which may or may not be zero, are given by:

$$\overrightarrow{r^{f^2(G)}} = \begin{bmatrix} r_0^{f^2(G)} \\ r_1^{f^2(G)} \\ r_2^{f^2(G)} \\ r_s^{f^2(G)} \\ \frac{M_r x_0 n_r}{H_0} f_G^2 \left[a_1 \frac{n^2}{n_r^2} + b_1 \frac{n}{n_r} + c_1 \right] \end{bmatrix} \tag{4.98}$$

Unlike the above saturation fault, the residue for this fault only appears if the turbine needs to be shutdown or the required power is suddenly reduced to a very low level when the system is under operation.

In the case of fault f^3 at the turbine wicket gate G, the residue is given by Equation (4.96) or Equation (4.98), whether the system is in normal operation mode or needs to be shutdown.

4.4.2 Residue Pre-Processing

Although there is some disturbance in the system's output or the residue, it is assumed that the disturbances in the power output, head pond, and surge tank are negligible. In the current case, some white noise is added to ponds 1 and 2 of the system approximating the sensor noise due to the water's bubbling or turbulent effect as it falls from the river into ponds 1 and 2. Therefore, the disturbance vector that will appear in the residue is given as:

$$\vec{d} = \begin{bmatrix} 0 \\ d_1 \\ d_2 \\ 0 \\ 0 \end{bmatrix} \tag{4.99}$$

So, the total residue in case of the occurrence of fault is given as:

$$\overrightarrow{r^{f^i(z)}} = \begin{bmatrix} r_0^{f^i(z)} \\ r_1^{f^i(z)} \\ r_2^{f^i(z)} \\ r_s^{f^i(z)} \\ r_P^{f^i(z)} \end{bmatrix} + \begin{bmatrix} 0 \\ d_1 \\ d_2 \\ 0 \\ 0 \end{bmatrix} \tag{4.100}$$

where z is the faulty component and i is the type of fault, both of which have been discussed above. As seen from Equation (122), the sensor noise is clearly not needed as it will tend to give a nonzero residue even if the system is running normally and no faults or unexpected disturbances have occurred. As the disturbances usually have relatively high-frequency components, while the system's hydraulic and power dynamics are in a lower frequency region, it makes sense to filter or average the residue to attenuate the effects of disturbance. In this case, a moving average is used to reduce the effects of disturbance. After the averaging, the residue is multiplied by a high gain to make it more sensitive to the effects of

the faults. This makes the residue sensitive and makes the effects of the fault more apparent when the effects of the faults appear in the system output. The residue given to the fault identification module is given as:

$$\overrightarrow{r^{f^1(z)}{}_{Final}} = g_r \frac{1}{T} \int_t^{t+T} \overrightarrow{r^{f^1(z)}}\, dt \tag{4.101}$$

Here, $\overrightarrow{r^{f^1(z)}{}_{Final}}$ is the residue vector for fault identification, T is the averaging time window, and g_r is the constant gain of the residue. In this way, all the faults' residues $\overrightarrow{r^{f^1(z)}{}_{Final}}$ are found and saved in the database for further usage. The simplified form of the residue generation and the preprocessing scheme is given in Figure 4.2. Note also that the 'Total System' in Figure 4.2 represents the whole of Figure 4.1 as the total system, which is the hydraulic system, turbine, and its control system.

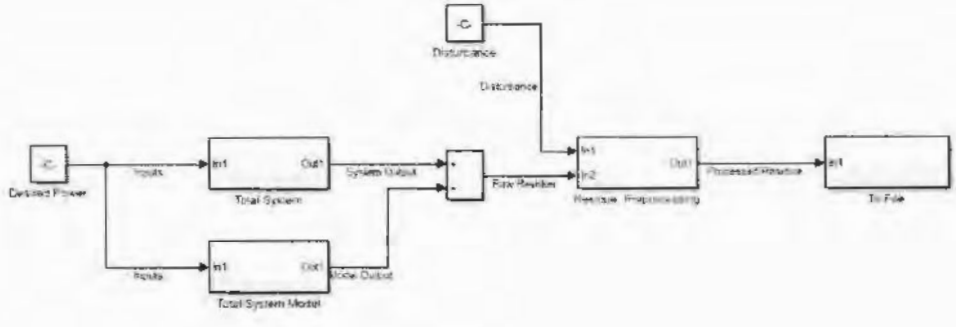

Figure 4.2. Residue generation and pre-processing.

4.4.3 Fault Identification

After the residue is generated, the next task is to identify and isolate the fault. As the residue is generated by the system and passed to the diagnostic module, it is processed to determine the system integrity and to identify any fault. The system residue is compared to all fault residues saved in the database beforehand to determine the presence or absence of a fault. The effects of the faults are more deterministic rather than probabilistic. According to assumptions, only one component can be faulty at a given time. It is more efficient to

compare the generated residue with the known fault residues from the database than any other method to identify the fault. A simplified form of the fault identification process is shown in Figure 4.3.

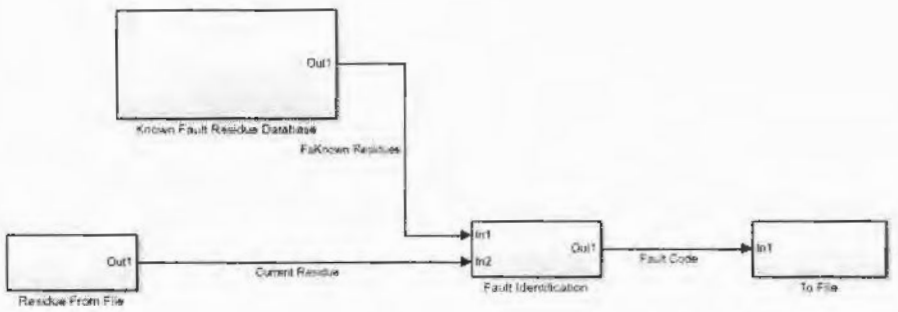

Figure 4.3. Fault identification module.

The residue comparison is given by taking the difference of the given residue with all the identified residues present in the database. The difference for a particular fault is given as:

$$\overrightarrow{d_{diff}{}^{f^i(z)}} = \overrightarrow{r^{Unidentified}{}_{Final}} - \overrightarrow{r^{f^i(z)}{}_{Final}} \tag{4.102}$$

Here, $\overrightarrow{r^{Unidentified}{}_{Final}}$ is the unidentified residue given by the system and $\overrightarrow{r^{f^i(z)}{}_{Final}}$ is one of the known residues of the system present in the database. Similarly, the given residue is compared with all of the residues present in the database and is prepared for the next step.

As we know that the residue is a set of five time-series and so is the difference of the residues, we need to make the difference vector independent from time while retaining all the information present in the difference vector. We square all of the five parts of the difference vector first. Writing the difference vector in its expanded form.

$$\overrightarrow{d_{diff}}^{f^i(z)} = \begin{bmatrix} d_0^{f^i(z)} \\ d_1^{f^i(z)} \\ d_2^{f^i(z)} \\ d_s^{f^i(z)} \\ d_p^{f^i(z)} \end{bmatrix} \tag{4.103}$$

The vector containing all the squared time series of the difference vector is donated by $\overrightarrow{D_{diff}}^{f^i(z)}$. We individually square all the elements of the difference vector as:

$$\overrightarrow{D_{diff}}^{f^i(z)} = \begin{bmatrix} \left(d_0^{f^i(z)}\right)^2 \\ \left(d_1^{f^i(z)}\right)^2 \\ \left(d_2^{f^i(z)}\right)^2 \\ \left(d_s^{f^i(z)}\right)^2 \\ \left(d_p^{f^i(z)}\right)^2 \end{bmatrix} \tag{4.104}$$

This makes $\overrightarrow{D_{diff}}^{f^i(z)}$ to retain the information in the difference vector by squaring the time series. Now, to turn the squared difference vector consisting of five time series, we integrate the squared difference vector over time to make it a time-independent vector consisting of five scalar values. The elimination of the time dependency is given as:

$$\overrightarrow{I^{f^i(z)}} = \int_0^t \overrightarrow{D_{diff}}^{f^i(z)} \, dt \tag{4.105}$$

Here, $\overrightarrow{I^{f^i(z)}}$ is the difference vector, consisting of five positive scalar elements each. Finally, the square of the magnitude of $\overrightarrow{I^{f^i(z)}}$ is found by having a dot product with itself.

$$K^{f^i(z)} = \left\| \overrightarrow{I^{f^i(z)}} \right\|^2 = \overrightarrow{I^{f^i(z)}} . \overrightarrow{I^{f^i(z)}} \tag{4.106}$$

The steps of Equation (4.102) to Equation (4.106) are repeated for each known fault residue in the database. This procedure generates a scalar for each known fault. After the scalar values are generated, the minimum of that is taken and compared to a predetermined threshold value. If the minimum value is lower than the threshold, that fault is determined to

have occurred and is identified. Each fault is given a unique code that describes the fault, which is then passed onto the fault tolerant control.

4.4.4 Fault Tolerance

In the event of fault occurrence, it corrects or modifies the system output parameters for the system to behave more desirably. Fault-tolerant action may not be necessary in the case of the occurrence of every fault. In the case of the faults discussed above, there are two possible cases for the effects of faults. If the effects of the fault are only apparent during the transient state and disappear when the system enters steady state, there is no need to have dedicated fault tolerance in this case. The second case is when the faults affect the outputs when the system is in steady state, fault-tolerant action is required. However, if the faults do not affect the output critical to the system, dedicated fault tolerant action may not be required. If the fault affects the critical outputs in the steady state, fault tolerance is required to correct the critical output. In the case of this system, the critical output which needs to have fault tolerance is the output power, while the actual levels of the ponds are not important.

In this case, the faults discussed are all the actuator faults, and it is rather hard to give corrective action to an already malfunctioning actuator. For this reason, fault tolerance is achieved by giving corrective action to the reference controller. The level reference controller gives the required level to the hydraulic system. By adjusting the required level to a corrected level, the effects of the fault are minimized and suppressed, thus achieving fault tolerance. By adjusting the reference, the rest of the system will behave more desirably while still being faulty. The fault-tolerant or fault-compensation process is shown in Figure 4.4.

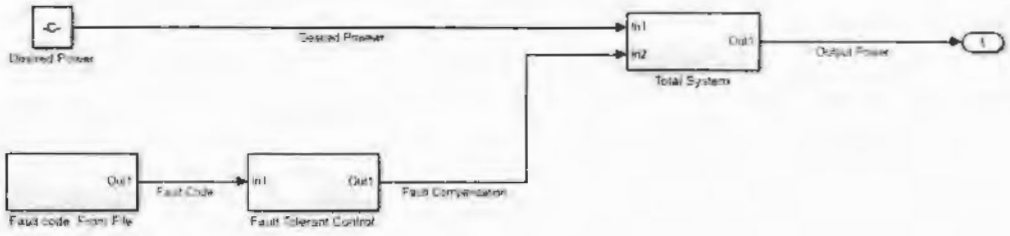

Figure 4.4. Fault tolerance and fault compensation process.

For each type of identified fault from the fault code given by the fault identification module, the actual name of the fault is given as output and whether it requires fault corrective action or not. In the case where fault corrective action is required, the fault corrective reference is added to the level reference as:

$$Level_{RefAdj} = Level_{Ref} + Level_{RefCorr} \tag{4.107}$$

So, this $Level_{RefAdj}$ is given as the required level to the level controller. When the fault tolerance action is not needed, $Level_{RefCorr}$ is given as zero to the level reference. Therefore, by combining the three steps of fault diagnostics, the fault diagnostic process is of the type shown in Figure 4.5.

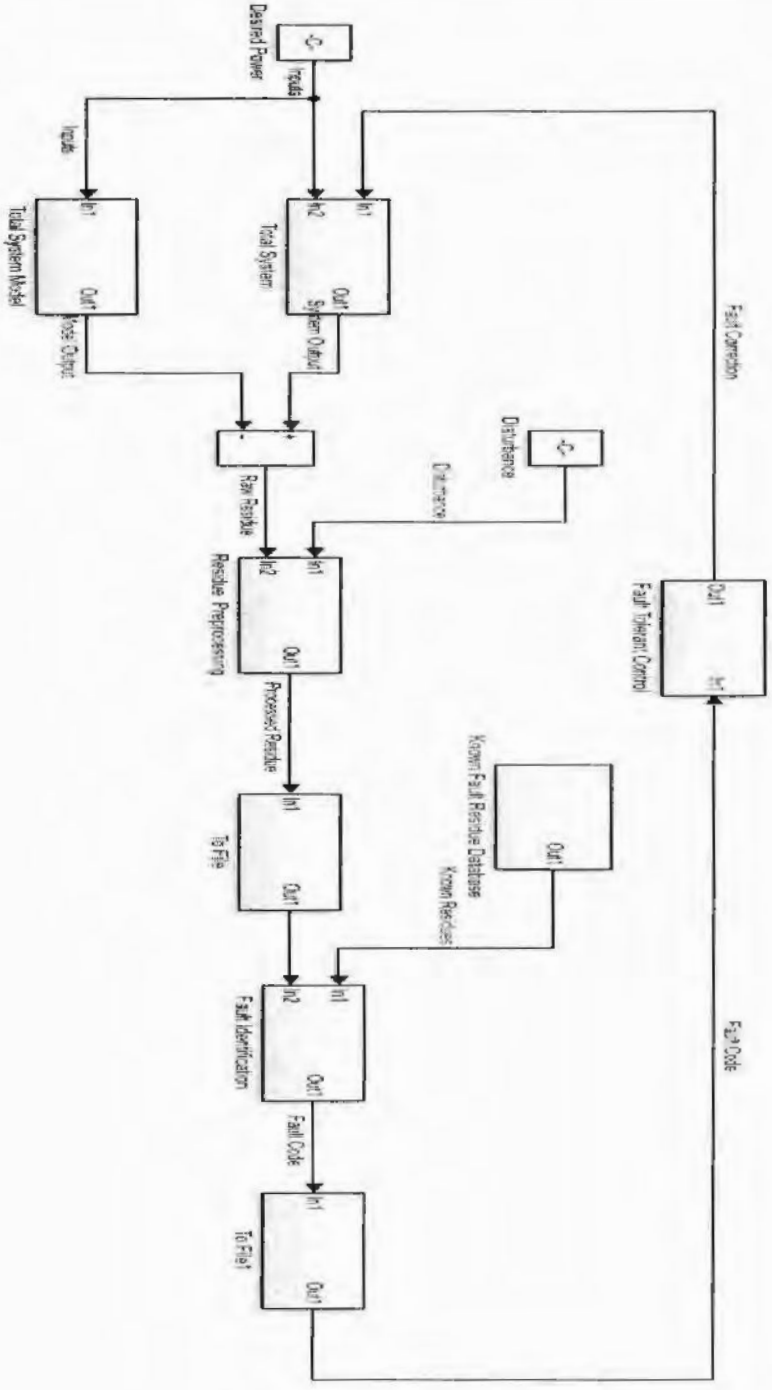

Figure 4.5. Fault diagnostic scheme.

4.5 Results and Discussions

The system was simulated in MATLAB and Simulink to analyze its validity. The basic three-pond hydraulic model is presented in the last chapter and is modified according to the requirements of this work. The Francis turbine model is taken from [44] and was implemented using MATLAB. First, the total system was simulated with the three-level control. After implementing faults and residue generation, the residue is saved in a memory unit. The saved unidentified residue is read by the fault identification module and identified. After identifying the fault or lack of it, a suitable error code is passed to the fault-tolerant module. The system is simulated in fault-tolerant mode in case of a fault. The model parameters were taken arbitrarily but taken to be in line with the parameters of the hydraulic system, which was also taken arbitrarily. So, the parameters of the hydraulic system for simulation are as follows:

$H_0 = H_1 = H_2$ = Height of pond 0,1,2 = 35 m;

H_s = Height of Surge Tank = 20 m;

C_t = Friction constant of headrace. = 0.98;

a = Cross sectional area of the ducts between T_1&T_0, T_2&T_0 = 6.25 m^2;

A = Area of the Ponds T_0,T_1,T_2 = 50 m x 50 m = 2500 m^2;

A_s = Area of Surge Tank.= 10 m x 10 m = 100 m^2;

L_t = Length of headrace. = 200 m;

A_t = Cross-sectional area of headrace = 6.25 m^2;

U_{max}= Maximum controllable inflow of water in ponds T_1 and T_2=100 $m^3/_{sec}$;

m = Base inflow of water in ponds T_1 and T_2 =75 $m^3/_{sec}$;

p = The maximum transient inflow of water in ponds T_1 and T_2 =25 $m^3/_{sec}$;

According to Equation (4.2) both the base and the transient flow rate will become equal at $50\ {}^{m^3}/_{sec}$.

The parameters of the turbine penstock were arbitrarily set as:

Q_r= Rated flow-rate through the turbine = 6.5 m^2;

n_r= Rated rotational speed of the turbine = 10 ${}^{rev}/_{sec}$;

n = Rotational speed at which the turbine is set = 8.33 ${}^{rev}/_{sec}$;

H_r= Rated height of the turbine which is same as the Height of Pond 0 =35 m;

M_r= Rated torque of the turbine = 200,655 Nm;

P_r= Rated maximum power of the turbine = 2,006,550 $Watts \cong 2\ MegaWatts$;

Although the turbine is rated at slightly more than 2 MW, the generated maximum power of the turbine maxes out at nearly 1.95 MW at the set conditions.

4.5.1 Power Generation

With all of the system parameters out of the way, the system operation was tested at some required power. The required power at which the system was tested was assumed to be the usual required power at which the system would operate most of the time. The required power was set at 1.65 MW, and the system's normal operation was tested. Although only the hydraulic system was tested in the last chapter, the hydraulic system had zero initial conditions. In this thesis, as stated earlier, the minimum level of the head pond is 20 m. Therefore, the initial conditions for the ponds were set at 20 m. The total system was tested with the required power of 1.65 MW and the initial conditions described.

The concerned outputs of the system were the pond levels 0, 1, and 2, and the output power is shown graphically. Furthermore, due to the massive difference between the output power and pond levels, it made sense to show both graphs separately for all the cases, such as the system

operation in normal or faulty conditions; also, the level and power graphs for the residue are shown separately for this reason.

For the case of the normal operation of the system, with a required power at 1.65 MW, the reference controller sets the required level to 30 m and the system is started from the initial conditions. The level and the power graphs are shown in Figures 4.6 and 4.7

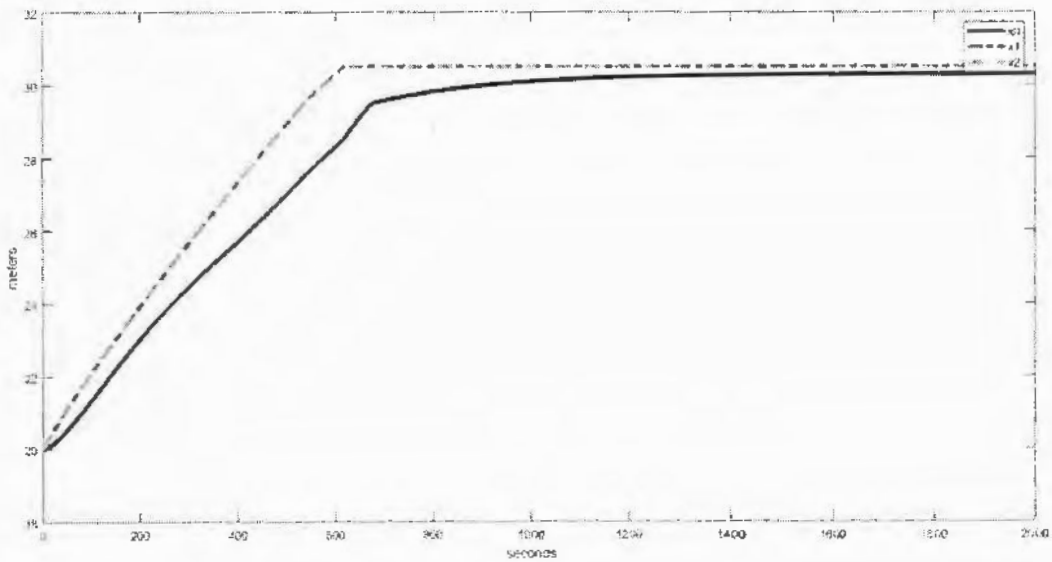

Figure 4.6. Pond levels (0, 1, and 2) in normal operation at the desired power of 1.65 MW

As shown in Figures 4.6 and 4.7, the system usually behaves and reaches both the required levels and required power in some time with aminimum error for both the pond levels and the generated power in steady state. Another point to consider is that there are comparisons of the level control of this model with the traditional single-pond model in the last chapter, which are not repeated here. Another comparison about the power regulation can be made with the results of [59], but the scale of power is different, and although [59] still uses a fuzzy controller as our work, their approach is different as [59] only deals with power regulation with a static head under different head conditions, such as a low, medium, and high head and

changing from power requirement from 2 MW to 10 MW or from 10 MW to 40 MW by only controlling the flow rate through the turbine.

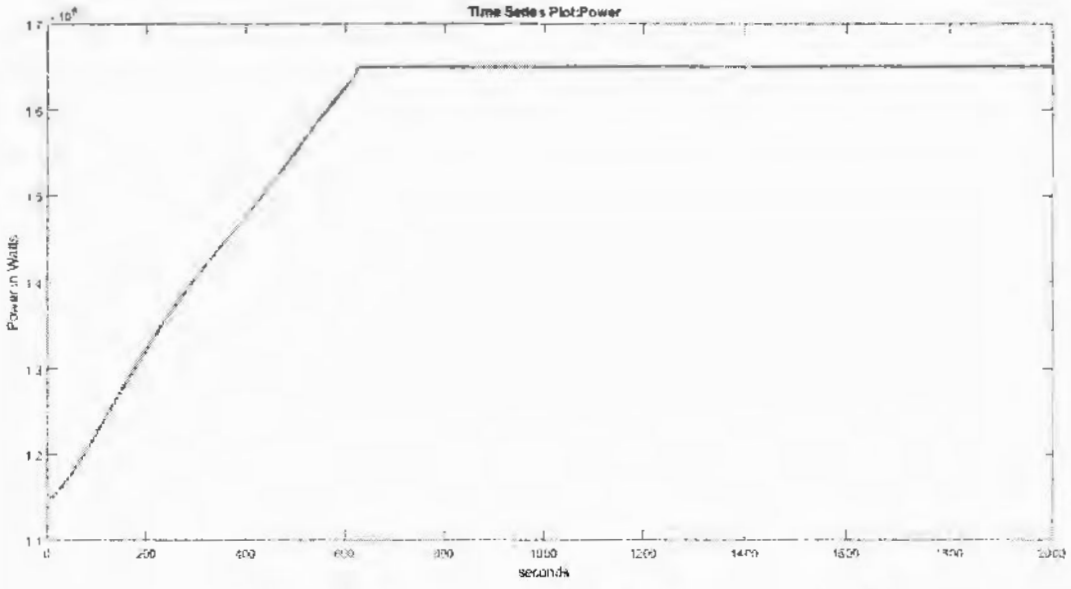

Figure 4.7. Power level in normal operation and desired power of 1.65 MW

4.5.2 Faults and Residues

As the main crux of this work relates to residue generation and fault identification, we shall be plotting the graphs for the residues of the faults. The residue generation mode consists of a fixed time window with the standard initial conditions and standard required power, which is 1.65 MW. It is unnecessary to plot the residue for the normal operation as it will be zero with noise added to r_1 and r_2. The magnitudes of the saturation and leakage faults are arbitrarily taken at 10%; i.e., the faulty valve or gate will be in saturation mode if it is equal to or greater than 90% of its opening and it will be in leakage mode when it is equal to or less than 10% of its opening. The graphs of the residues are generated through the system sensors in MATLAB/Simulink, while to aid in calculations, the fault effects were taken mathematically. Now, let us look at the residues for each fault discussed above with the exception of those which do not have any effect on the residue in the normal mode of operation and also faults

that are redundant after discussing these faults; i.e., faults of sluice gate w_2 and pond valve s_2.

4.5.2.1 Saturation Fault of Sluice Gate

As discussed earlier, Equation (4.86) is used to generate the residue of fault f^1 of the sluice gates w_1 or w_2; it also was noted earlier that the effects of the saturation fault are only visible in the residue when the sluice gate is in its saturation region. This occurs when the system is in a transient region, and the levels of the ponds are below the required levels. When the system reaches its steady state, the sluice gate is no longer in its saturation mode, and the system starts behaving in its normal mode. Therefore, the residue for this fault is only visible in the transient region of the system. Although the exact mathematical model of this fault was only given for the directly affected pond (in this case pond 1), it was also stated that the effects of this fault would be transmitted to the other ponds and the output power. The residue graph for the saturation fault of w_1 is given in Figure 4.8. If the same fault is in w_2, Residues 1 and 2 are swapped, while the rest of the residues will remain the same.

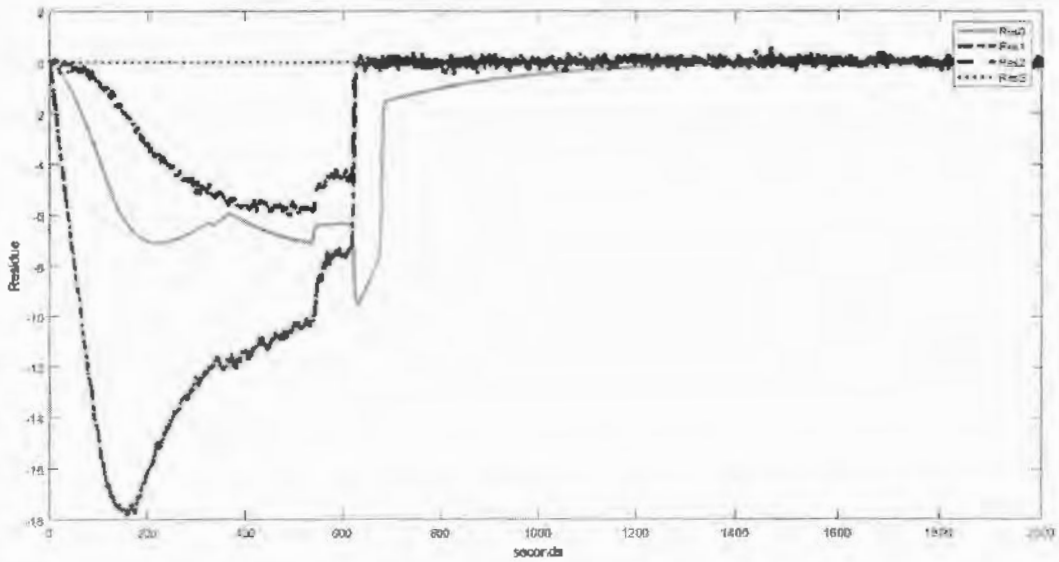

Figure 4.8. Pond residues for the saturation fault of sluice gate w_1

As the magnitude and the scales of the power residue are very different from the other residues, the power residue is shown separately for all the faults discussed here. When the pond levels are lower than the required levels in the transient state, the power generated depends on the head pond level as the turbine wicket gate may be fully open. As the head pond level is lower than the normal transient state, these effects appear in the power residue in the transient state and disappear as soon as the system reaches steady state, as shown in Figure 4.9. In the case of the saturation fault of w_2, the power residue will remain the same.

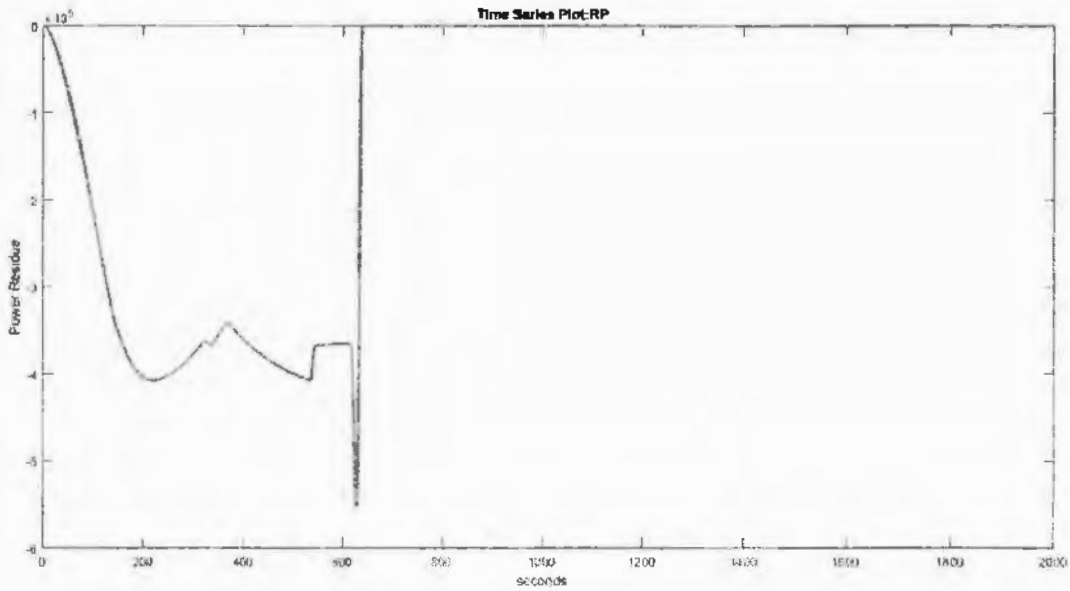

Figure 4.9. Power residue for the saturation fault of sluice gate w_1.

4.5.2.2 Leakage Fault of Sluice Gate

Equation (4.88) is used to compute the residue in case of the leakage fault f^2 of the sluice gate w_1 or w_2. As discussed before, the effects of that fault are only visible when the system is in steady-state mode or when the pond levels are greater than the required levels. When the ponds are in the steady-state mode, i.e., the current levels are equal to or greater than the required level, the sluice gate goes into leakage mode. Due to this leakage, the amount of water entering the pond is greater than the water leaving it, causing a slow rise in the water level. The effect is more apparent in the primarily affected pond, then transmitting to head pond 0 and forward to the power and surge tank and back to the other pond. The residue graphs for the leakage fault f^2 of the sluice gate w_1 are shown in Figure 4.10. In the case of fault of w_2, residues 1 and 2 are swapped.

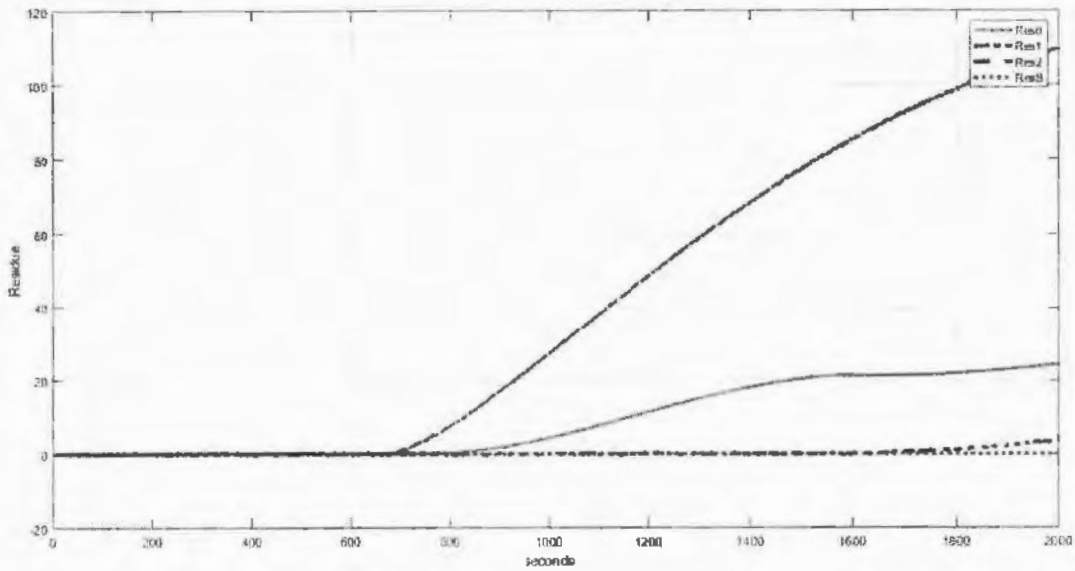

Figure 4.10. Pond residues for the leakage fault of sluice gate w_1

The effects of the leakage fault are also transmitted to the output power of the turbine, and the output power will also start creeping up after the system has reached steady-state mode; therefore, the power will also creep up, as shown by the residue graph in Figure 4.11.

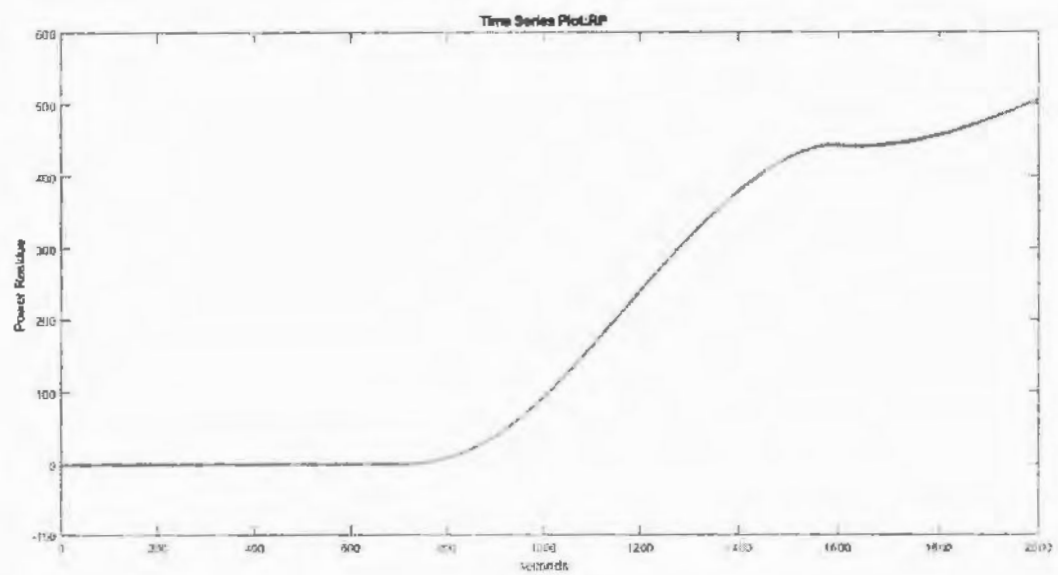

Figure 4.11. Power residue for the leakage fault of sluice gate w_1

4.5.2.3 Saturation and Leakage Fault of Sluice Gate

As discussed earlier, the f^3 fault is a combination of saturation and leakage faults, and its effect on the residue is during both the transient and steady-state regions. The residue graph for fault f^3 of the sluice gate w_1 is given in Figure 4.12. As stated before, for the same fault of w_2, residues 1 and 2 are swapped.

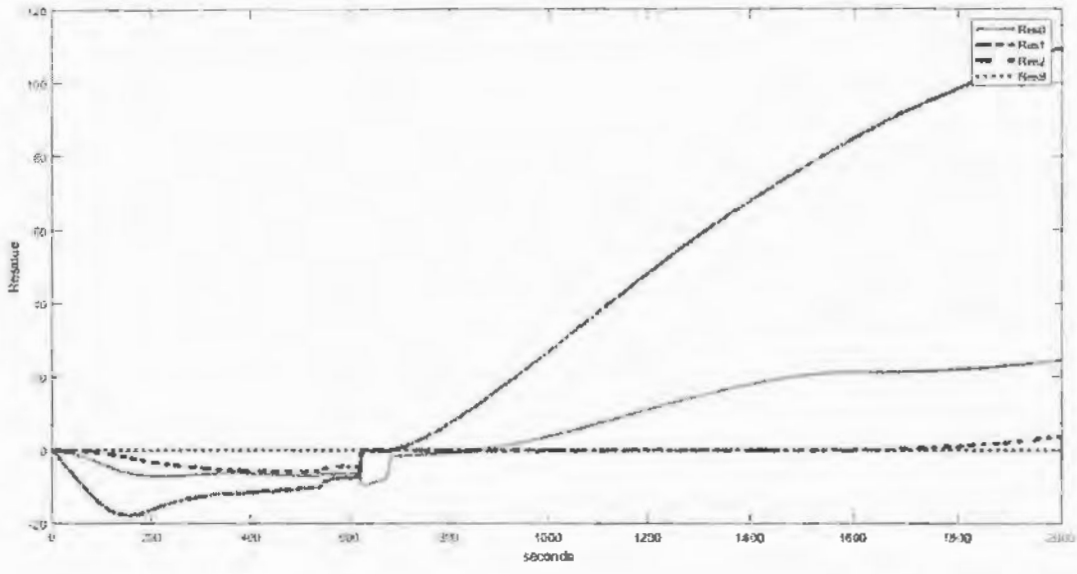

Figure 4.12. Pond residues for the saturation and leakage fault of sluice gate w_1

Similarly, the power residue combines the previous two faults and is given in Figure 4.13. Although the power residue graph looks the same as in Figure 4.9, it is a combination of Figures 4.9 and 4.11, this is because the power residue in Figure 10 has a very large magnitude as compared with Figure 12, and its effect looks suppressed.

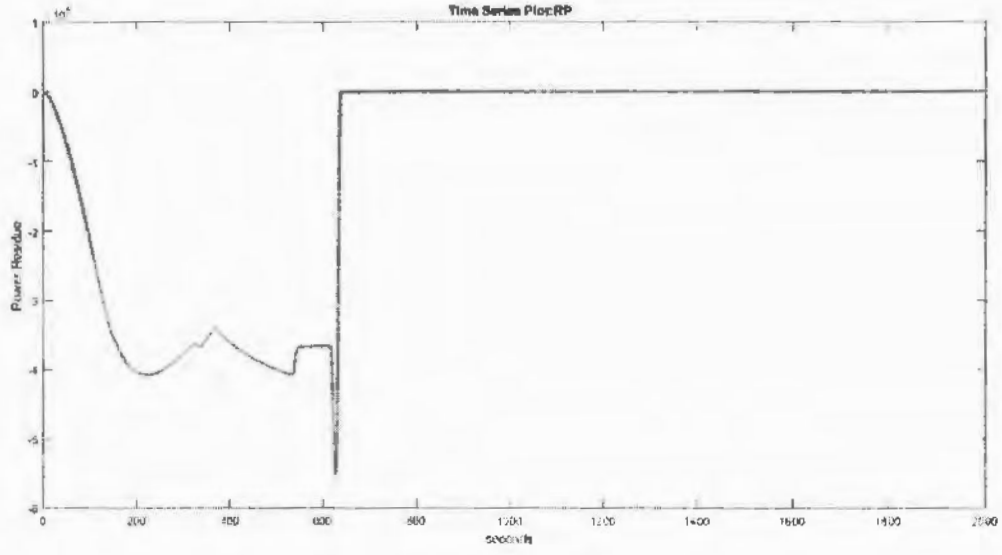

Figure 4.13. Power residue for the saturation and leakage fault of sluice gate w_1

4.5.2.4 Saturation Fault of the Pond Valve

Equation (4.91) is used to compute the residue in case of the fault f^1 of the pond valves s_1 or s_2. As the effect of the saturation fault of the pond valve only appears when the system is in the transient region when the current pond level is lower than the required level, the valve cannot be fully opened and goes into saturation mode. Therefore, the effects of the saturation fault for the valves$_1$ appear in the residue as shown below. As the effects of the leakage fault of the pond valve only appear when the system's required levels are lower than the current level, the leakage fault of the pond valve is also undetectable in the current residue generation mode, as the residue is unchanged. The effects of the saturation fault for valves$_1$ appear in the residue as shown in Figure 4.14; also, both the fault type f^1 and f^3 have exactly the same residue for valve s_1.

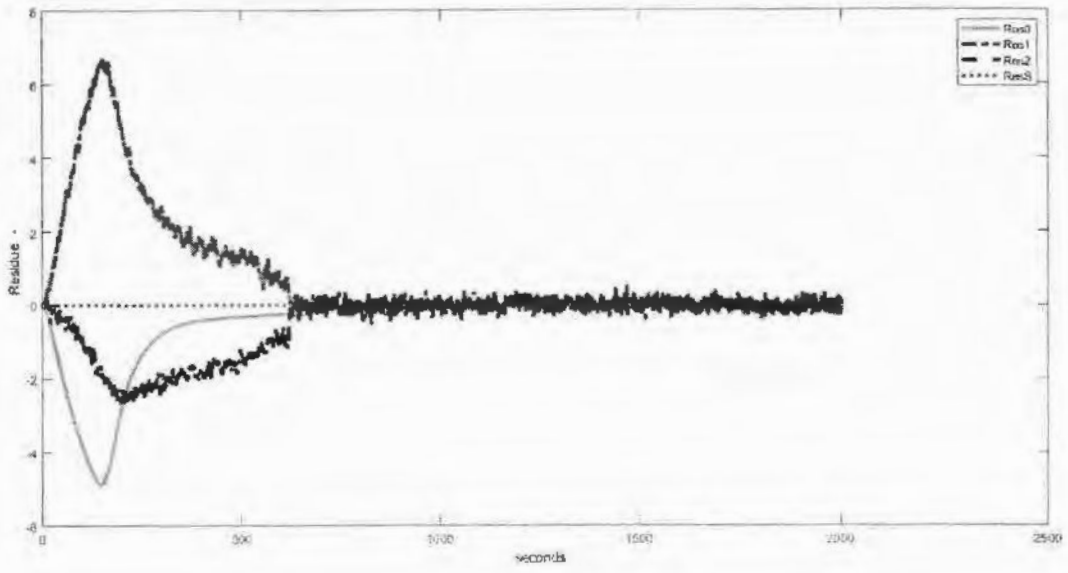

Figure 4.14. Pond residues for the saturation fault of the pond valve s_1.

Similarly, the effects of the fault f^1 of the pond valves appear only during the transient mode. The power residue graph for the f^1 fault of the pond valve s_1 is given in Figure 4.15; also, it is exactly the same as the f^3 fault.

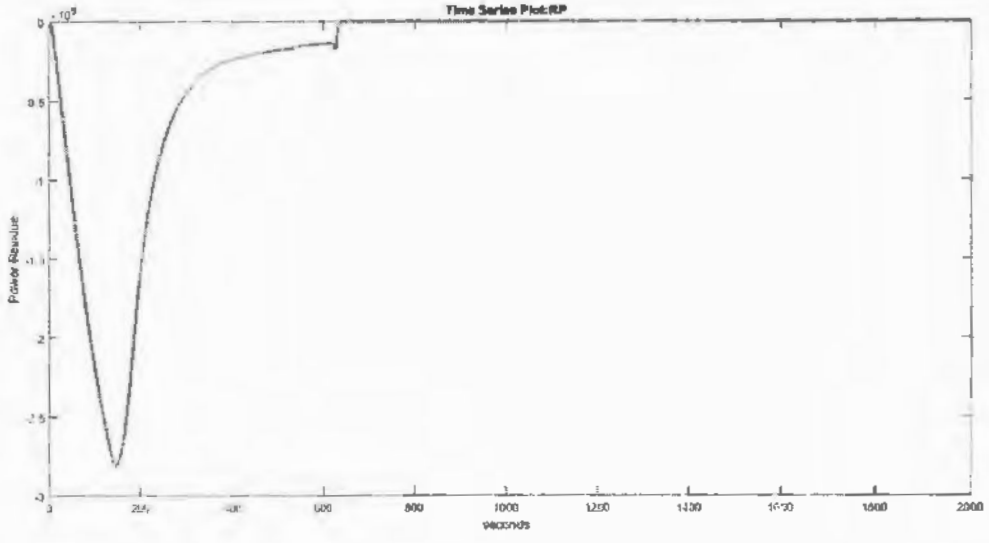

Figure 4.15. Power residue for the saturation fault of the pond valve s_1

4.5.2.5 Saturation Fault of the Turbine Wicket Gate

Equation (4.96) gives the residue in case of fault f^1 of the turbine wicket gate G. As stated before, the turbine operates at near or more than 90% gate opening for most of the time during operation. When the system is in transient state, and the current pond and power levels are below the required levels, at this time, the turbine gate is at nearly full throttle to try to reduce the power error as soon as possible. If a saturation fault exists in the turbine gate, its effects will appear in the power residue. When the system reaches its steady state, the turbine is still in its saturation mode, and the power residue will continue to be nonzero. Although the effects of this fault only appear in the power residue, they are not back propagated towards the ponds and hydraulic system. As all the saturation and leakage faults tested have a 10% magnitude, the effects of the fault are limited to the turbine. However, if the saturation fault increases significantly, then the effects of the fault will also back propagate towards the hydraulic system, starting with the surge tank. In the current situation, the hydraulic system's residue for the turbine gate's saturation fault is the same as a normal residue (near zero). However, the power residue is always nonzero. Furthermore, as the effects of the leakage fault do not appear in the normal residue generation mode, the power residue for fault f^3 of the turbine wicket gate G is the same as the saturation fault as shown in Figure 4.16.

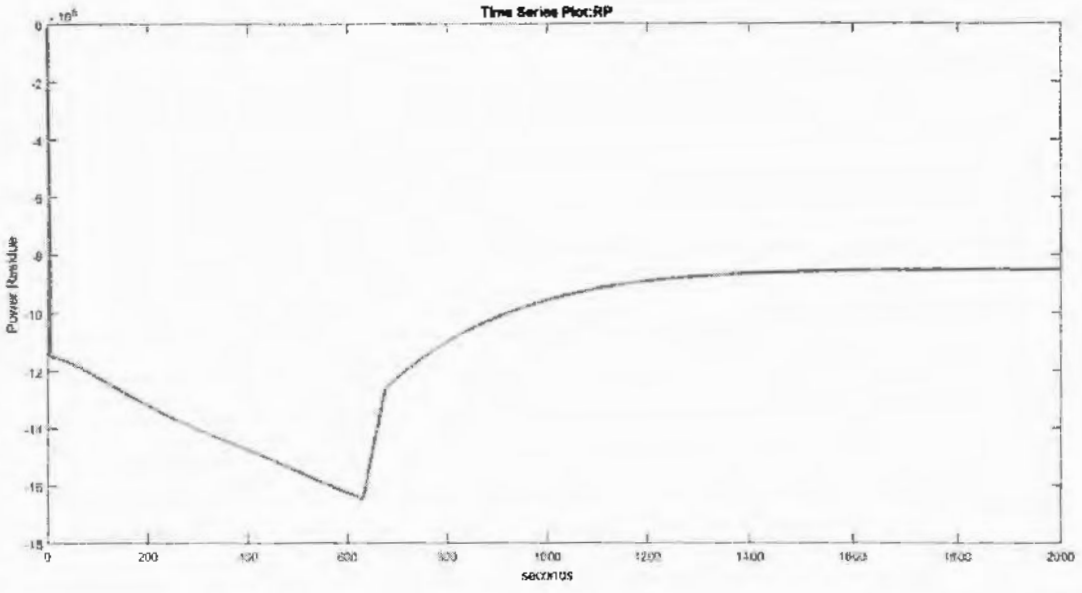

Figure 4.16. Power residue for the saturation fault of turbine gate *G*

4.5.2.6 Undetectable Faults

Due to the nature of the saturation and leakage faults, the system behavior is indistinguishable from a faultless system. As long as the faulty component of the system is not operating in a faulty (saturation or leakage) region, these faults will remain undetected. Examples of these are the leakage faults of the pond valves and the turbine wicket gate, whose effects are only visible if the pond level is needed to be lowered significantly or the turbine is shutdown. Therefore, another special residue generation mode needs to be implemented, forcing the pond valves and the turbine gate to go into leakage mode, thus making the leakage faults detectable. By implementing the special residue generation mode, all the discussed faults can be detected by running it in conjunction with the normal residue generation mode. Implementation of a special residue generation mode is left for future work as these faults do not affect the system in steady state and thus do not require the intervention of fault-tolerant control.

4.5.3 Effect of Fault-Tolerant Control

As stated in the fault description section, the faults affect the system in a transient or steady state. The requirement for fault tolerance arises if the system starts behaving undesirably in the steady state or its behavior is harmful to the system in the transient state. In these cases, while any fault must be detected and taken care of during scheduled maintenance, it is often not feasible for the system to be stopped during the operation. For this reason, it is more efficient for the system to take countermeasures and operate it in lower efficency mode rather than shutting down the system running it in faulty mode. Although fault compensation or tolerant action is not required to occur in the case of detection of each and every fault, some faults have long-term effects on the system outputs. In the case of the faults discussed above, fault tolerance is required only for two cases of faults. The first case is the leakage fault of the sluice gate, and the other is the saturation fault of the turbine. In the current system, the output power is most important for the system's proper operation. Therefore, for fault tolerance control, the output power is targeted for correction of a fault, while the pond levels are disregarded in favor of the output power. In the following section, the two cases that require fault tolerance are discussed below.

4.5.3.1 Sluice Gate Leakage Fault Tolerance

For the residue graphs for the sluice gate leakage faults, the power residue is nonzero in the steady state and keeps increasing. This will result in a slow but steady increase in the power output if left unchecked. The power residue graph shows that the residue is around 500 mark at the end of the simulation. This is due to the residue's very high residue gain (around 100). The undesirable increase in the level of the head pond is due to the uncontrolled increase in pond 1 or 2. Although the power output increases by 5–6 watts compared to the normal operation, it will tend to snowball later and cause the plant to behave in unpredictable ways. So, a fault-tolerant action is needed to avoid or at least delay that unpredictable behavior. One

of the easiest ways to delay that undesirable behavior is to keep the head pond at a lower level than normal and have the turbine compensate for it. The fault tolerant controller sets the desired level of the head pond to a lower level and has the turbine compensate for the lower pond level. As shown in the power graph (Figure 4.17), although the power level of the fault-tolerant system reaches the desired level a little while after the faulty system, it will remain at the desired level a lot longer than the faulty system. The pond graphs for this case is shown in Figures 4.18 and 4.19, while the power graph is shown in Figure 4.17.

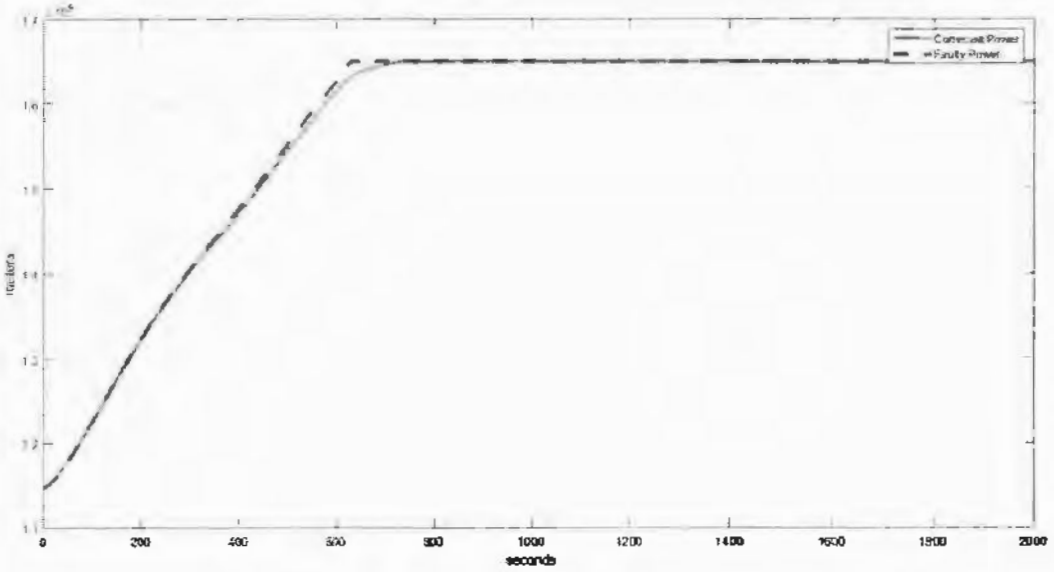

Figure 4.17. Power with faulty and fault-corrected operation given a sluice gate w_1 leakage fault

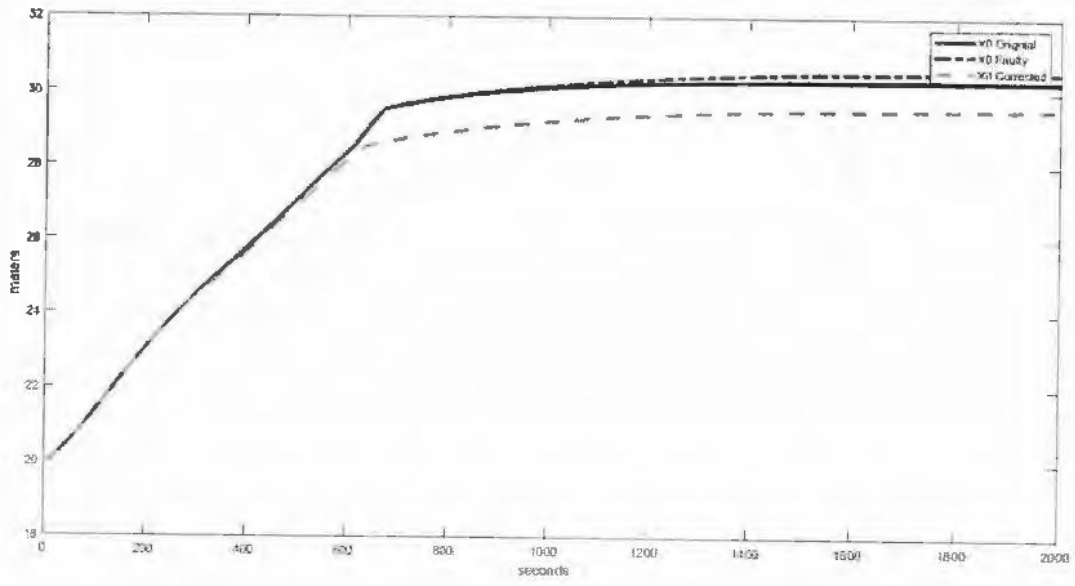

Figure 4.18. Pond 0 with normal, faulty, and fault-corrected operation given a sluice gate w_1 leakage fault

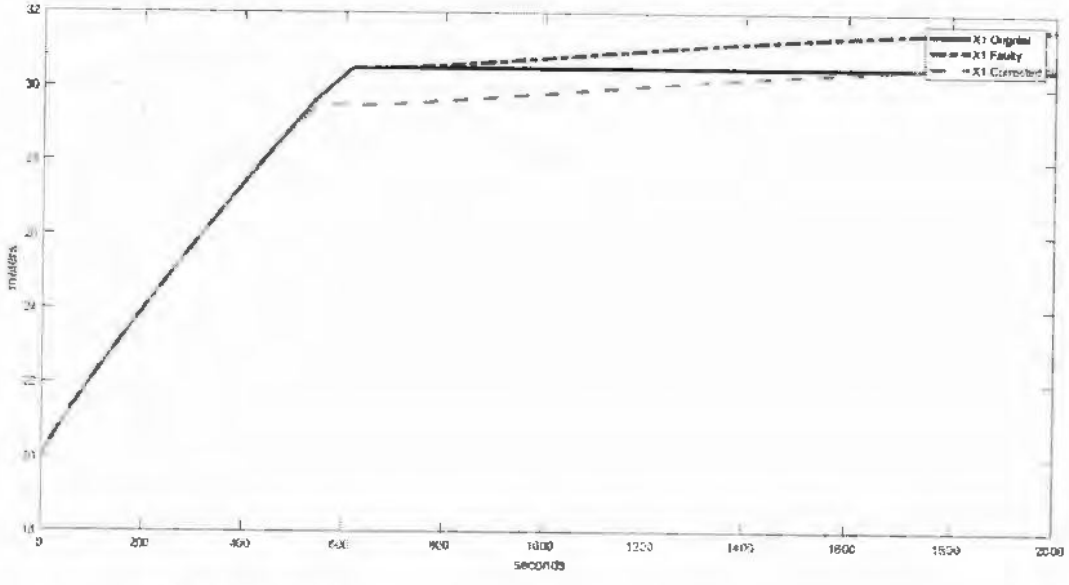

Figure 4.19. Pond 1 with normal, faulty, and fault-corrected operation given a sluice gate w_1 leakage fault

4.5.3.2 Turbine Saturation Fault Tolerance

As discussed in the earlier section, the effects of turbine saturation faults are present 99% of the time when it occurs. The saturation fault of the turbine also directly affects the power of the turbine, which is the most important output of the system. Therefore, including fault compensation or fixing the fault as soon as possible is vital. The output power is reduced due to the reduction in the flow-rate through the turbine, as shown in Equation (4.12). Furthermore, it cannot be increased, so the water level needs to be increased to increase the output power of the turbine. Therefore, after identifying the turbine saturation fault, the fault-tolerant controller increases the required level of the pond as shown in Figure 4.20, and the system functions as usual. Looking at the power graphs, compared to the normal and the faulty operation (Figure 4.21), we see that the fault tolerant mode takes a somewhat longer time to reach the desired power level compared to the faultless system, while the faulty system fails to reach the desired level.

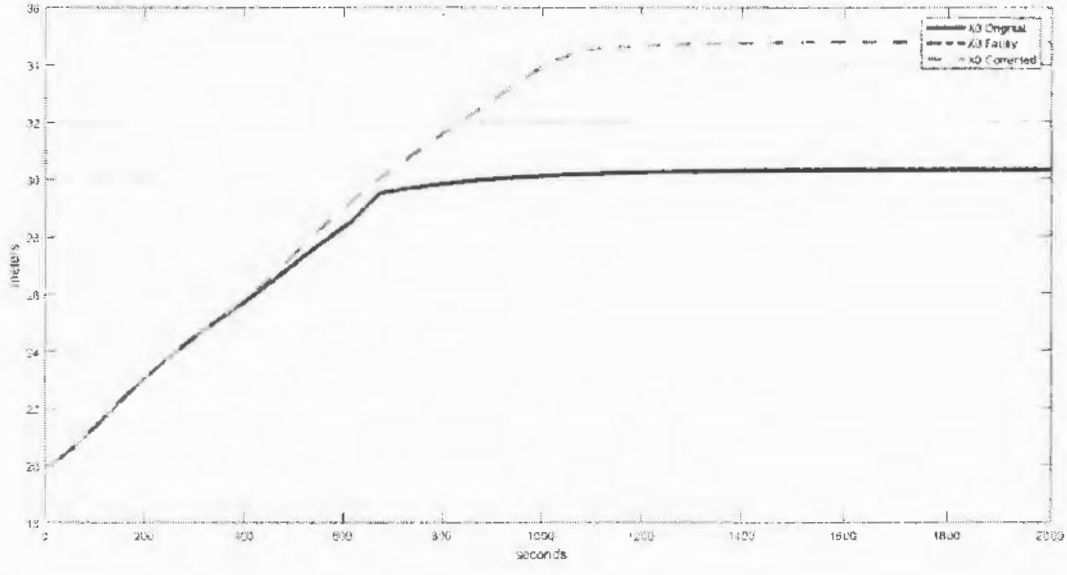

Figure 4.20. Pond 0 with normal, faulty, and fault-corrected operation given a turbine gate *G* saturation fault

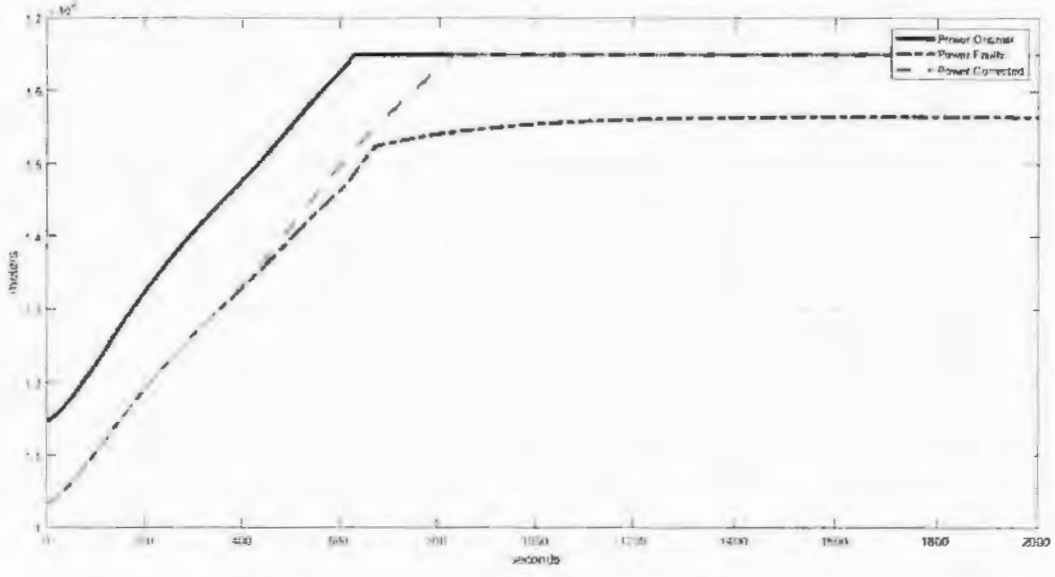

Figure 4.21. Power with normal, faulty, and fault-corrected operation given a turbine gate *G* saturation fault

In this chapter, the concept of three pond hydropower model is extended from the previous chapter and a Francis turbine is integrated with the system for power regulation. Next, Fault modelling, diagnostics and tolenrance is completed for the system.

CHAPTER 5

CONCLUSIONS AND FUTURE DIRECTIONS

5.1. Conclusions

In this thesis, a new solution to the water level regulation of a hydro power plant is proposed by using three pond system as a way to regulate water level. This concept is explored and is tested against several disturbances and compared to a single pond model. The simulations show that the proposed three-pond system is more robust against disturbances. The second contribution analyzes integrating a three-pond hydraulic system with a Francis turbine and adds two levels of control to the power generation. Next, some faults are added to the system, and the second part of the work deals with fault identification and then fault tolerance. The power control presented in the thesis is adequate as it reduces the power error to nearly 100 watts of error. This error could be reduced further by introducing a different control scheme.

5.2. Future Directions

The main future direction of this work is to identify more types of faults in the system and a combination of faults. Another future direction is to discuss the detailed fault models in this thesis, an example of which is discussed in Appendix A in a separate thesis. Furthermore, the fault tolerance is done by manipulating the required level of the head ponds to compensate for the faults; also, by having a fast technique to identify faults on the fly rather than running the system in fault identification mode periodically to identify the faults in the system. As the fauts considered in this thesis are only actuator faults, another future direction is to model

and consider sensor faults in the future. Also, in the fault detection module we did not consider the inclusion of the disturbances which were considered in chapter 3, that is also another future direction.Another future direction is to have a rather large database of faults and fault combinations that could be identified by the fault identification system and the fault-tolerant control having more autonomy in manipulating the parameters of the system variables to run the system more effectively in fault-tolerant model.

APPENDIX A

In the main thesis, we discussed the explicit effects of the faults on the directly affected state variables. As an extension to the above fault models, we shall discuss the implicit effects of the faults on the state variables that are not directly affected. As an example, we shall be taking the effects of the saturation fault f^1 for the pond valve s_1. Rewriting the effected Equations (4.59) and (4.60).

The total effect of fault on pond 1 is given by rewriting Equation (4.59).

$$x_1 = -\frac{n.a}{A}\int_0^t s_1\sqrt{2g|x_1 - x_0|}sgn(x_1 - x_0)dt - \frac{n.a}{A}\int_0^t f_{s_1}^1\sqrt{2g|x_1 - x_0|}sgn(x_1 - x_0)dt + \int_0^{At}\frac{w_1 l_1}{A}dt \tag{A1}$$

Similarly, the total effect of fault on pond 0 is given by rewriting Equation (4.60):

$$x_0 = \frac{n.a}{A}\int_0^t \left[s_1\sqrt{2g|x_1 - x_0|}sgn(x_1 - x_0) + f_{s_1}^1\sqrt{2g|x_1 - x_0|}sgn(x_1 - x_0) + s_2\sqrt{2g|x_2 - x_0|}sgn(x_2 - x_0)\right]dt - \int_0^t \frac{Q_t}{A}dt \tag{A2}$$

Now for ease of notation, let us donate the x_1 and x_0 from the Equations (A1) and (A2) as $x_1^{f_{s_1}^1}$ and $x_0^{f_{s_1}^1}$, respectively. For the duration of the appendix, let us assume the normal state variables, x_1 and x_0, as faultless, modifying Equations (A1) and (A2) in new notations as:

$$x_1^{f_{s_1}^1} = -\frac{n.a}{A}\int_0^t s_1\sqrt{2g|x_1 - x_0|}sgn(x_1 - x_0)dt - \frac{n.a}{A}\int_0^t f_{s_1}^1\sqrt{2g|x_1 - x_0|}sgn(x_1 - x_0)dt + \int_0^{At}\frac{w_1 l_1}{A}dt \tag{A3}$$

$$x_0^{f_{s_1}^1} = \frac{n.a}{A}\int_0^t \left[s_1\sqrt{2g|x_1 - x_0|}sgn(x_1 - x_0) + f_{s_1}^1\sqrt{2g|x_1 - x_0|}sgn(x_1 - x_0) + s_2\sqrt{2g|x_2 - x_0|}sgn(x_2 - x_0)\right]dt - \int_0^t \frac{Q_t}{A}dt \tag{A4}$$

Now let us rewrite Equations (A3) and (A4) in a simpler form as a combination of a normal value and faulty component:

$$x_0{}^{f_{s_1}^1} = x_0 + \frac{n_v a}{A}\int_0^t f_{s_1}^1 \sqrt{2g|x_1 - x_0|}\, sgn(x_1 - x_0)dt \tag{A5}$$

Similarly,

$$x_1{}^{f_{s_1}^1} = x_1 - \frac{n_v a}{A}\int_0^t f_{s_1}^1 \sqrt{2g|x_1 - x_0|}\, sgn(x_1 - x_0)dt \tag{A6}$$

Now, with the effects of the faults present in simplified terms in Equations (A5) and (A6), let us discuss the effects of the saturation fault of the pond valve on the other state variables. Now, rewriting Equation (4.9) for pond 2 with fault effects as:

$$x_2{}^{f_{s_1}^1} = -\frac{n_v a}{A}\int_0^t s_2\sqrt{2g|x_2 - x_0|}\, sgn\left(x_2 - x_0{}^{f_{s_1}^1}\right)dt + \int_0^t \frac{w_2 l_2}{A}dt \tag{A7}$$

Now, putting the value of $x_0{}^{f_{s_1}^1}$ in Equation (A7):

$$\begin{aligned} x_2{}^{f_{s_1}^1} = -\frac{n_v a}{A}\int_0^t s_2\sqrt{2g|x_2 - x_0|}\, sgn\Bigg(x_2 \\ -\left\{x_0 + \frac{n_v a}{A}\int_0^t f_{s_1}^1\sqrt{2g|x_1 - x_0|}\, sgn(x_1 - x_0)dt\right\}\Bigg)dt + \int_0^t \frac{w_2 l_2}{A}dt \end{aligned} \tag{A8}$$

Now simplifying the equation:

$$\begin{aligned} x_2{}^{f_{s_1}^1} = -\frac{n_v a}{A}\int_0^t s_2\sqrt{2g|x_2 - x_0|}\, sgn\Bigg(x_2 - x_0 \\ -\frac{n_v a}{A}\int_0^t f_{s_1}^1\sqrt{2g|x_1 - x_0|}\, sgn(x_1 - x_0)dt\Bigg)dt + \int_0^t \frac{w_2 l_2}{A}dt \end{aligned} \tag{A9}$$

and

$$\begin{aligned} x_2{}^{f_{s_1}^1} = -\frac{n_v a}{A}\int_0^t s_2\sqrt{2g|x_2 - x_0|}\, sgn(x_2 - x_0)dt + \int_0^t \frac{w_2 l_2}{A}dt \\ +\frac{n_v a}{A}\int_0^t s_2\sqrt{2g|x_2 - x_0|}\, sgn\left(\frac{n_v a}{A}\int_0^t f_{s_1}^1\sqrt{2g|x_1 - x_0|}\, sgn(x_1 - x_0)dt\right) \end{aligned} \tag{A10}$$

Therefore, the expression for the level of pond 2 becomes:

$$x_2{}^{f_{s_1}^1} = x_2 + \frac{n_v a}{A}\int_0^t s_2\sqrt{2g|x_2 - x_0|}\, sgn\left(\frac{n_v a}{A}\int_0^t f_{s_1}^1\sqrt{2g|x_1 - x_0|}\, sgn(x_1 - x_0)dt\right)dt \tag{A11}$$

For finding the effect of the fault on the surge tank, we consider Equation (47), but it depends upon the flow rate through the headrace, which in turn depends on the level of pond 0. Therefore, we consider the equation of head race (29):

$$\frac{d}{dt}Q_t = \frac{gA_t}{L_t}(x_0 - x_s) - C_t Q_t|Q_t| \tag{A12}$$

Integrating Equation (A12) to find the value of Q_t as:

$$Q_t = \frac{gA_t}{L_t}\left(\int_0^t x_0 dt - \int_0^t x_s\, dt\right) - \int_0^t C_t Q_t|Q_t|dt \tag{A13}$$

Now, with the explicit value of the flow-rate through the headrace, let us consider Equation (4.23) of the surge tank with the occurrence of the fault:

$$x_s{}^{f_{s_1}^1} = \int_0^t \frac{Q_t{}^{f_{s_1}^1}}{A_s}dt - \int_0^t \frac{Q}{A_s}dt \tag{A14}$$

Now, using the value of $Q_t{}^{f_{s_1}^1}$ from Equation (A13) in the above Equation (A14):

$$x_s{}^{f_{s_1}^1} = \int_0^t \frac{\frac{gA_t}{L_t}\left(\int_0^t x_0{}^{f_{s_1}^1}dt - \int_0^t x_s\, dt\right) - \int_0^t C_t Q_t|Q_t|dt}{A_s}dt - \int_0^t \frac{Q}{A_s}dt \tag{A15}$$

Simplifying:

$$x_s{}^{f_{s_1}^1} = \frac{1}{A_s}\int_0^t \left[\frac{gA_t}{L_t}\left(\int_0^t x_0{}^{f_{s_1}^1}dt - \int_0^t x_s\, dt\right) - \int_0^t C_t Q_t|Q_t|dt\right]dt - \int_0^t \frac{Q}{A_s}dt \tag{A16}$$

Now putting the value of $x_0{}^{f_{s_1}^1}$ in Equation (A16):

$$\begin{aligned} x_s{}^{f_{s_1}^1} = \frac{1}{A_s}\int_0^t \Bigg[\frac{gA_t}{L_t}\Bigg(\int_0^t \Bigg\{x_0 + \frac{na}{A}\int_0^t f_{s_1}^1\sqrt{2g|x_1 - x_0|}\,sgn(x_1 - x_0)dt\Bigg\}dt - \int_0^t x_s\, dt\Bigg) \\ - \int_0^t C_t Q_t|Q_t|dt\Bigg]dt - \int_0^t \frac{Q}{A_s}dt \end{aligned} \tag{A17}$$

After separating the faulty term from Equation (A17);

$$\begin{aligned} x_s{}^{f_{s_1}^1} = \frac{1}{A_s}\int_0^t \left[\frac{gA_t}{L_t}\left(\int_0^t x_0 dt - \int_0^t x_s\, dt\right) - \int_0^t C_t Q_t|Q_t|dt\right]dt - \int_0^t \frac{Q}{A_s}dt \\ + \int_0^t \frac{1}{A_s}\left[\int_0^t \frac{na}{A}\left\{\int_0^t f_{s_1}^1\sqrt{2g|x_1 - x_0|}\,sgn(x_1 - x_0)dt\right\}dt\right]dt \end{aligned} \tag{A18}$$

Now Equation (A18) can be rewritten as a combination of faultless and faulty state using Equation (A16):

$$x_s^{f_{s_1}^1} = x_s + \int_0^t \frac{1}{A_s}\left[\int_0^t \frac{n.a}{A}\left\{\int_0^t f_{s_1}^1\sqrt{2g|x_1 - x_0|}sgn(x_1 - x_0)dt\right\}dt\right]dt \tag{A19}$$

Now to find the effect of saturation fault of the pond valve on the output power, we consider the power Equation (4.12) as:

$$P^{f_{s_1}^1} = \frac{M_r x_0^{f_{s_1}^1} n_r}{H_0} G\left[a_1\frac{n^2}{n_r^2} + b_1\frac{n}{n_r} + c_1\right] \tag{A20}$$

Now putting the value of $x_0^{f_{s_1}^1}$ in the power equation:

$$P^{f_{s_1}^1} = \frac{M_r\left\{x_0 + \frac{n.a}{A}\int_0^t f_{s_1}^1\sqrt{2g|x_1 - x_0|}sgn(x_1 - x_0)dt\right\}n_r}{H_0} G\left[a_1\frac{n^2}{n_r^2} + b_1\frac{n}{n_r} + c_1\right] \tag{A21}$$

Simplifying:

$$\begin{aligned} P^{f_{s_1}^1} = {} & \frac{M_r x_0 n_r}{H_0} G\left[a_1\frac{n^2}{n_r^2} + b_1\frac{n}{n_r} + c_1\right] \\ & + \left\{\frac{n.a}{A}\int_0^t f_{s_1}^1\sqrt{2g|x_1 - x_0|}sgn(x_1 - x_0)dt\right\}\frac{M_r n_r}{H_0} G\left[a_1\frac{n^2}{n_r^2} + b_1\frac{n}{n_r}\right. \\ & \left. + c_1\right] \end{aligned} \tag{A22}$$

After further simplification the power becomes:

$$\begin{aligned} P^{f_{s_1}^1} = P + {} & \left\{\frac{n.a}{A}\int_0^t f_{s_1}^1\sqrt{2g|x_1 - x_0|}sgn(x_1 - x_0)dt\right\}\frac{M_r n_r}{H_0} G\left[a_1\frac{n^2}{n_r^2} + b_1\frac{n}{n_r}\right. \\ & \left. + c_1\right] \end{aligned} \tag{A23}$$

After further simplification the power becomes:

$$P^{f_{s_1}^1} = P + \left\{\frac{n.a}{A}\int_0^t f_{s_1}^1\sqrt{2g|x_1 - x_0|}sgn(x_1 - x_0)dt\right\}\frac{M_r n_r}{H_0} G\left[a_1\frac{n^2}{n_r^2} + b_1\frac{n}{n_r} + c_1\right] \tag{A24}$$

Therefore, we can find the explicit and implicit effects of the saturation fault f^1 for the pond valve s_1 as Equations (A3), (A4), (A11), (A19), and (A24) as a linear combination of faultless

state variables and fault effects. Similar calculations can be done for the other faults discussed in the thesis.

REFERENCES

[1] Demirbaş, Ayhan. "Global renewable energy resources." *Energy sources* 28, no. 8 (2006): 779-792.

[2] Gupta, Gaurav, and Paul Bogdan. "Distributed placement of power generation resources in uncertain environments." In *Proceedings of the 8th International Conference on Cyber-Physical Systems*, pp. 71-79. 2017.

[3] Egré, Dominique, and Joseph C. Milewski. "The diversity of hydropower projects." *Energy policy* 30, no. 14 (2002): 1225-1230.

[4]Hill, Donald. *A history of engineering in classical and medieval times*. Routledge, 2013.]

[5] Kiran, D. "Hydroelectric Power Plant: Layout, Working and Types. Electricaleasy. Com." (2015).

[6] Vytvytskyi, Liubomyr, Roshan Sharma, and Bernt Lie. "Model based control for run-of-river system. Part 1: Model implementation and tuning." Modeling, Identification and Control, 36, no 4 pp 237-249 (2015).

[7] Sarasua, Jose I., Jesus Fraile-Ardanuy, Juan I. Perez, Jose R. Wilhelmi, and Jose A. Sanchez. "Control of a run of river small hydro power plant." In *2007 International Conference on Power Engineering, Energy and Electrical Drives*, pp. 672-677. IEEE, 2007.

[8] Yadav, Omkar, Nand Kishor, Jesus Fraile-Ardanuy, Soumya R. Mohanty, Juan I. Pérez, and José I. Sarasúa. "Pond head level control in a run-of-river hydro power plant using fuzzy controller." In *2011 16th International Conference on Intelligent System Applications to Power Systems*, pp. 1-5. IEEE, 2011.

[9] Guoqing, Chen, Bi Weiming, and Zhang Cheng. "The design of AGC program adapted for the run-off-river hydropower plant." In *Proceedings. International Conference on Power System Technology*, vol. 4, pp. 2308-2312. IEEE, 2002.

[10] Belhadji, Lakhdar, Seddik Bacha, Daniel Roye, and Toufik Rekioua. "Experimental validation of direct power control of variable speed micro-hydropower plant." In *IECON 2012-38th Annual Conference on IEEE Industrial Electronics Society*, pp. 995-1000. IEEE, 2012.

[11] Kim, Jinho, Vahan Gevorgian, Yusheng Luo, Manish Mohanpurkar, Vladimir Koritarov, Rob Hovsapian, and Eduard Muljadi. "Supercapacitor to provide ancillary services with control coordination." *IEEE Transactions on Industry Applications* 55, no. 5 (2019): 5119-5127.

[12] Buaphan, Isara, and Suttichai Premrudeepreechacharn. "Development of expert system for fault diagnosis of an 8-MW bulb turbine downstream irrigation hydro power

plant." In *2017 6th International Youth Conference on Energy (IYCE)*, pp. 1-6. IEEE, 2017.

[13] Jiang, Jiheng, Ying Qiao, and Zongxiang Lu. "The probabilistic production simulation for renewable energy power system considering the operation of cascade hydropower stations." In *2018 International Conference on Power System Technology (POWERCON)*, pp. 331-338. IEEE, 2018.

[14] Molina, Marcelo G., and Mario Pacas. "Improved power conditioning system of micro-hydro power plant for distributed generation applications." In *2010 IEEE International Conference on Industrial Technology*, pp. 1733-1738. IEEE, 2010.

[15] Tessarolo, Alberto, F. Luise, P. Raffin, and M. Degano. "Traditional hydropower plant revamping based on a variable-speed surface permanent-magnet high-torque-density generator." In *2011 International Conference on Clean Electrical Power (ICCEP)*, pp. 350-356. IEEE, 2011.

[16] Hug-Glanzmann, Gabriela. "Predictive control for balancing wind generation variability using run-of-river power plants." In *2011 IEEE Power and Energy Society General Meeting*, pp. 1-8. IEEE, 2011.

[17] Borkowski, Dariusz, and Tomasz Węgiel. "Small hydropower plant with integrated turbine-generators working at variable speed." *IEEE Transactions on Energy Conversion* 28, no. 2 (2013): 452-459.

[18] Blanco, HJ Eslava, LA Rojas Castellar, and MG Herrera Sanabria. "Intelligent integration based on optical telecommunications to optimize distributed generation." CIRED Workshop: Integration of Renewables into the Distribution Grid (2012): 102-102.

[19] Avram, Camelia, Dan Mircescu, Adina Aştilean, and Ovidiu Gbiran. "Fluid Stochastic Petri Nets based Modelling and simulation of Micro Hydro Power stations behaviour." In *2014 IEEE International Conference on Automation, Quality and Testing, Robotics*, pp. 1-6. IEEE, 2014.

[20] Xu, Huiting, Wenxia Liu, Lili Wang, Meng Li, and Junpeng Zhang. "Optimal sizing of small hydro power plants in consideration of voltage control." In *2015 International Symposium on Smart Electric Distribution Systems and Technologies (EDST)*, pp. 165-172. IEEE, 2015.

[21] Wen, Xiankui, Qiang Fan, Wenxia Liu, Chenghui Lin, and Wen Peng. "Design and Application of Multiple Intermittent Energy Grid Integration Evaluation System." In *2018 2nd IEEE Advanced Information Management, Communicates, Electronic and Automation Control Conference (IMCEC)*, pp. 1022-1028. IEEE, 2018.

[22] Sabir, Mohammad Amjad, Syed Husnain Ali Shah, and Umer Habib. "Establishment of hydroelectric microgrids, need of the time to resolve energy shortage problems." In *2017 3rd International Conference on Power Generation Systems and Renewable Energy Technologies (PGSRET)*, pp. 16-21. IEEE, 2017.

[23] Borkowski, Dariusz. "Small hydropower plant as a supplier for the primary energy consumer." In *2015 16th International Scientific Conference on Electric Power Engineering (EPE)*, pp. 148-151. IEEE, 2015.

[24] Diniz, André Luiz, Ana Lucia Saboia, and R. M. Andrade. "An exact multi-plant hydro power production function for mid/long term hydrothermal coordination." In *2016 Power Systems Computation Conference (PSCC)*, pp. 1-7. IEEE, 2016.

[25] Chen, Yue, Feng Liu, Wei Wei, Shengwei Mei, and Naichao Chang. "Robust unit commitment for large-scale wind generation and run-off-river hydropower." *CSEE journal of power and energy systems* 2, no. 4 (2016): 66-75.

[26] Yuan, Liu, Jianzhong Zhou, Chuyang Chang, Peng Lu, Chao Wang, and Muhammad Tayyab. "Short-term joint optimization of cascade hydropower stations on daily power load curve." In *2016 IEEE International Conference on Knowledge Engineering and Applications (ICKEA)*, pp. 236-240. IEEE, 2016.

[27] Fan, Qiang, Xiankui Wen, Chenghui Lin, Wen Peng, and Yan Zhang. "Research on influence factors analysis and countermeasures of improving prediction accuracy of run-of-river small hydropower." In *2017 2nd International Conference on Power and Renewable Energy (ICPRE)*, pp. 548-552. IEEE, 2017.

[28] Paravan, Dejan, T. Stokelj, and Robert Golob. *Selecting input variables for hpp reservoir water inflow forecasting using mutual information*. Vol. 2. IEEE, 2001.

[29] Martins, L. S. A., and S. Soares. "Insights on short-term hydropower scheduling: on the representation of water continuity equations." In *2016 Power Systems Computation Conference (PSCC)*, pp. 1-6. IEEE, 2016.

[30] Shaktawat, Anuja, and Shelly Vadhera. "Fuzzy logic based determination of cost overrun of hydro power plant." In *2016 International Conference on Electrical Power and Energy Systems (ICEPES)*. pp. 301-304. IEEE, 2016.

[31] Wijesinghe, Anuradha, and Loi Lei Lai. "Small hydro power plant analysis and development." In *2011 4th International Conference on Electric Utility Deregulation and Restructuring and Power Technologies (DRPT)*, pp. 25-30. IEEE, 2011.

[32] Macabiog, Rose Ellen N., Jennifer C. Dela Cruz, and Timothy Amado. "Water Quality Analysis: Ecological Integrity Conformance of Run-of-River Hydropower

Plants." In *2018 IEEE 10th International Conference on Humanoid, Nanotechnology, Information Technology, Communication and Control, Environment and Management (HNICEM)*, pp. 1-4. IEEE, 2018.

[33] Qiang, Fan, Lin Chenghui, Wen Xiankui, Wen Peng, and Chen Yuanyuan. "Research on application of run-of-river small Hydropower Station group short-term power forecast system in Guizhou Power Grid." In *2016 IEEE International Conference on Power and Renewable Energy (ICPRE)*, pp. 328-334. IEEE, 2016.

[34] Desingu, Karthik, Thanga Raj Chelliah, and Deepak Khare. "Sustainable operation of small hydropower schemes in changing climatic conditions." In *2017 IEEE PES Asia-Pacific Power and Energy Engineering Conference (APPEEC)*, pp. 1-6. IEEE, 2017.

[35] Azrulhisham, E. A., and M. Arif Azri. "Application of LISST instrument for suspended sediment and erosive wear prediction in run-of-river hydropower plants." In *2018 IEEE International Conference on Industrial Technology (ICIT)*, pp. 886-891. IEEE, 2018.

[36] Fang, Fang, and Rajesh Karki. "Reliability Implications of Riverflow Variations in Planning Hydropower Systems." In *2018 IEEE Conference on Technologies for Sustainability (SusTech)*, pp. 1-6. IEEE, 2018.

[37] Wang, Yaochun, Naicheng Wu, Tao Tang, Yuyu Wang, and Qinghua Cai. "Small run-of-river hydropower dams and associated water regulation filter benthic diatom traits and affect functional diversity." *Science of The Total Environment* 813 (2022): 152566.

[38] Sasthav, Colin, and Gbadebo Oladosu. "Environmental design of low-head run-of-river hydropower in the United States: A review of facility design models." *Renewable and Sustainable Energy Reviews* 160 (2022): 112312.

[39] Bernardes Jr, Jose, Mateus Santos, Thiago Abreu, Lenio Prado Jr, Danilo Miranda, Ricardo Julio, Pedro Viana, Marcelo Fonseca, Edson Bortoni, and Guilherme Sousa Bastos. "Hydropower Operation Optimization Using Machine Learning: A Systematic Review." *AI* 3, no. 1 (2022): 78-99.

[40] Sojka, Mariusz. "Directions and extent of flows changes in Warta river basin (Poland) in the context of the efficiency of run-of-river hydropower plants and the perspectives for their future development." *Energies* 15, no. 2 (2022): 439.

[41] Arévalo, Paul, Marcos Tostado-Véliz, and Francisco Jurado. "A novel methodology for comprehensive planning of battery storage systems." *Journal of Energy Storage* 37 (2021): 102456.

[42] Jovan, David Jure, Gregor Dolanc, and Boštjan Pregelj. "Utilization of Excess Water Accumulation for Green Hydrogen Production in a Run-of-River Hydropower Plant." *Available at SSRN 4028659*.

[43] Arai, Ryosuke, Yasushi Toyoda, and So Kazama. "Streamflow maps for run-of-river hydropower developments in Japan." *Journal of Hydrology* 607 (2022): 127512.

[44] Simani, Silvio, Stefano Alvisi, and Mauro Venturini. "Fault tolerant control of a simulated hydroelectric system." *Control Engineering Practice* 51 (2016): 13-25.

[45] He, JiangBiao, Qichen Yang, and Zheng Wang. "On-line fault diagnosis and fault-tolerant operation of modular multilevel converters—A comprehensive review." *CES Transactions on Electrical Machines and Systems* 4, no. 4 (2020): 360-372.

[46] Moloi, K.; Jordaan, J.A.; Abe, B.T. Development of a hybrid fault diagnostic method for power distribution network. In Proceedings of the 2019 IEEE AFRICON, Accra, Ghana, 25–27 September 2019; pp. 1–4

[47] Moloi, K.; Akumu, A.O. Power distribution fault diagnostic method based on machine learning technique. In Proceedings of the 2019 IEEE PES/IAS PowerAfrica, Abuja, Nigeria, 20–23 August 2019; pp. 238–242

[48] Trnka, P.; Hofreiter, M.; Sova, J. Combination of techniques for the fault diagnostics. In Proceedings of the 2017 18th International Carpathian Control Conference (ICCC), Sinaia, Romania, 28–31 May 2017; pp. 499–502

[49] Mattera, C.G.; Quevedo, J.; Escobet, T.; Shaker, H.R.; Jradi, M. A Method for Fault Detection and Diagnostics in Ventilation Units Using Virtual Sensors. *Sensors* **2018**, *18*, 3931.

[50] Rombach, Katharina, Gabriel Michau, and Olga Fink. "Contrastive learning for fault detection and diagnostics in the context of changing operating conditions and novel fault types." *Sensors* 21, no. 10 (2021): 3550.

[51] De, V. Lima, T.L.; Filho, A.C.L.; Belo, F.A.; Souto, F.V.; Silva, T.C.B.; Mishina, K.V.; Rodrigues, M.C. Noninvasive Methods for Fault Detection and Isolation in Internal Combustion Engines Based on Chaos Analysis. *Sensors* **2021**, *21*, 6925.

[52] Komorska, Iwona, and Andrzej Puchalski. "Rotating machinery diagnosing in non-stationary conditions with empirical mode decomposition-based wavelet leaders multifractal spectra." *Sensors* 21, no. 22 (2021): 7677.

[53] Dong, L.; Guo, H.; Guo, Z.; Zheng, T. Fault Diagnosis Technique for Hydroelectric Generators using Variational Mode Decomposition and Power Line Communications. *J. Phys.* **2019**, *1176*, 062058

[54] Xia, Xin, Wei Ni, and Yingjun Sang. "A novel analysis method for fault diagnosis of hydro-turbine governing system." *Proceedings of the Institution of Mechanical Engineers, Part O: Journal of Risk and Reliability* 231, no. 2 (2017): 164-171.

[55] Chen, W. Fault Detection and Isolation in Nonlinear Systems: Observer and Energy-Balance Based Approaches. Ph.D. Thesis, University of Duisburg-Essen, Duisburg, Germany, 2012.

[56] Khan, A.Q. Observer-Based Fault Detection in Nonlinear Systems. Ph.D. Thesis, University of Duisburg-Essen, Duisburg, Germany, 2010

[57] Abid, M. Fault Detection in Nonlinear Systems: An Observer-Based Approach. Ph.D. Thesis, University of Duisburg-Essen, Duisburg, Germany, 2010

[58] Priyadharson, A.S.M.; Saravanan, M.S.; Gomathi, N.; Joshua, S.V.; Mutharasan, A. Energy efficient flow and level control in a hydro power plant using fuzzy logic. *J. Comput. Sci.* **2014**, *10*, 1703–1711